PROCESS SIMULATION OF AMMONIA PLANT

A Thesis Submitted
in Partial Fulfilment of the Requirements
for the Degree of
DOCTOR OF PHILOSOPHY

By
CHANDRA PRAKASH PRASAD SINGH

to the
DEPARTMENT OF CHEMICAL ENGINEERING
INDIAN INSTITUTE OF TECHNOLOGY, KANPUR
MARCH, 1978

CERTIFICATE

It is certified that this work 'PROCESS SIMULATION OF AMMONIA PLANT' has been carried out under my supervision and it has not been submitted elsewhere for a degree.

March 22, 1978

D.N. Saraf

[D.N. Saraf]
Professor
Department of Chemical Engineering
Indian Institute of Technology, Kanpur
Kanpur-208016, India

CHE-1978-D-SIN-PRO

ACKNOWLEDGEMENTS

The author wishes to express his gratitude and indebtedness to Professor D.N. Saraf, the Guru, for guidance, flexibility shown in the style of working and all help called for throughout the course of this work.

The author is also indebted to Sri Sunil Sahasrabudhey for shouldering the more important responsibilities for the sake of completion of the work and to Sri Jag Narain Mahto for invaluable discussions during the initial stage of the work.

The permission by Fertilizer Corporation of India Ltd., to use its plant data, and the cooperations from Sri K.C. Sharma, Chairman and Managing Director, Sri B.B. Chandra, G.M. (Namrup Division), Sri J.P. Gupta, G.M.(Barauni Division), Sri A.K. Mitra, G.M. (Durgapur Division), Sri B.S. Kalia, D.G.M.(Namrup Division) and Sri Dutta Majumdar (Durgapur Division) are gratefully acknowledged. The author is very much thankful to Sarvasri Anirudh Prasad, Binay Kumar, Vinay Kumar, B. Banerjee, Dutta Mitra, G.K. Mohata, R.L. Sanger, all engineers of FCI Ltd. for their cooperation, in collection of plant data and general information, important for the work ; to Sri G. Narsimhan and Miss Veena Joshi for checking the manuscript, and to Sri T. Swaminathan and Sri Srikant Kulkarni for general assistance at completion.

Acknowledgement is also made to Sri A.S. Athayde, Additional Chief Engineer, F.C.I., Trombay for arranging visit to the Plant and providing all the additional help required in collecting data.

Thanks are due to Sri B.S. Pandey for the care taken in typing the manuscript, to Sri D.S. Panesar for the drawings, Sri Hari Ram for cyclostyling the manuscript and Sri Jai Ballabh for the ammonia prints. Thanks are also due to the staff of Computer Center, IIT-Kanpur for their general assistance.

Lastly, the author wishes to express his gratitude to his wife, Mrs. Madhuri Singh, for her help in many ways.

Author

CONTENTS

LIST OF FIGURES

LIST OF TABLES

PROCESS SIMULATION OF AMMONIA PLANT

A Thesis Submitted
In Partial Fulfilment of the Requirements
For the Degree of

DOCTOR OF PHILOSOPHY

by

CHANDRA PRAKASH PRASAD SINGH

to the

Department of Chemical Engineering
Indian Institute of Technology, Kanpur

March, 1978

SYNOPSIS

A mathematical description of the process units is necessary for the design, optimization and control of a chemical plant. These mathematical relationships are often obtained by regression analysis of historical plant data. The reliability of these regression models is limited by system noise. Also these models are valid only for the range of the variables in which data were collected.

A better model can be obtained by considering all the physical and chemical processes taking place in any differential section of the unit under consideration. This work describes process simulation of ammonia plant wherein, for each important

unit such mathematical models have been developed.

Ammonia, which is a basic fertilizer ingredient, is industrially synthesized from nitrogen and hydrogen. The process consists of steam reformation of a hydrocarbon (natural gas or naphthas), conversion of CO in the reformed product to CO_2, removal of CO_2 by absorption, conversion of any residual carbon oxides to methane and finally synthesis of ammonia from this gas which contains N_2, H_2, CH_4 and Ar. The important process units are primary and secondary reformer high and low temperature shift reactors and ammonia synthesis reactor.

In the primary reformer model development, a method to calculate transfer of heat to reformer tubes from flames in addition to those from flue gases in the fire box, has been developed. The total transfer of heat, from flames and flue gases, to a differential section of a reformer tube is considered simultaneous with the transfer of heat to the reacting gases and the reaction taking place inside it. Kineti rate expressions describing steam-hydrocarbon reactions, under varying conditions of pressure, have been obtained by modifi-cations in the available ones. This model has been used to check performance of reformers of different sizes (reformer tube heated length -3.28 to 12.2 meters), using different hydrocarbon feeds (natural gas or naphthas) and operating

under different pressures (13.7 to 35.0Kg/cm^2) and feed temperatures (371 to 456.4°C). Agreement between plant data and simulation results is generally very good.

In the secondary reformer model, the temperature and composition at the inlet, due to mixing of air with high temperature product from primary reformer, is calculated. Rate of reformation reaction is calculated by considering diffusion of methane to the catalyst pellet surface to be the limiting factor. Match of the calculated inlet temperature, amount of air used and the outlet temperature and composition with the respective plant data confirms the validity of the method of calculation.

Rate equation for water-gas shift reaction over a high temperature shift catalyst (Fe_2O_3-Cr_2O_3) has been developed. This rate equation takes into account the effects of temperature, pressure, age of the catalyst, H_2S content of the reacting gases as well as the intraparticle diffusional resistance in the catalyst pores. It has been used in the high-temperature shift reactor model to check the performance of reactors having single or multiple beds and working under different conditions of temperature (603-744°K), pressure (16.4 to 30 Kg/cm^2), composition of the reacting system (CO - 9.0 to 40.6 per cent), catalyst age (60 to 560 days), H_2S concentration (less than 0.5 to 60 ppm) and steam to carbon monoxide ratio (5 to 21.7). The close agreement between the

plant data and predicted values validated the model.

For low-temperature shift catalyst (CuO-ZnO), the effects of temperature, pressure, age of the catalyst and intraparticle diffusional resistance on the rate of reaction are accounted along the same lines as for high temperature catalyst. Performance of reactors using catalysts of differer age (60 to 560 days) and working under different conditions of pressure (16.0 to 28.9 Kg/cm^2) and temperature (183-228°C) can satisfactorily be predicted with this model. However, the change in composition as well as temperature is rather low in this reactor and hence the significance of the model is not obvious.

A workable method to calculate the effectiveness factor, for a complex reaction, by partially solving the transport equations has been developed. Appropriate rate equation describing synthesis of ammonia over an iron catalyst has been selected. This, along with the method developed to calculate effectiveness factor, has been used in a mathematica model to describe the ammonia synthesis reactor performance. Both adiabatic as well as non-adiabatic beds have been consi- dered. The model very successfully represents the plant performance.

These unit models are finally unified in an overall plant simulation which assumes ideal performance for the units which have not been separately considered. This program

is used to check the performance of two existing ammonia plants each of 600 tons/day capacity, working with natural gas and naphtha as the feed stock and at different conditions of operation. The agreement between plant performance and simulation results have been checked at various points throughout the plant.

The simulation models have been used only to check the performance of existing units or plants. However, in view of their validity over diverse conditions of operation, these models could as well be used for design purposes.

CHAPTER 1

INTRODUCTION

With increase in world fertilizer demand the need for the basic fertilizer ingradient, ammonia, has also increased. The design development in mid sixties, of single train ammonia plants employing centrifugal compressors, facilitated large scale production capacity. As a result, numerous plants have been constructed around the world which produce 600-1500 tons of ammonia per day. The plants use feed stock ranging from natural gas to naphthas in the boiling range upto 220°C.

Figure 1.1 shows a simplified process flow diagram for such an ammonia plant. After being mixed with steam, the desulphurised process hydrocarbon enters a Primary Reformer (PR). The outlet stream containing H_2, CO, CO_2, CH_4 and steam, is mixed with air at the Secondary Reformer (SR) inlet. The quantity of air used is such that after complete conversion of CH_4 and CO to CO_2 the hydrogen to nitrogen ratio (H_2/N_2) in the process gas is slightly more than three. The high temperature SR product is cooled (Heat recovery) and sent to High Temperature shift reactor (HT) where CO reacts with steam to yield additional CO_2 and H_2. In the Low Temperature shift reactor (LT) that follows, the CO concentration in the

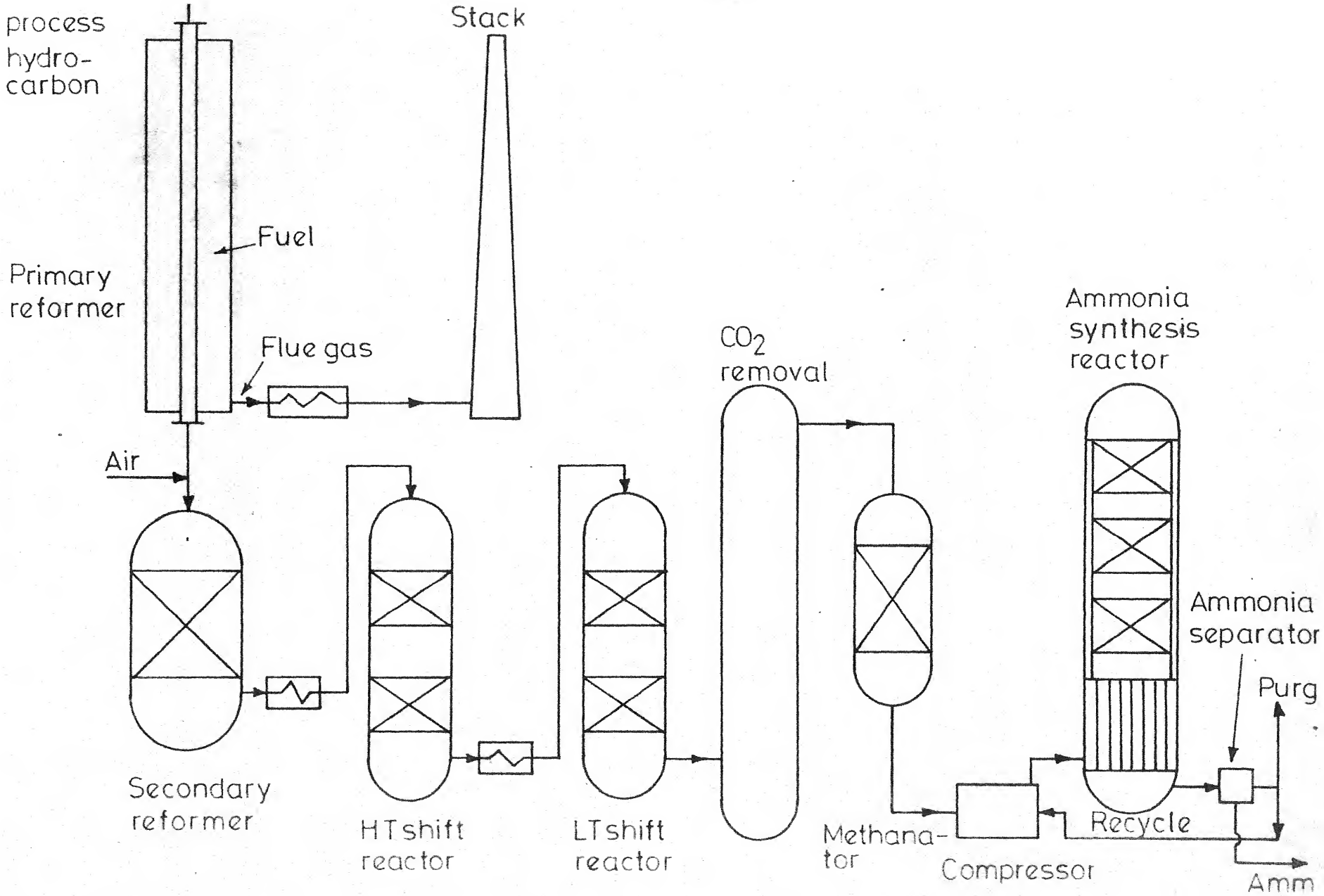

Fig. 1-1 - Simplified flow diagram for an ammonia plant

gas is reduced to a very low value closely approaching equilibrium at a lower temperature. Carbon dioxide is subsequently removed from the process gas in CO_2 absorber and remaining carbon oxides are converted to methane in the methanator. The methanator exit i.e. synthesis gas, is compressed and mixed with the recycle gas to make feed for the ammonia synthesis reactor. Reaction in this reactor, between nitrogen and hydrogen of the synthesis gas, yields ammonia which is the final product. Ammonia is separated from the product stream, a part of the remaining gas is purged to maintain low concentration of inerts in synthesis gas and the rest of it is recycled.

The general engineering philosophy behind the single train ammonia plants is to employ higher pressures in the reforming section (PR and SR) and lower pressure in ammonia synthesis section, compared to those in older plants which use reciprocating compressors. The centrifugal compressors used in these plants are driven by steam turbines. Required steam is generated by the utilization of sensible heat from the product gases of the synthesis reactor and the SR as well as waste heat from the PR flue gas. While a major advantage of this design is to obtain an extremely efficient utilization of the heat generated in the plant, its operation is highly sensitive to both process and equipment performance.

This work takes only the process performance into consideration

A mathematical description of all important process units taking into consideration all the important physical and chemical processes taking place inside them is necessary for a successful design and operation of the plant. Moreover, when a computer is used for control of a chemical process, a mathematical description of the process units is necessary to perform such tasks as feed forward and feed back control, as well as off line and on line optimization. Historical plant data are often used to obtain such a mathematical description by means of regression analysis. However, reliability of these regression models is limited by system noise. Also these models are valid only for the range in which the values of the variables were obtained and extrapolation is generally not very useful.

Availability of a priori knowledge of the behaviour of the critical units greatly facilitates the design of computer control strategy of a plant. Off line simulation of the actual plant units by means of analog or digital computer can provide such a knowledge, provided that the mathematical models chosen for simulation describes the plant with reasonable accuracy. Once the accuracy and generality of the plant simulation in predicting the plant behaviour is

established, the same models can be used for designing new plants. Also this could be reduced by various simplification techniques for use in on-line control and optimization.

The important process units in the ammonia plant are the primary and secondary reformers, the high and low temperature shift reactors and the ammonia synthesis reactor. Simulation model for each of these units is described in this work. These unit models have been tested under diverse conditions of operation and finally a unified computer program using all these models has been prepared to check the performance of two ammonia plants. Each of these are of 600 tons/day capacity but one of the plants is based on natural gas while the other uses straight run naphtha in the boiling range 200 to 210°C, as feed stock.

Chapter 2 describes the models for primary and secondary reformers. In Chapter 3 model development of high and low temperature shift reactors is discussed. Model for ammonia synthesis reactor is discussed in Chapter 4. The 5th Chapter deals with unification of all these unit models in an overall simulation program for ammonia plant.

CHAPTER 2

SIMULATION OF STEAM-HYDROCARBON REFORMERS

Steam reformation of hydrocarbons is carried out in two consecutive reactors, namely, Primary Reformer (PR) and Secondary Reformer (SR). PR consists of rectangular furnaces in parallel. In each furnace, catalyst tubes are arranged in two rows parallel to the two walls in which a large number of burners are embedded (Figure 2.1). Reactions over the latest steam-reforming catalysts are so fast that thermodynamic equilibrium, corresponding to the process temperature, is closely approached. Since higher temperature favours low methane content in the process gas, it is desirable to attain high PR exit temperature. However, limitations of heat transfer at higher temperature through metallic tubes put a limit to which the temperature can be raised.

Process condition close to equilibrium at higher temperature is attained in SR. Air is added to the SR inlet stream (PR exit) to provide nitrogen for ammonia production and the necessary heat, obtained by the combustion, for conversion of the resi'ual methane in PR exit. There is no heat transfer through the reactor (SR) walls and performance is dependent on adiabatic partial combustion of inlet stream

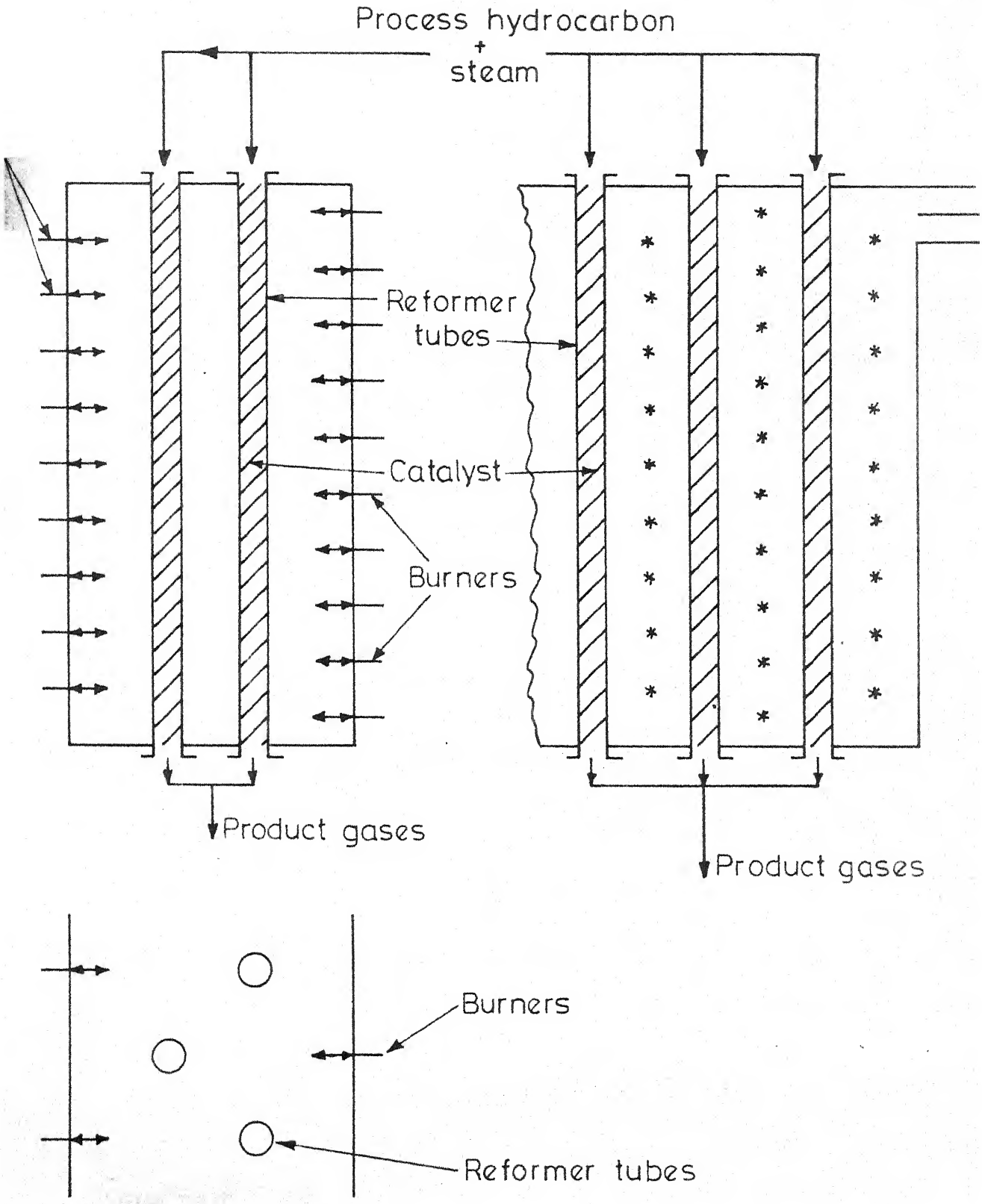

Fig. 2·1 - Side-wall fired reformer furnace.

followed by reforming over the SR (nickel) catalyst.

2.1 PRIMARY REFORMER

The feed to PR (hydrocarbon-steam mixture) enters the catalyst packed reformer tubes at the top. Endothermic heat of reaction as well as heat to increase process gas temperature is supplied by large number of burners distributed uniformly over the walls (Figure 2.1).

There are some works reported in literature which deal with the problem of heat transfer in top-fired [27,30] and side fired [16] steam -hydrocarbon reformers. Some others have simulated steam hydrocarbon reactions in a reformer [23,24]. The studies related to heat transfer in a side-fired reformer consider only the total amount of heat transferred over the entire length of reformer tubes. In the studies on simulation of reformer reactions, tube wall temperature profile has been assumed. The objective here is to find the conditions of the process stream at any point inside the reformer tube given the inlet conditions of process feed and burners.

For this purpose, kinetic rate expressions describing reactions inside a reformer tube have been developed. Transfer of heat from flames and flue gas to reformer tubes has also been modelled. With the help of these, a mathematical

model, taking into account the processes inside a differential reformer tube section and transfer of heat to it by flames and flue gas, is developed. Calculation program used for its integration provides the composition, temperature and pressure at each point inside the tubes and at the exit. It also gives the temperatures at all points on outside and inside surfaces of the reformer tubes and the amount of heat transferred through these surfaces to the process gas.

2.1.1 RATE EQUATIONS

The steam-reforming process generally uses nickel catalysts and feedstocks ranging from natural gas to naphthas of final boiling point 220°C. The chemical reactions that take place in catalytic reforming of these hydrocarbons are exceedingly numerous. Particularly in case of naphthas, which have very large number of components, it is practically impossible to determine the mechanisms and kinetic rate expressions of different reactions taking place. Therefore, many speculations have been made regarding the mechanism of steam-naphtha reaction and consequently to the development of models for the same. The model generally proposed, used in this work and elsewhere [23,24] is based on reformation experiments carried out with hydrocarbons heavier than methane e.g. propane, butane, hexane and benzene [6,12,32]. From

such experiments it is deduced that methane is the primary product of reaction between steam and heavier hydrocarbons. Accordingly, in the present model, methanation is taken to be completed at the entrance to the reformer i.e. all hydrocarbons heavier than methane are assumed to hydrocrack to methane. Consequently, the reaction system inside a reformer tube is described by the kinetic rate expressions for steam-methane reaction, irrespective of the process feed hydrocarbon.

Any pair of the following four reversible reactions will account for the stoichiometry in steam-methane reforming

$$CH_4 + H_2O \rightleftharpoons CO + 3H_2 \qquad (2.1)$$

$$CO + H_2O \rightleftharpoons CO_2 + H_2 \qquad (2.2)$$

$$CH_4 + 2H_2O \rightleftharpoons CO_2 + 4H_2 \qquad (2.3)$$

$$CO_2 + CH_4 \rightleftharpoons 2CO + 2H_2 \qquad (2.4)$$

While the choice of equations is important when dealing with kinetic relationships, any pair of these given here may be selected when dealing with equilibrium relationship

Taking different pairs from among the four reversible reactions described above, many kinetic models for steam-methane reactions have been proposed [1,2,7,12,29]. These rate equations differ considerably from one another but there are some common features as well. Firstly, the rate of

disappearance of methane is first order with respect to its concentration for almost all the cases referred to, although the pair of reactions used to describe the process are different. Secondly the forward rate constant, is dependent on pressure.

The differences among the equations, for rate of disappearance of methane, could be due to more than one reason. However, the most probable one seems to be the neglect of pore diffusional resistance, which is significant in large size catalyst pellets when the reaction is very fast. The inter-particle mass transfer resistance is insignificant under the high mass velocity conditions existing in primary reformer. Moreover, in case of shift reaction (reaction 2.2), seemingly different rate equations obtained by various workers [3,9,10,18,22,25,28] could be reduced to a single (intrinsic) rate equation by accounting for pore diffusional resistance [31, 33]. Based on these observations it has been assumed that pore diffusional resistance for reformation reactions is very high. Pair of reactions (2.1) and (2.2) has been taken to describe the reaction and the rate is evaluated by the following first order kinetic expressions [19]

$$r_1 = a_1 \exp(-Ea_1/RT) \left(p_{CH_4} - \frac{p_{H_2}^3 \cdot p_{CO}}{K_{eq_1} \cdot p_{H_2O}}\right) \qquad (2.5)$$

$$r_2 = a_2 \cdot \exp(-Ea_2/RT)\left(p_{CO} - \frac{p_{H_2} \cdot p_{CO_2}}{K_{eq_2} \cdot p_{H_2O}}\right) \quad (2.6)$$

where r_1 and r_2 are rates of reactions (2.1) and (2.2) respectively; a_1 and a_2 are the pre-exponential factors, constant at given pressure; Ea_1 and Ea_2 are apparent energies of activation, K_1 and K_2 are equilibrium constants, P is the total pressure and p_j is the partial pressure pressure of component j.

The values of apparent energies of activation and pre-exponential factors used in this work are

Ea_1 = 8,780 K.cal/kg.mole

a_1 = 127 Kg.mole/hr.Kg.of Catalyst.atm.

Ea_2 = 13880 K.cal/Kg.mole

a_2 = exp(8.23) Kg.mole/hr.Kg. of catalyst. atm.

The values of a_1 and a_2 are at a total pressure of 1 atmosphere. Values of Ea_1 and a_1 are due to Akers and Camp[1]. Those of Ea_2 and a_2 have been taken to be the same as those over an iron oxide catalyst (shift reaction catalyst). Values of Ea_2 and a_2 are from Singh and Saraf [33].

If the rate of a first order reversible reaction, with significant pore diffusion resistance, is expressed in terms of partial pressures of reacting components, the rate constant is inversely proportional to square root of the total

pressure [31]. So the values of pre-exponential factors, a_1 and a_2, at any pressure other than one atmosphere could be obtained by dividing its value at one atmosphere by square root of total pressure i.e. $\sqrt{P}$. Assuming the ideal gas conditions to hold and expressing the partial pressures as multiples of total pressure and mole fractions we have from equations (2.5) and (2.6)

$$r_1 = 127\sqrt{P} \exp\left(-\frac{8\,780}{RT}\right)\left(x_{CH_4} - \frac{x_H^3 \cdot x_{CO_2} \cdot P^2}{K_{eq_1} \cdot x_{H_2O}}\right) \quad (2.7)$$

$$r_2 = \exp\left(-\frac{13880}{RT} + 8.23\right)\sqrt{P}\left(x_{CO} - \frac{x_{H_2} \cdot x_{CO_2}}{K_{eq_2} \cdot x_{H_2O}}\right) \quad (2.8)$$

The above equations are valid under all operating conditions.

2.1.2 HEAT TRANSFER

The arrangement of tubes and burners alongwith the path of flue gas flow in a side fired reformer is shown in Figure 2.1. The heat transfer problem in such reformers can be conveniently split into two parts, namely, the transfer of heat from flames and flue gas to the reformer tubes and from inside walls of the reformer tubes to the reacting gas mixture.

Radiation is the prevailing mode for transfer of heat from flue gas and flames. Heat transferred by conduction

and convection is negligible compared to the total amount of heat received by the reformer tubes. Flue gas contributes larger part of heat in total transfer where as flames emanating from large number of burners provide the rest. For the sake of ease in calculation, the flames and flue gas are assumed as two distinct sources. Radiative transfer from these two sources to the tubes is assumed not to interfere with one another and the sum of the two is the total heat transferred. Both these sources consist of a mixture of radiating gases and the their emissivities enter all calculatio

Emissivities of Flames and Flue Gas:

The flames and fully burnt combustion products (flue gas) of most conventional gas and oil fuels are real gases, since the radiation from them is mainly due to carbon dioxide and water vapour which emit in discrete bands. However, the form of the relations for radiative heat transfer in an enclosure is greatly simplified if the gray gas assumption is made. Therefore, it is advantageous that the mathematical formulation which characterises a gray-gas system is retained in the representation of a real gas emission.

This is achieved by representing the emissivity of a real gas as the sum of the weighted emissivities of a number of gray gases [20]. The emissivity of a gray gas is given by

$$\varepsilon_g = 1 - \exp\ (-k_g\ pL_m)$$

where k_g is the absorption coefficient, p is the partial pressure of gas and L_m is the mean beam length. The total emissivity of a real gas, in terms of weighted emissivities of a number of gray gases, is given by

$$\varepsilon_g = \sum_{n=1}^{N} a_{g,n}\ [(1-\exp(-k_{g,n}\ pL_m)] \qquad (2.9)$$

where $a_{g,n}$ and $k_{g,n}$ are weighting and absorption coefficients for component n respectively and N is the total number of components. If the number of terms in the above summation i.e. N, is very large, $a_{g,n}$ may be considered as the fraction of energy in a blackbody spectral region in which the effective absorption coefficient is $k_{g,n}$. However, $k_{g,n}$ and $a_{g,n}$ may be more correctly considered as numbers which make the series in equation (2.9) fit the given function of ε_g vs pL_m. Although in theory the emissivity of a gas approaches one as the value of pL_m becomes very large, at all practically attainable values of it the emissivity is considerably less than one. Therefore, in fitting the emissivities of real gases with finite number of terms, it is common to have one term with $k_{g,n}$=0. This physically corresponds to the windows in the spectrum between strong emission bands and is sometimes referred to as the clear gas component.

In such a representation $k_{g,n}$ is held constant and temperature dependence of emissivity is transferred to weighting coefficients by expressing $a_{g,n}$ as

$$a_{g,n} = b_{1,n} + b_{2,n} T_g \qquad (2.10)$$

where $b_{1,n}$ and $b_{2,n}$ are constants for each value of n and T_g is the gas temperature. In the above representation Taylor and Foster [35] have used a 1 clear + 3 gray gas components model to fit the emissivities of combustion products of commonly employed gas and fuel oils as

$$\varepsilon_g = \sum_{n=1}^{4} (b_{1,n}+b_{2,n} T_g) (1-e^{-k_{g,n}(p_c+p_w)L_m}) \qquad (2.11)$$

where p_c and p_w are partial pressures of carbon dioxide and water vapour respectively, in the radiating gas mixture (flue gas or flames). This correlation, with values for constants in the reference, have been used here.

(i) Transfer of Heat to Reformer Tubes:

(a) Radiative Transfer from Flue Gas:

The enclosing refractory walls of a reforming furnace (fire-box) do not transfer any heat except that lost to atmosphere. This loss is generally assumed to be equal to the amount of heat transferred to it by convection and conduction from flue gas. So, there is no net radiative exchange between the enclosing walls and radiating gas and

tubes. Such a surface is termed a no flux surface.

A uniform flue gas temperature is assumed. The burning gas emanates at considerable momentum, from the burners, leading to a thorough mixing of gases inside the furnace. Measurement of temperature at different points throughout a reforming furnace also showed an insignificant variation, justifying the assumption.

It is further assumed that reformer tubes are gray and the disposition of surfaces is such that the view factor of the tube (sink) surface from a point on the refractory walls is same as that from any other point. The latter assumption implies that sink and walls are intimately mixed i.e. the walls are speckled.

In view of all the assumptions made, the problem can be visualized as that of radiative heat exchange between an isothermal gray gas and a single sink zone (tube surface), the enclosure being completed by refractory surfaces grouped together into a single no flux zone. From the available derivation for such a case [20] the net exchange between flue gas and reformer tubes can be written as

$$\dot{Q}_{g \rightleftharpoons t} = (\overline{GS}_t)_R \, (E_g - E_t) \tag{2.12}$$

where

$$\frac{1}{(\overline{GS}_t)_R} = \frac{1}{A_t} \left(\frac{1}{\varepsilon_t} - 1\right) + \frac{1}{(\overline{GS}_t)_{R,\text{black}}} \tag{2.13}$$

$$(\overline{GS}_t)_{R,\text{black}} = \varepsilon_g[A_t + \frac{A_R}{1 + \varepsilon_g/(1-\varepsilon_g)F_{Rt}}] \qquad (2.14)$$

$E_g = \sigma T_g^4$, $E_t = \sigma T_o^4$, σ is the Stefan-Boltzmann constant, T_g and T_o are the gas and outer tube surface temperatures respectively, $(\overline{GS}_t)_R$ is the total exchange area between flue gas and reformer tubes and $(\overline{GS}_t)_{R,\text{black}}$ is the total exchange area when tube surfaces are assumed to be black, ε_g and ε_t are emissivities of gas and tubes respectively, A_t and A_R are the surface areas of tubes and refractory walls, and F_{Rt} is the view factor of tubes with respect to refractory walls. F_{Rt} can be determined from charted values [20, 26] by considering an imaginary surface parallel to the tubes (and just outside them) and multiplying the view factor between the refractory and this surface by that between the surface and tubes.

It is clear from equations (2.13) and (2.14) that the total exchange area, $(\overline{GS}_t)_R$, is independent of the tube surface temperature. In addition, the assumed intimate mixing of reformer tube surface and that of the refractory wall makes it clear that there is no distinction between different elements of reformer tube surface due to geometrical disposition. Hence, the exchange area for a unit reformer tube surface is constant irrespective of its location and it is equal to the total exchange area divided by the total tube surface area. So the net exchange between furnace gas and an element of

unit area on a reformer tube can be written as (Equation (2.12)

$$\dot{q}_{g \rightleftharpoons t} = \frac{\dot{Q}_{g \rightleftharpoons t}}{N_t \cdot A_t} = \frac{(\overline{GS}_t)_R}{A_t \cdot N_t} (E_g - E_t) \qquad (2.15)$$

where N_t is the total number of reformer tubes, $A_t (=\pi D_o L)$ is the total outer tube surface of a reformer tube and D_o and L are outside diameter and length of a reformer tube respectively.

(b) Radiative Transfer from Flames:

Following assumptions are made:

1. Burners are evenly distributed over the refractory walls,
2. There is no distinction between different elements of reformer tube surface due to geometrical disposition or proximity to burners,
3. The flames are spherical in shape and radiate at adiabatic flame temperature,
4. Burner cup surfaces are no flux surfaces,
5. All radiations starting from flames reach the reformer tubes directly, the only loss to it is in passing through absorbing flue gas media. These radiations are completely absorbed on the tube surface

and

6. The amount of radiations from flue gas and tubes absorbed by flames, is negligible. It should be

noted here that the errors incurred due to this assumption and those due to assumption 5 are of opposite signs.

Based on these assumptions the amount of heat transferred to reformer tubes by flames can be written as

$$\dot{Q}_{f \rightleftharpoons t} = N_B A_f \varepsilon_f (1-\varepsilon_g)\varepsilon_t E_f \qquad (2.1$$

where N_B is total number of burners in use, $A_f = \pi D_B^2$, D_B is the diameter of hemispherical burner cup, ε_f is the emissivity of flames, $E_f = \sigma T_f^4$ and T_f is the adiabatic flame temperature, ε_f is calculated from equation (2.11) at flame temperature, T_f, using a mean beam length equal to 0.63 D_B i.e. 0.63 times the diameter of spherical gas shape [20].

Since one element of reformer tube surface is no different from another, the transfer of heat to an unit tube surface by flames can be represented as

$$\dot{q}_{f \rightleftharpoons t} = \frac{N_B A_f \varepsilon_f (1-\varepsilon_g)\varepsilon_t E_f}{N_t A_t} \qquad (2.17)$$

The total transfer of heat to an unit tube surface can now be written as

$$q = \dot{q}_{g \rightleftharpoons t} + \dot{q}_{f \rightleftharpoons t}$$

$$= \frac{1}{N_t A_t} [(\overline{GS}_t)_R (E_g - E_t) + N_B A_f \varepsilon_f (1-\varepsilon_g)\varepsilon_t E_f] \qquad (2.18)$$

In the above equation it is easy to visualize the total transfer as the radiative transfer from flue gas on which that from flames have been superimposed.

(ii) Transfer of Heat from Reformer Tube Inner Wall to the Process Gas:

It is assumed that heat transfer from inner tube wall is mainly by forced convection. Transfer by radiation and conduction have been neglected. It is reported that the radial temperature gradient inside a reformer tube is insignificant [5]. Therefore, a one dimensional model for heat transfer has been used. However, considering the two important resistances; one adjacent to the wall and the other in catalyst bed, the heat transfer has been calculated from the correlation of Beek [4]. It gives heat transfer coefficien h_{in}, as

$$h_{in} = \frac{K}{D_p} [2.58\ (Re_p)^{1/3}(Pr)^{1/3} + 0.094(Re_p)^{0.8}(Pr)^{0.4}] \qquad (2.19)$$

where $Re_p = D_p G/\mu$, $Pr = \overline{C}_p \mu/K$, D_p is the diameter of the catalyst particles, K, μ and $\overline{C_p}$ are the conductivity, viscosity and specific heat of process gas respectively. Hyman [23] has reported that for ring-shaped catalyst particles in a reformer tube the heat transfer coefficient is approximately 40 per cent of the value calculated from equation (2.19). In the

present work this is used for all particle shapes and the amount of heat transferred from unit surface of inner tube wall is

$$q_{in} = 0.4\ h_{in}\ (T_{in}-T) \qquad (2.20)$$

where T_{in} is the inner tube wall temperature and T is the process gas temperature.

2.1.3 DESCRIPTION OF THE MATHEMATICAL MODEL

The basis of the mathematical model is a differential reformer tube section of length dz filled with nickel catalyst. It is shown in Figure 2.2.

Heat Transfer:

It is assumed that there is no transfer of heat in the axial direction. This implies that the heat transferred to the outer surface of the tube element is conducted through it to the inner surface, in the radial direction. The inner surface in turn, transfers it to the process gas enclosed within the differential section. Since there is no accumulation or loss in transfer through the tube element, the heat received by it can be equated to the amount conducted through it and both of these could be equated to the amount of heat transferred to the process gas. These equalities could be expressed in terms of heat transfer per unit outer tube surface, q, as

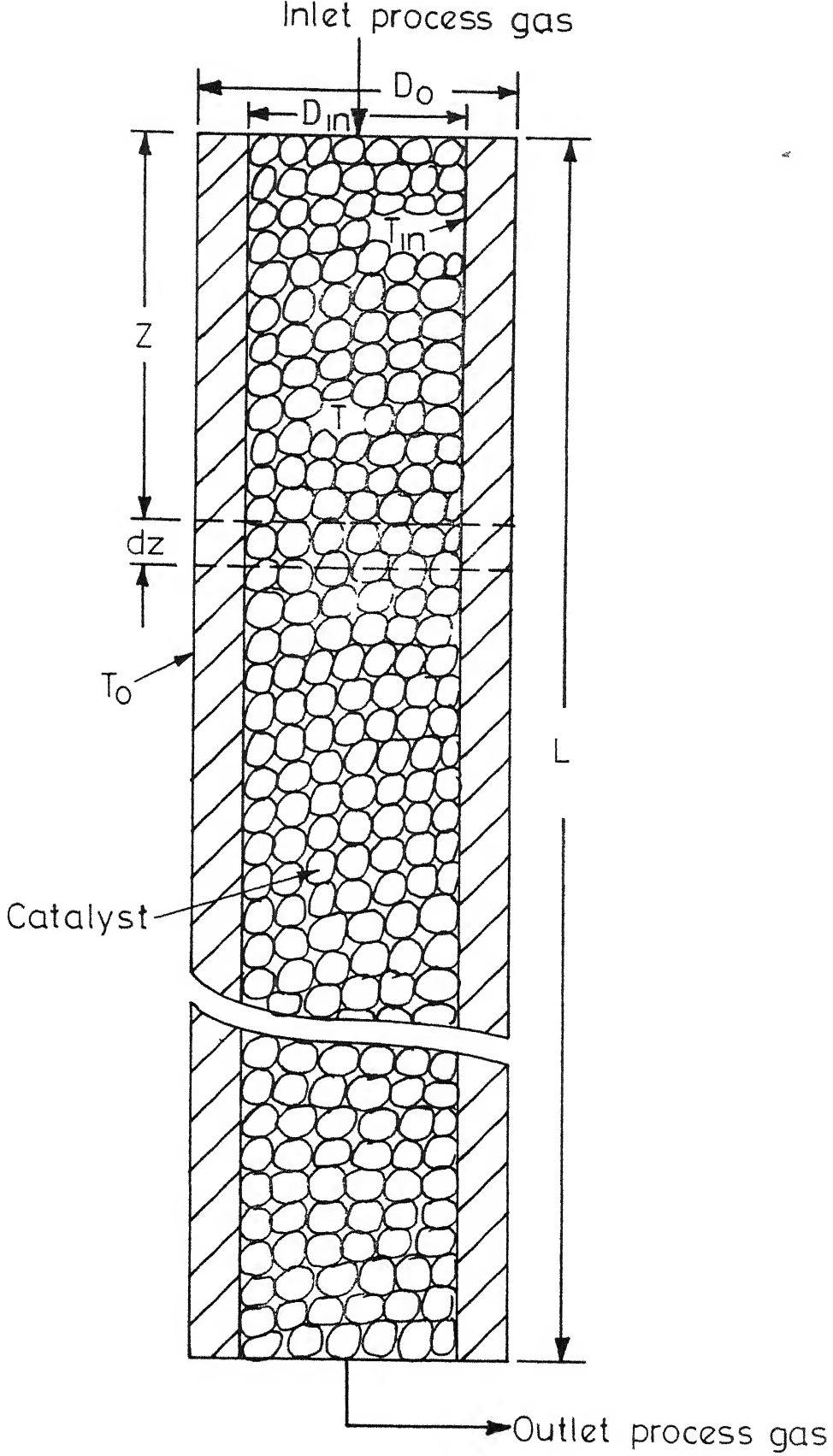

Fig 2 2 - Catalyst filled reformer tube

$$q = \frac{2 \times K (T_o - T_{in})}{D_o \ln D_o/D_{in}} \qquad (2.21)$$

and

$$q = D_{in}\, q_{in}/D_o \qquad (2.22)$$

where D_o and D_{in} are the outer and inner tube diameters respectively and T_o and T_{in} are the outside and inside surface temperatures.

Mass and Heat Balance:

It is assumed that the performance of a single reformer tube is representative of any other tube in the furnace. The temperature, pressure and composition through a general cross section of the catalyst bed in a reformer tube has been assumed to be uniformly distributed and axial diffusion of heat and mass has been neglected. With these assumptions the material and energy balance equations over the differential section, dz,(Figure 2.2) can be written as

$$\frac{d\xi_i''}{dz} = \frac{r_i \rho_c}{G} \qquad \text{for } i=1,2 \qquad (2.23)$$

ξ_i'' is defined by

$$g_j = g_j^o + \sum_{i=1}^{2} \alpha_{ij} M_j \xi_i'' \qquad (2.24)$$

and

$$\frac{dT}{dz} = \sum_{i=1}^{2} \left(-\frac{\Delta H_i}{\bar{C}_p}\right) \frac{r_i \rho_c}{G} + \frac{4}{D_{in} G} \frac{h_{in}}{\bar{C}_p} (T_{in}-T) \qquad (2.25)$$

where r_i is the rate of ith reaction, ρ_c is the catalyst bulk density, G is the mass velocity, ΔH_i is the heat of the ith reaction, $\bar{C}_p$ is average specific heat of the process gas, g_j and g_j^o are the mass fractions of component j at any point and the entrance respectively, M_j is the molecular weight of component j and α_{ij} is the stoichiometric coefficient of component j in the ith reaction, with a negative sign when the component is a reactant.

Pressure Drop:

Several investigators have proposed correlations for finding gas pressure drop for flow in a packed bed. Yen [36] evaluated three such methods and found the Ergun [15] equation to match his experimental data within 45 per cent. The Ergun equation is

$$\frac{dP}{dz} = -\left[\frac{150(1-v)}{Re_p} + 1.75\right]\left(\frac{G^2}{\rho}\right)\left(\frac{1}{D_p}\right)\left(\frac{1-v}{v^3}\right) x \frac{1}{(32.2)(144)(14.7)(3600)^2} \qquad (2.26)$$

where v is the void fraction and ρ is the density of gas. For hydrocarbon reforming, particle Reynolds number, Re_p, is in thousands. Therefore, the equation being used neglects the first term in the bracket.

It is noted that the mass velocity, G, is a constant throughout the entire tube length and for the moderate pressure

and high temperature employed in reformers it can be written as

$$\rho = \frac{M.P.}{RT}$$

where M is the average molecular weight of the process gas. The values of K_f and μ_f have been taken from values tabulated by Ghoshal et al.[17]. These have been expressed as linear functions of temperature and used in this work. $\bar{C}_p$ has been obtained by averaging specific heats of constituent molecules. Heats of reactions, ΔH_i expressed as linear functions of temperature have been used [14]. Equations (2.7, 2.8, 2.11, 2.13, 2.14, 2.18, 2.19 through 2.26) describe the mathematical model.

2.1.4 CALCULATION PROCEDURE

Process feed hydrocarbon is assumed to hydrocrack completely to methane at the entrance and heat effect associated with the process is neglected. The conversion of hydrocarbon (represented as CH_{2y} molecule) to methane is expressed by the following stoichiometric relation

$$3\ CH_{2y} + (2-y)\ H_2O \rightleftharpoons (1+y)\ CH_4 + (2-y)\ CO \qquad (2.27)$$

from which the amounts of CH_4 and CO are calculated. Amounts of H_2 and CO_2 in the gas are obtained from equilibrium considerations of reactions (2.1) and (2.2) respectively.

These calculations are repeated till the equilibrium conditions of both the reactions are simultaneously satisfied. This yields the feed gas composition for the primary reformer.

Adiabatic flame temperature is calculated by balancing the sensible heat in incoming fuel and air plus the heat generated by combustion with the heat in flames [21]. Amount of excess air used is calculated from the percent of oxygen in the combustion product (flue gas). Measured flue gas temperature and calculated adiabatic flame temperature are used in equation (2.11) to evaluate emissivities of flue gas and flames respectively. In these calculations beam length for flames is taken to be 0.63 times the diameter of hemispherical burner cup whereas that for flue gas is 1.8 times the gap between reformer tube row and the facing wall [20].

To evaluate the heat transferred to a differential tube section or the change in the process conditions inside it, the tube wall temperatures are to be known. Equations (2.18) through (2.22) are used for this purpose. In the calculation scheme, a suitable value for T_o is assumed and q is calculated from equation (2.18). Subsequently, q_{in} is evaluated from equation (2.22). Equations (2.19) and (2.20) in turn lead to the value of T_{in}. Finally, to check the validity of assumed value, T_o is calculated from equation (2.21) and in case it differs from the assumed value, the

calculated one is used as the new value of T_o for next iteration. The process is continued till assumed and calculated values of T_o agree within the desirable accuracy limits ($\leq 0.1^oC$).

Inlet process conditions and T_{in} for the differential section being known, equations (2.23) through (2.26) are simultaneously integrated using Runge-Kutta method of fourth-order [13] to obtain the conditions of outlet which, in turn, is the feed to succeeding differential section. Integration is started at the inlet end of reformer tubes and continued upto the outlet yielding composition, temperature and pressure at each point inside the reformer tubes. Values of T_{in}, $q_{g \rightleftharpoons t}$, $q_{f \rightleftharpoons t}$, q and q_{in} are also evaluated simultaneously along the whole length. Size of the integration step is varied according to the length of reformer tubes.

Calculation Program:

On the basis of the mathematical model described in the proceeding section, a calculation program in Fortran IV has been prepared for IBM 7044 computer. The calculation time for checking the performance of a reformer is 3 minutes and 5 secs, when the step size is 1/1000th of the heated tube length.

2.1.5 RESULTS AND DISCUSSION

The calculation results for three reformers of different sizes, using different hydrocarbon feeds and fuel (naphthas or natural gas) and working under various process conditions are presented in Tables 2.1, 2.2 and 2.3. Figures 2.3, 2.4 and 2.5 show the temperature profiles of process gas and reformer tube inner and outer wall for different cases. Figure 2.6 shows a typical calculated concentration profile of the component molecules along the reformer length (Table 2.3 Case I).

The calculated values for process variables are in very close agreement with the corresponding measured values. Since the rate of reaction is very fast, process gas outlet temperature is the most important process variable. The maximum difference between the measured and calculated values of process gas outlet temperature is 3 per cent (Table 2.3, Case I).

The amount of heat calculated as the difference between sensible heat of the flames and that of flue gas leaving the reforming furnace has been tabulated as total heat absorbed. The calculated values of total heat absorbed and total heat transferred are in very close agreement. Only in the case of short tube reformer (Table 2.2) this difference is 8 per cent, in other cases the values are within one per cent.

TABLE 2.1

CALCULATED AND EXPERIMENTAL DATA FOR STEAM-NAPHTHA PRIMARY REFORMER

Process and fuel hydrocarbon - Naphtha [final boiling point $<210^{\circ}C$, C/H ratio 6.27

Total number of reformer tubes	-	160
Heated tube length, meters	-	11.36
Inside tube diameter, mm	-	115.3
Outside tube diameter, mm	-	147.6
Burner cup diameter, mm	-	356.0
Catalyst shape and size	-	Raschig rings 16x16x6 mm
Bulk density of catalyst, Kg/m^3	-	1358.0
Calorific value of fuel, K.cal/Kg	-	10200

	Case I	Case II
Number of burners in use	526	521
Fuel naphtha flow, kg/hr	6320	5180
Flue gas temperature, $^{\circ}C$	1058	1010
Oxygen in flue gas, per cent	2.0	4.3
Total heat absorbed, K.cal/hr	4.03×10^7	3.406×10^7
Process Inlet:		
Process naphtha flow, Kg/hr	14100	11900
Calculated methane equivalent, kg.mole/hr	695	587
Steam flow, Kg/hr	67200	56000
Temperature, $^{\circ}C$	443	440
Pressure, kg/cm^2	24.8	24.3

Table 2.1 (contd)

	Case I		Case II	
	Plant	Calculated	Plant	Calculated
Process Outlet				
Dry gas flow, Nm^3/hr	61300	63723	54100	53850
Steam flow, kg/hr	45600	44188	35800	36500
Temperature, ^oC	761	770.1	775	771.5
Pressure, kg/cm^2	21.9	21.75	21.6	21.65
Composition of Gas, Mole per cent (Dry basis)				
CO	9.93	11.21	12.6	11.32
CO_2	17.43	16.97	17.2	17.01
H_2	64.16	64.44	63.3	64.38
CH_4	8.13	7.38	6.9	7.29
Heat Transfer:				
Heat transfer from flue gas, K.cal/hr		2.989×10^7		2.5025×10^7
Heat transfer from flames, K.cal/hr		1.005×10^7		0.8605×10^7
Total heat transfer, K.cal/hr		3.994×10^7		3.363×10^7
Outside Tube Wall Temperature, ^oC				
Reformer Tube Length (Fractional)				
0.2	777	802	740	770
0.4	832	842	825	813
0.6	866	872	870	857
0.8	900	897	880	885

TABLE 2.2

CALCULATED AND EXPERIMENTAL DATA FOR SHORT-TUBE PRIMARY REFORMER

Process and fuel hydrocarbon	-	Naphtha [final boiling point $<210^{\circ}C$, C/H ratio 6.27]
Total number of reformer tubes	-	176
Heated tube length, meters	-	3.28
Inside tube diameter, mm	-	90.5
Outside tube diameter, mm	-	117.2
Catalyst shape and size	-	6x6 mm pellets
Bulk density of catalyst, kg/m^3	-	1112
Calorific value of fuel, K.cal/Kg	-	10200
Number of burners in use	-	160
Fuel naphtha flow, Kg/hr	-	1814.1
Flue gas temperature, $^{\circ}C$	-	1045
Oxygen in flue gas, per cent	-	3.2
Total heat absorbed, K.cal/hr	-	10.083×10^6
Process Inlet:		
Process naphtha flow, Kg/hr	-	2215.3
Calculated methane equivalent, kg.mole/hr	-	114.72
Steam flow, Kg/hr	-	13960
Temperature, $^{\circ}C$	-	371
Pressure, Kg/cm^2	-	13.7

Table 2.2 (contd)

Process Outlet:	Plant	Calculated
Dry gas flow, Nm^3/hr	15800.0	15236.2
Steam flow, Kg/hr	9980.0	10327.0
Temperature, ^oC	796	785.3
Pressure, Kg/cm^2	13.0	13.1
Dry gas composition, mole per cent		
CO	11.15	10.79
CO_2	13.23	14.36
H_2	74.00	72.52
CH_4	1.52	2.33

Heat Transfer:

Heat transfer from flue gas, K.cal/hr	-	6.046×10^6
Heat transfer from flames, K.cal/hr	-	3.224×10^6
Total heat transfer, K.cal/hr	-	9.27×10^6

Outside Tube Wall Temperature, ^oC:

Reformer Tube Length (Fractional)		
0.25	875	860.4
0.50	904	897.3
0.75	940	938.4

TABLE 2.3

PLANT AND CALCULATED DATA FOR STEAM-NATURAL GAS PRIMARY REFORMER

Process and fuel hydrocarbon	-	Natural gas [Average composition, mole per cent CH_4 - 81.5, C_2H_6 - 7.0, C_3H_8 - 5.5, C_4H_{10} - 4.5, CO_2 - 1.5]
Total number of reformer tubes	-	200
Heated tube length, meters	-	12.2
Inside tube diameter, mm	-	96.0
Outside tube diameter, mm	-	133.8
Burner cup diameter, mm	-	356
Catalyst shape and size	-	Raschig rings 16x16x6 mm
Bulk density of catalyst, Kg/m^3	-	1182
Calorific value of fuel, $K.cal/Nm^3$		10800

	Case I	Case II
Number of burners in use	584	568
Fuel natural gas flow, Nm^3/hr	7786	7069
Flue gas temperature, ^oC	1030	1038
Oxygen in flue gas, per cent	2.5	3.8
Total heat absorbed, K.cal/hr	3.96×10^7	3.69×10^7
Process Inlet:		
Process natural gas flow, Nm^3/hr	13920	12014
Calculated methane equivalent, Kg.mole/hr	689.83	598.6

Steam flow, Kg/hr	61000	55000
Temperature, ^{o}C	456.4	447.0
Pressure, Kg/cm^2	35.0	32.3

Process Outlet:	Case I		Case II	
	Plant	Calculated	Plant	Calculated
Dry gas flow, Nm^3/hr	62400	61362.7	54160	53342.2
Steam flow, Kg/hr	44000	44417.0	39600	39852.3
Temperature, ^{o}C	773	796.8	793	784.3
Pressure, Kg/cm^2	31.3	31.56	28.8	29.12
Composition of gas, mole per cent (dry basis)				
CO	10.17	9.56	9.86	9.90
CO_2	12.27	12.56	11.79	12.01
H_2	67.22	69.61	69.03	69.19
CH_4	9.83	8.27	9.32	8.90
Heat Transfer:				
Heat transfer from flue gas, K.cal/hr		2.926×10^7		2.721×10^7
Heat transfer from flames, K.cal/hr		1.004×10^7		0.936×10^7
Total heat transfer, K.cal/hr		3.93×10^7		3.657×10^7
Outside Tube Wall Temperature, ^{o}C				
Reformer Tube Length (Fractional)				
0.2	772	792.8	754	775.3
0.4	836	831.0	830	724.2
0.6	866	864.5	849	848.0
0.8	891.3	892.3	871	875.8

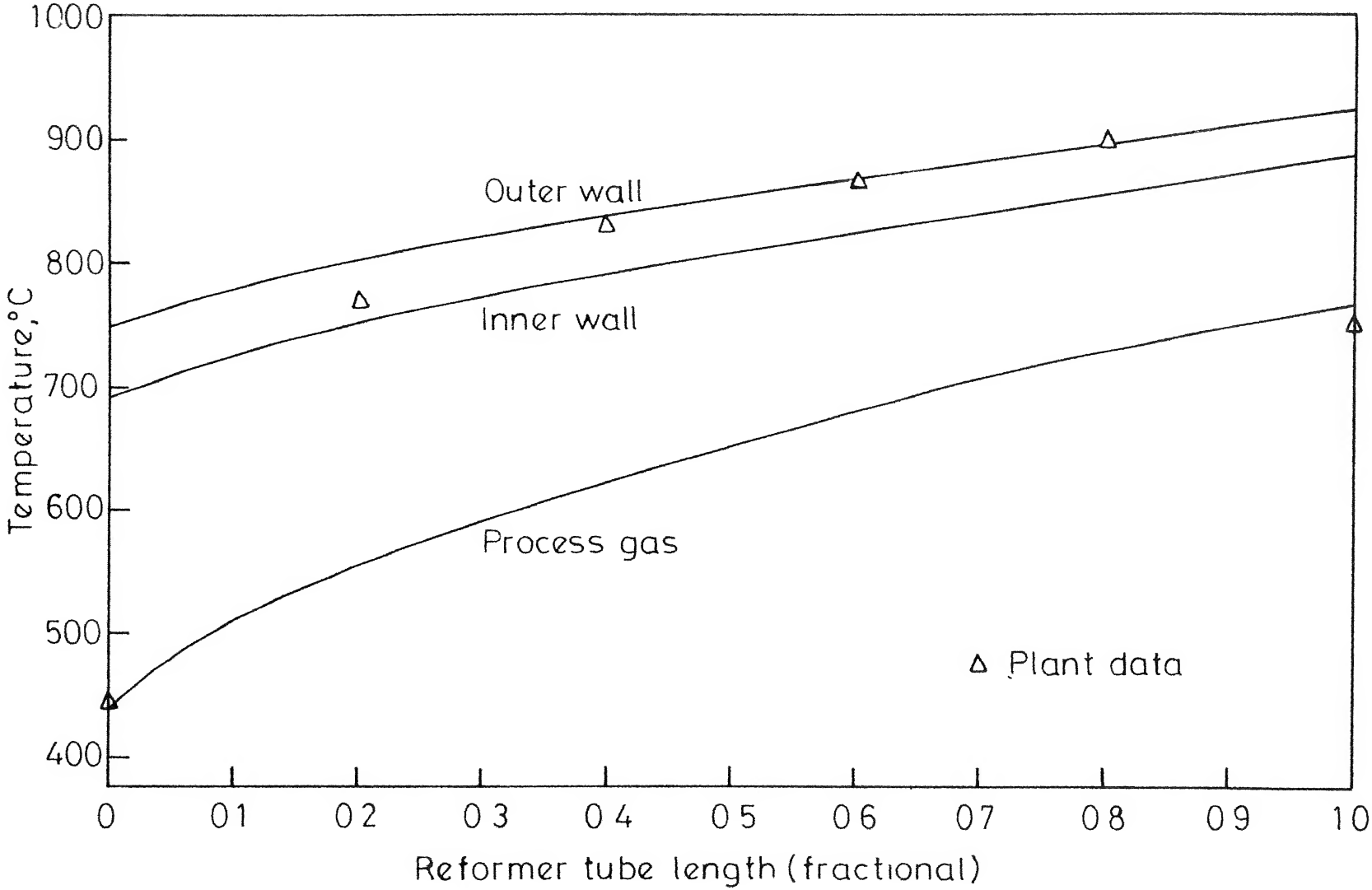

Fig 2 3 - Temperature profiles of process gas and reformer tube surfaces.
[Table 2 1, Case 1]

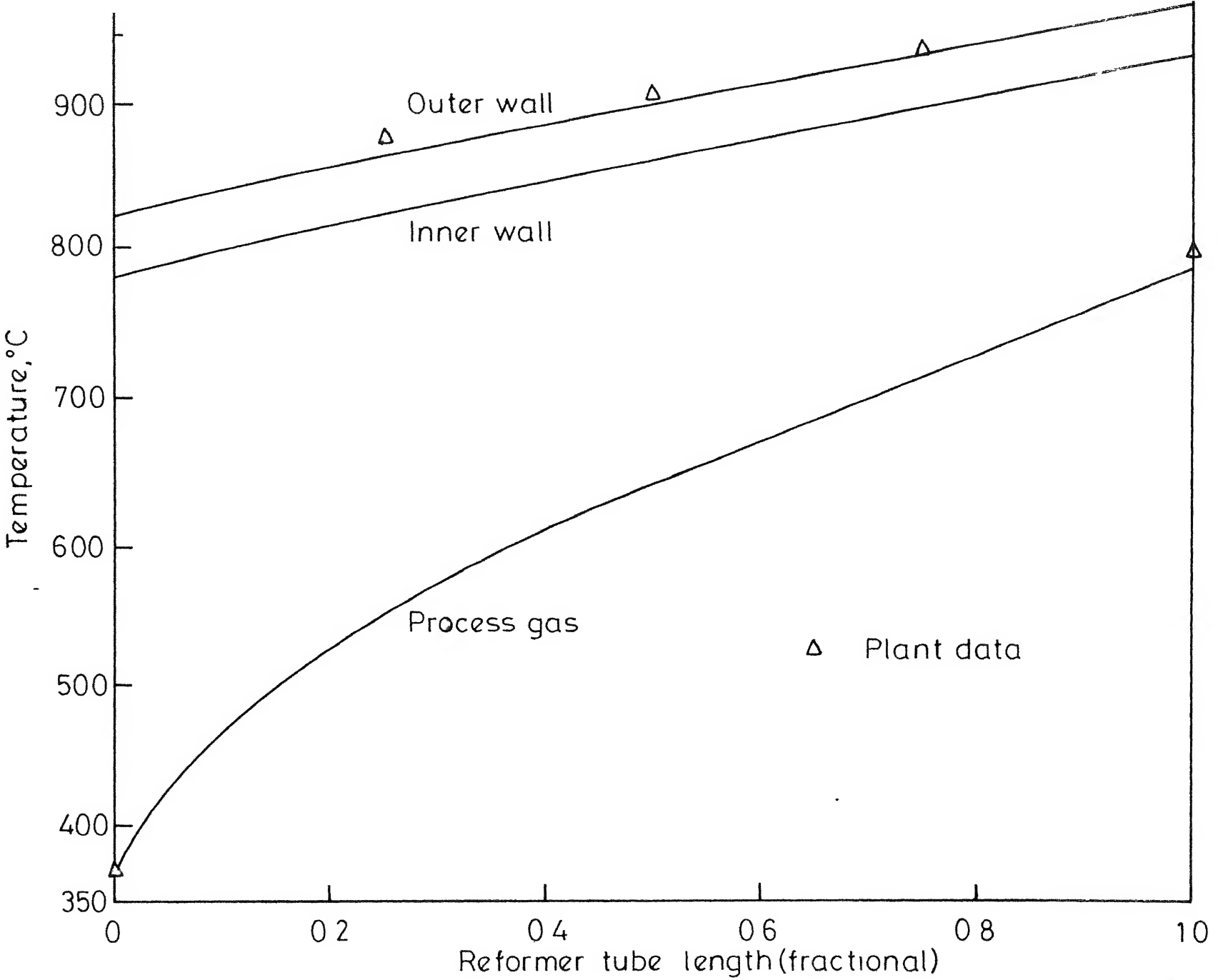
Outer wall
Inner wall
Process gas
Plant data
Temperature, °C
900
800
700
600
500
400
350
0
0 2
0 4
0 6
0 8
10
Reformer tube length (fractional)

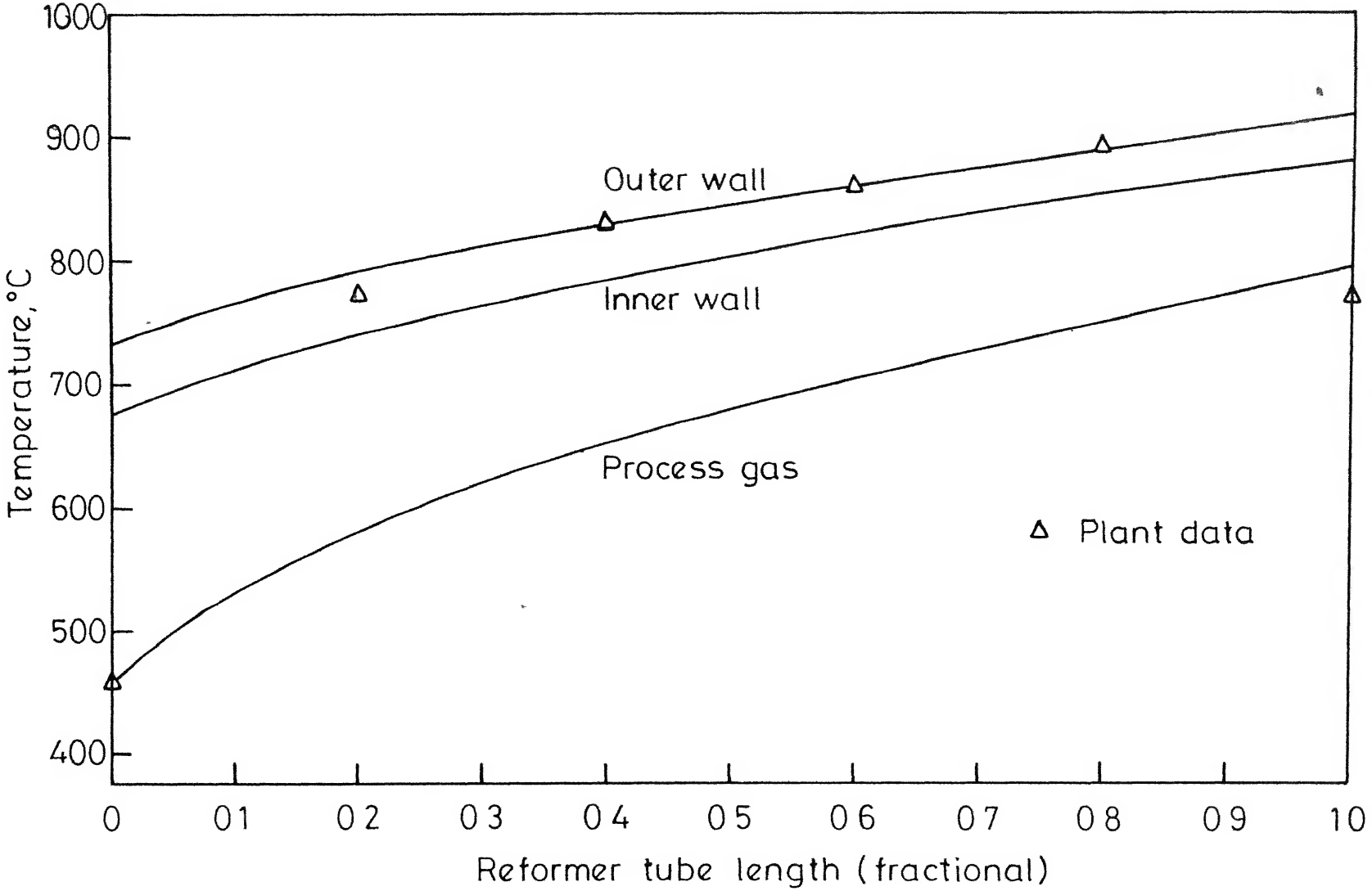

Fig 2·5 - Temperature profiles of process gas and reformer tube surfaces.
[Table 23, Case I]

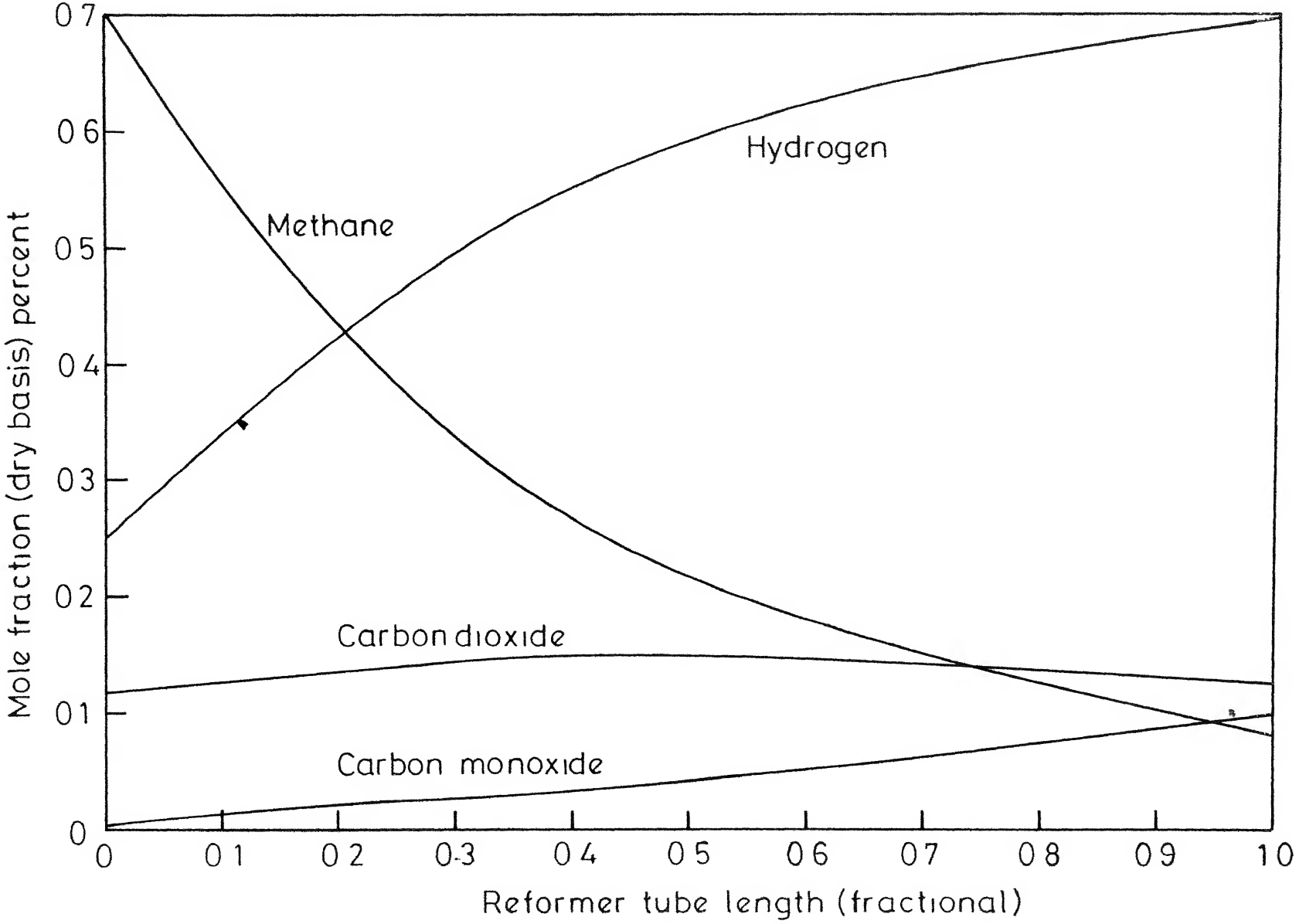

Fig 2·6 – Calculated concentration profile of component molecules in a

The heat transfer model is more accurately validated from the data on reformer tube outside wall temperature, at various points along the length, presented in Tables 2.1 through 2.3 and Figures 2.3 through 2.5. These figures show the calculated temperature profiles of tube wall surface and that of process gas along with measured values. The agreement is generally very good. However, the measured temperature near the inlet end (0.2 fractional length) is lower compared to the calculated value except in the case of short tube reformer (Table 2.2, Fig. 2.4). This could be because of the assumptions of uniform flue gas temperature and uniform distribution of burners throughout the wall. In actual practice the flue gas temperature at the outlet (reformer tube inlet end) is lower and less number of burner are used in this section. This effect is insignificant in the short tube reformer because of the smaller length which reduces the effect of a localized section.

In absence of any measurements of composition of process gas at various points inside the tube, a proper justification of reaction model is lacking. However, the close agreement between all the values measured with the corresponding calculated values is a reasonable justification of the validity of the reaction rate equations.

The results obtained do justify all the assumptions made to obtain the reaction rate and heat transfer models.

However, it should be noted that the accuracy achieved in the calculations is more because of the contradictory effects of various assumptions made rather than the correctness of any single assumption. For example, the number of burners used in middle section of the reforming furnace is generally more than those in the top or bottom sections. Therefore, the assumption of uniform distribution of burners over the walls leads to higher values of calculated heat transfer rates in the top and bottom sections and lower values in the middle section compared to the actual ones, whereas the neglect of end effects has just the reverse effect. Similarly the neglect of heat loss through the refractory walls and the heat effects associated with the conversion of higher hydrocarbons to methane have opposite heat effects.

2.2 SECONDARY REFORMER

The feed to secondary reformer consists of PR exit to which air is mixed. The SR feed condition is therefore dependent on the amount of air used. Too little air means insufficient nitrogen and unconverted methane while too much air leads to excessive temperature and excess nitrogen. The amount of air mixed should be such that at ammonia synthesis reactor inlet H_2/N_2 ratio is 3. Since a small per cent of methane remains unconverted, the H_2/N_2 ratio, based on 100 per cent conversion is, taken as 3.1. It is further assumed that no oxygen remains after combustion stage.

2.2.1 FEED CONDITION

Mixing of PR exit with air at SR inlet leads to adiabatic combustion of H_2, CO and CH_4 molecules in the gas. The rate as well as equilibrium for the burning (reaction with oxygen) of each of them is different and therefore for evaluating the exact composition of the product, all the combustion reactions should be considered in simultaneous equilibrium [14]. However, the rate at which hydrogen burns is much faster than the other two. Therefore, in this work, it has been assumed that the extent of combustion of CO and CH_4 is negligible compared to that of H_2. Close agreement was found between the combustion product temperature calculated on this basis

and that calculated by Davis and Lihou [14]. In this model the amount of air required is calculated as follows:

$$F^{o}_{air} = \frac{F^{o}_{CO} + F^{o}_{H_2} + 4\,F^{o}_{CH_4}}{3.1\,a_{N_2} + 2\,a_{O_2}} \qquad (2.28)$$

where F^{o}_{air}, F^{o}_{CO}, $F^{o}_{H_2}$ and $F^{o}_{CH_4}$ are the inlet rates of air, CO, H_2 and CH_4 respectively, Nm^3/hr and a_{N_2} and a_{O_2} are the mole fractions of N_2 and O_2 in air. Amount of H_2, N_2 and Ar in the combustion product are obtained from the following relations

$$F_{H_2} = F^{o}_{H_2} - 2\,a_{O_2} x\, F^{o}_{air} \qquad (2.29)$$

$$F_{N_2} = F^{o}_{air} x\, a_{N_2} \qquad (2.30)$$

and

$$F_{Ar} = F^{o}_{air} x\, a_{Ar} \qquad (2.31)$$

where F_{H_2}, F_{N_2} and F_{Ar} are the rates of flow of H_2, N_2 and Ar in the process gas after combustion is complete. Amounts of other components in the PR exit remain unaffected since they do not participate in the reaction with air.

Temperature of the process gas after combustion, and before it reaches SR catalyst bed, is calculated by equating the sum of sensible heats in air and PR exit and the heat from combustion to the sensible heat in combustion product. This is calculated by a trial and error procedure [21].

2.2.2 RATE EQUATIONS

As in PR, a nickel catalyst is used in this reactor also with the only difference that this catalyst is capable of standing relatively higher temperatures. The pair of equations used to describe the reactions is same as that for PR catalyst i.e.

$$CH_4 + H_2O \rightleftharpoons CO + 3H_2 \qquad (2.1)$$

$$CO + H_2O \rightleftharpoons CO_2 + H_2 \qquad (2.2)$$

The same kinetic expressions (Equations (2.7) and (2.8)) can also be used here. However, at the SR temperature condition, rate of reaction (2.1) is so fast that it could be assumed that the methane molecules hydrocrack instantaneously at the catalyst surface. The surface concentration of methane is, therefore, taken as that in equilibrium corresponding to catalyst surface temperature.

In such situations the rate of reaction is governed by the rate at which the reactant diffuses to catalyst surface from the bulk gas [34] which could be expressed as follows:

$$r_1 = K_m a_m (C_{CH_4} - C^s_{CH_4}) \qquad (2.32)$$

where C_{CH_4} and $C^s_{CH_4}$ are CH_4 concentrations in the bulk gas and at the surface respectively, Kg.mole/Nm^3; K_m is the mass transfer coefficient between bulk gas and solid surface, meters/hr. and a_m is the external surface area per unit mass

of the catalyst pellets, $m^2/Kg.$ of catalyst. $C^s_{CH_4}$ and the catalyst surface temperature, T^s are evaluated from an energy balance on the pellet which could be written, after proper manipulations and approximations [34] as follows

$$T-T^s = 0.7 \times (-\Delta H) \times \frac{(C_{CH_4} - C^s_{CH_4})}{C \cdot \bar{C}_p} \qquad (2.33)$$

where C is the total concentration of the process gas, $Kg.mole/m^3$. For the solution of above correlation, which involves trial and error solution, reaction (2.2) is assumed to be absent.

Rate of shift reaction is described by equation (2.8) i.e.

$$r_2 = \exp(-\frac{13880}{RT} + 8.23)\sqrt{P}\ (X_{CO} - \frac{X_{H_2} \cdot X_{CO_2}}{K_{eq_2} X_{H_2O}}) \qquad (2.8)$$

2.2.3 DESCRIPTION OF MATHEMATICAL MODEL

The basis of the mathematical model is a differential section of length dz, of the adiabatic catalyst bed. The assumptions and material, energy and pressure balance equations over this section are same as those for PR catalyst sections except that heat transfer term in equation (2.25) is zero. Equation (2.25) can be rewritten for this case as

$$\frac{dT}{dz} = \sum_{i=1}^{2} \left(\frac{-\Delta H_i}{\bar{C}_p}\right) \frac{r_i \rho_c}{G} \qquad (2.34)$$

Equations (2.8),(2.23), (2.24), (2.26), (2.32), (2.33) and (2.34) adequately describe the performance of SR adiabatic catalyst bed.

Simultaneous solution of equations (2.23), (2.24),(2.26) and (2.34), using Runge-Kutta method of fourth order [13], yields temperature, composition and pressure throughout the catalyst bed.

2.2.4 RESULTS AND DISCUSSION

The calculation results for three reformers are presented in Tables 2.4, 2.5 and 2.6. Figure 2.7 shows the variation of calculated temperature along the catalyst bed length alongwith the measured values at the inlet and exit (Table 2.4, Case I).

The calculated SR inlet temperature (after mixing with air) agrees well with those reported by Davies and Lihou [14] who have considered simultaneous combustion of H_2, CO and CH_4. It is to be noted that in the present calculations, combustion of only H_2 is considered being the fastest among the three. The calculated values also agree with the measured SR inlet temperatures which are available (Table 2.4). These agreements validate the assumptions made.

The agreement between measured and calculated composition and temperature for all cases, at the SR outlet, shows the correctness of the assumptions made in the calculation of steam-methane reaction over SR catalyst. However, the validity of the method of calculation cannot be ascertained because of lack of data on temperature or composition at intermediate points in the SR catalyst bed (Figure 2.7).

TABLE 2.4

CALCULATED AND EXPERIMENTAL DATA FOR SECONDARY REFORMER

Catalyst, tons	25.0
Diameter of catalyst filled space, meters	3.492
Height of catalyst bed, meters	1.62
Catalyst shape and size	Raschig rings 16x16x6 mm

	Case I		Case II	
Process Inlet:	Plant	Calculated	Plant	Calculated
Inlet process gas	Outlet from PR	Case I in Table 2.1	Outlet from PR	Case II Table 2.1
Air inlet rate, Nm^3/hr	22620	23247	20600	19523
Air inlet temperature, ^oC	231		231	
Temperature after mixing with air i.e. process gas inlet temperature, ^oC	1100	1096.6	1121	1092.4
Pressure, Kg/cm^2	21.6		21.4	
Process Outlet:				
Dry gas flow, Nm^3/hr	84000	86257	74000	71649
Steam, Kg/hr	47500	47935	40800	39783
Pressure, Kg/cm^2	21.1	21.1	21.0	20.9
Temperature, ^oC	905	902.3	925	905.4
Dry Gas Composition, Mole per cent:				
CO	13.36	13.18	14.1	13.36
CO_2	15.06	12.75	12.8	12.42
H_2	52.26	52.13	50.9	52.26
CH_4	0.36	0.34	0.1	0.29
N_2	20.73	21.34	21.9	21.42
Ar	0.20	0.26	0.2	0 25

TABLE 2.5

CALCULATED AND EXPERIMENTAL DATA FOR SECONDARY REFORMER

Catalyst weight, tons				2.86	
Catalyst volume, m^3				2.49	
Catalyst shape and size				Raschig rings, 18x18x6 mm	
Process Inlet:					
Dry gas flow, Nm^3/hr				11900	
Dry gas composition, mole per cent	CO	CO_2	H_2	CH_4	
	6.24	14.28	70.99	8.49	
Steam, kg/hr	7860				
Pressure Kg/cm^2	16.8				
	Experimental		Calculated		
Air flow rate, Nm^3/hr	4060		4023		
Air inlet temperature, °C	108				
Process Outlet:					
Dry gas flow, Nm^3/hr	1354		1309		
Steam, Kg/hr	19520		19800		
Pressure, kg/cm^2	16.2		16.2		
Temperature, °C	876		868		
Dry Gas Composition (mole per cent):					
CO	8.98		9.10		
CO_2	11.37		11.27		
H_2	57.73		57.45		
CH_4	0.33		0.38		
N_2	21.26		21.56		
Ar	0.27		0.24		

TABLE 2.6

CALCULATED AND EXPERIMENTAL DATA FOR SECONDARY REFORMER

Catalyst, tons	14.83
Diameter of catalyst filled space, m	3.192
Height of catalyst bed, m	1.56
Catalyst shape and size	Raschig rings, 16x16x6 mm

Process Inlet:	Case I		Case II	
	Plant	Calculated	Plant	Calculated
Inlet process gas	Outlet from PR Table 2.3 Case I		Outlet from PR Table 2.3 Case II	
Air inlet rate, Nm^3/hr	24300	23831	21000	20753
Air inlet temperature, ^oC	460		460	
Temperature after mixing with air i.e., process gas inlet temperature, ^oC		1179		1140
Pressure, kg/cm^2	30.9		28.4	
Process Outlet:				
Dry gas flow, Nm^3/hr	85300	84493	72500	72983
Steam, Kg/hr	47500	48234	42800	43836
Pressure, kg/cm^2	30.2	30.4	28.0	28.3
Temperature, ^oC	962	957	932	927
Dry Gas Composition, Mole per cent:				
CO	12.20	11.96	12.40	12.52
CO_2	9.40	9.44	9.60	9.26
H_2	55.58	55.73	55.37	55.43
CH_4	0.32	0.34	0.33	0.33
N_2	22.11	22.26	22.10	22.
Ar	0.38	0.27	0.40	0.36

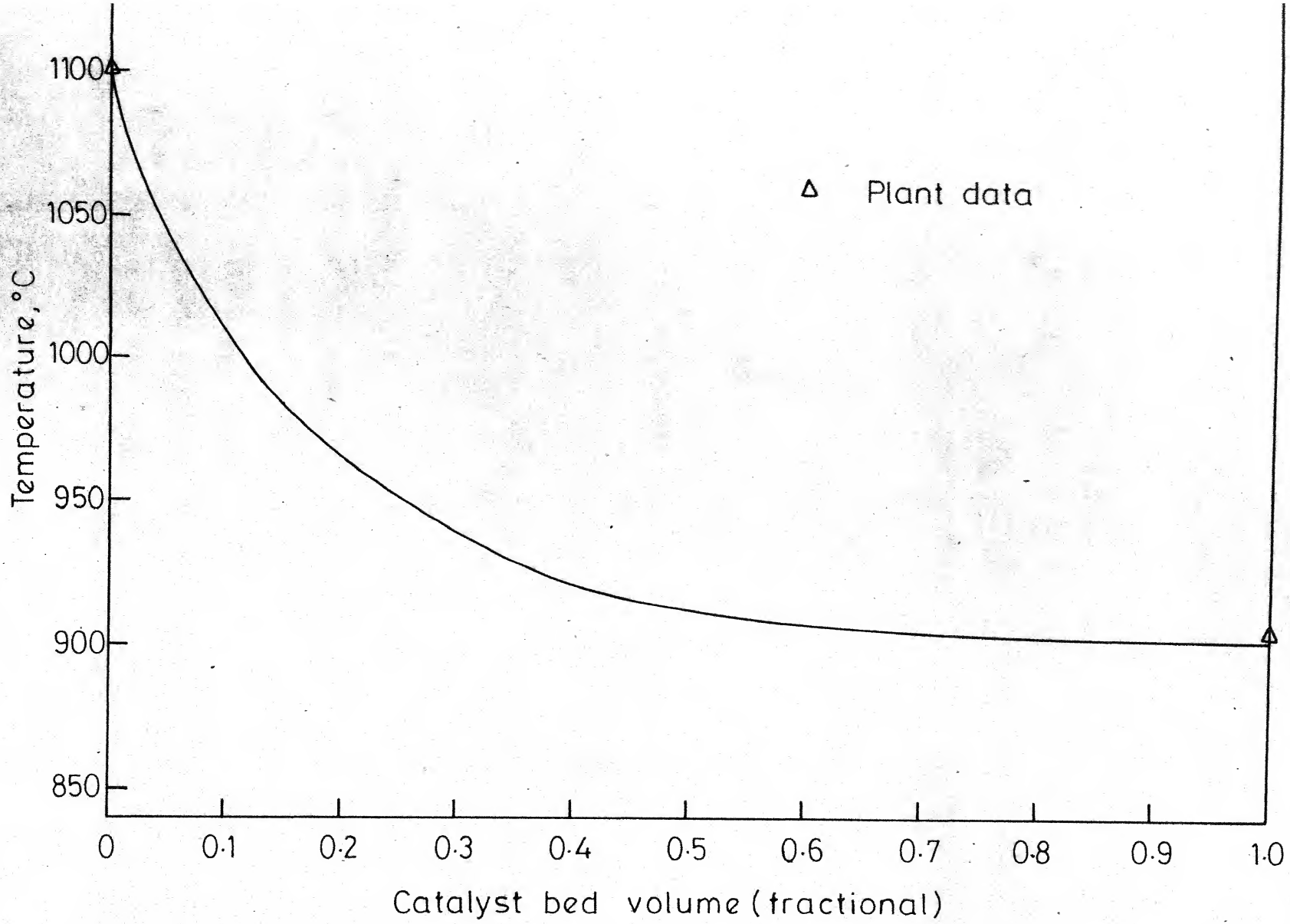

Fig. 2·7 - Temperature variation in SR catalyst bed. [Table 2·4, Case I]

NOMENCLATURE

A	Surface area, m^2
a	Pre-exponential factor
a_m	External surface area per unit mass of catalyst, m^2/Kg. of catalyst
a_{O_2}, a_{N_2}, a_{Ar}	Mole fraction of O_2, N_2, Ar in air respectively
$\bar{C}_p$	Average specific heat capacity of process gas, K.Cal/Kg.$^{\circ}$C
C_{CH_4}	Concentration of methane, Kg.mole/Nm^3
D	Diameter, meter
E	Emissive power, K.Cal/m^2.hr
E_a	Apparent energy of activation, K.Cal/Kg.mole
F_{Ar}, F_{H_2}, F_{N_2}	Flow rate of air, Ar, H_2, N_2 respectively, Nm^3/hr
F_{Rt}	View factor of reformer tube surface with respect to refractory wall surface
G	Mass velocity, Kg./m^2.hr
g	Mass fraction
$\triangle H$	Heat of reaction, K.cal/kg.mole
h	Heat transfer coefficient, K.Cal/(m^2.$^{\circ}$C.hr)
K	Conductivity, Btu/(m.$^{\circ}$K.hr)
K_{eq}	Equilibrium constant
k_g	Absorption coefficient of gas
K_m	Mass transfer coefficient, meters/hr.
L	Length of a reformer tube, meters

L_m Mean beam length, meters

M Molecular weight

N_B Number of burners

N_t Number of tubes

P Total pressure, atms.

p Partial pressure, atms

$\dot{Q}_{g \rightleftharpoons t}$ Rate of total heat transfer from furnace gas to reformer tubes, K.Cal/hr.

$\dot{q}_{f \rightleftharpoons t}$ Rate of heat transfer from flames to unit area of tube surface, K.Cal/(m^2.hr)

q Rate of heat transfer per unit area of reformer tube surface, K.Cal/m^2.^oK.hr.

R Gas constant

r Rate of reaction, Kg.mole/Kg.of catalyst.hr

T Temperature, ^oK

v Void fraction

x Mole fraction

y A variable

dz Integration step size

$a_{g,n'}$, $b_{1,n'}$, $b_{2,n'}$, $k_{g,n}$ Constants

μ Viscosity, Kg/m.hr

ε Emissivity

ρ Density, Kg/m^3

ρ_c Bulk density of catalyst, Kg/m^3

ξ Extent of reaction

α Stoichiometric coefficient

Subscripts

1 Reaction 1

2 Reaction 2

i Reaction i

j Component j

f Flames

g Gas

R Refractory wall

t Reformer tube

o Outside wall of reformer tube

in Inside wall of reformer tube

Superscript

o Inlet condition

s Catalyst surface condition

REFERENCES

1 Akers, W.W. and Camp, D.P., AIChEJ, 1, 471 (1955).

2 Allen, D.W., Gerhard, E.R. and Lıkıns, Jr., M.R. I and EC Proc. Des. Dev., 14, 256 (1975).

3 Atroshenko, V.I. and Bıbr, B., J. Appl. Chem. USSR p. 102((1959).

4 Beek, J., 'Advances ın Chemıstry ın Chemical Engıneerıng' Academıc Press, New York, 1962.

5 Beskov, V.S., Intl.Chem. Engg., 5, 201 (1965).

6 Bhatta, K.S.M. and Dixon,G.M., Trans. Farad.Soc. 63, 2217 (1967).

7 Badrov, I.M., Apel'baum, L.O. and Tımkın, M.I., Kınet. Katal. 8, 821, (1967).

8 Bodrov, I.M., Apel'baum, L.O. and Tımkin, M.I., Kinet. Katal., 9, 1065 (1968).

9 Bohlbro, H., J.Catalysis, 3,207 (1964).

10 Bortolını, P., Chem.Eng.Sci., 9, 135 (1958).

11 Bridger, G.W., Chem. and Proc. Engg. 53, 38 (1972).

12 Bridger, G.W., and Wyrwas, W., Chem. and Proc. Engg. 48,101 (1967).

13 Carnahan, B., Luther, H.A. and Wılkes, J.O., 'Applied Numerıcal Methods' John Wıley and Sons Inc., 1969.

14 Davıs, J. and Lıhou, D.A., Chem. and Proc. Engg. 52, 71 (1971).

15 Ergun, S., Chem.Eng. Prog. 48, 89 (1952).

16 Ganderton, R., Godfrey, K.R. and Finkelstein, L., Measr. Contl., 3, T73 (1970).

17 Ghoshal, S R., Roy, D. and Dutta, B.K., Technol. 1(4) (1964).

18 Goodridge, F. and Quazi, H.A., Trans. Inst. Chem. Engrs., 45, T274 (1967).

19 Haldor Topsoe, 'Some Aspects of Catalytic Cracking', Communication 698, The Institution of Gas Engineers, 31st Autumn Research Meeting, Nov. 1965.

20 Hottel, H.C. and Sarofim, A.F., 'Radiative Transfer', McGraw Hill, New York, 1967.

21 Hougen, O.A., Watson, K.M. and Ragatz, R.A., 'Chemical Process Principles' Part I, John Wiley and Sons Inc., 1954.

22 Hulburt, H.M. and Srinivasan, C.D., AIChEJ, 7, 143 (1961).

23 Hyman, M.H., Hydro. Proc., 47, 131 (1968).

24 Malik, R.K., M.Tech. Thesis, I.I.T., Kanpur, 1973.

25 Mars, P., Chem. Eng. Sci., 14, 375 (1961).

26 McAdams, W.H., 'Heat Transmission' (3rd Edition), McGraw Hill, New York, 1954.

27 McGreavy, C. and Newmann, M., 'Development of a Mathematical Model of a Steam Reformer', Instn. Electrical Engineers Conference on the Industrial Applications of Dynamic Modelling, Durham, September 1969.

28 Moe, J.M., Chem. Eng. Prog., 58, 33 (1962).

29 Moe, J.M. and Gerhard, E.R. 'Chemical Reaction and Heat Transfer Rates in the Steam Methane Reaction' AIChE Symposium, Fiftysixth National Meeting, SanFrancisc Calif. May 1965.

30 Roesler, F.C. Chem. Eng. Sci., 22, 1325 (1967).

31 Ruthven, D.M., Canadian J. Chem. Engg. 47, 327 (1969).

32 Schnell, C.R., J. Chem. Soc. (B), 1. 158 (1970).

33 Singh, C.P.P. and Saraf, D.N., I and EC, Proc. Des. Dev. 313, 16 (1977).

34 Smith, J.M.,'Chemical Engineering Kinetics', IInd Ed., McGraw Hill Book Company, 1970.

35 Taylor, P.B. and Foster, P.J., Int. J. Heat Mass Transfer, 17, 1591 (1974).

36 Yen, I. Kuan, Chem. Eng. 173-176 (March 13, 1967).

means low carbon monoxide content in the exit gas.

Some of the old units have only high temperature shift reactors. Multiple beds with interstage cooling are used with progressively lower temperatures in the subsequent beds. However, the lowest temperature has to be kept high enough in order that the HT catalyst is still effective. Current practice is to provide an LT reactor in conjunction with a single bed HT reactor. Use of LT reactors has several advantages [16]. Very low (< 0.2 per cent) concentration of carbon monoxide in the exit from LT can be attained. With such low concentration of CO, methanation catalyst can conveniently be used for removal of last traces of carbon monoxide and dioxide without involving high purge loss.

3.1 HIGH TEMPERATURE WATER-GAS SHIFT REACTOR (HT)

For reaction over HT catalyst (chromia promoted iron oxide) some workers propose a first order [3,26,28] or a second order [29,31] rate equation to explain the conversion but many others [4-6,8.9,15,20,22-25, 32, 37] propose different rate equations. Each of the latter rate equations is of complex order and different from those proposed by others. It has experimentally been observed that catalysts of different manufacturers give different rate equations even under identical conditions [15]. The specific surface area of the catalyst is reduced considerably during use due to sintering [18] and the surface composition of the catalyst changes depending on the composition of the reacting gases which are a mixture of oxidizing and reducing gases. All these may help in qualitatively explaining the difference in rate equations obtained by different workers but it is not very useful in getting a general rate equation which is not available in literature. So in this work the approach is to start with a rate equation which explains the conversion under some constraints. Each of these constraints are subsequently eliminated, one at a time, by introducing suitable correction terms. These are mostly empirical correlations obtained from experimental results of different workers on the same catalyst.

3.1.1 DEVELOPMENT OF THE RATE EQUATION

The rate equation most frequently referred to in literature is first-order or pseudo-first order in carbon monoxide concentration or partial pressure [3,26,28] and all attempts to correlate the rate data by power function models give reaction rates which are almost consistently first order with respect to partial pressures of carbon monoxide [5,8,15]. So a first order rate equation of the form given by equation (3.2) has been selected.

$$r = k' (P_{CO} - P^*_{CO}) \qquad (3.2)$$

where, r = rate of reaction, cc/hr.gm. of catalyst,

k' = rate constant, cc/hr. gm. of catalyst. atms.,

P_{CO} = partial pressure of CO, atms. and

P^*_{CO} = partial pressure of CO in equilibrium conditions, atm

It is noted that this rate equation has been used under low pressures (of the order of 1 atmosphere), high steam to carbon monoxide ratio and below a temperature of 500°C. In commercial reactors latter two conditions are met but the operating pressure is generally high (15 to 30 atms). So the above rate equation is used at a constant pressure of 1 atmosphere, and the variation in pressure is accounted for separately. At one atmosphere pressure, equation (3.2) can be written as

$$r = k (x_{CO} - x^*_{CO}) \qquad (3.3)$$

where, k = rate constant, cc/hr. gm. of catalyst,

x_{CO} = mole fraction of CO,

x^*_{CO} = mole fraction of CO in equilibrium conditions

$$= \frac{x^*_{H_2} \times x^*_{CO_2}}{x^*_{H_2O} \times K_{eq}}$$

and K_{eq} = equilibrium constant

The rate constant, k is generally expressed in the form of Arrhenius Equation as

$$k = a\ e^{-E/R_g T} \qquad (3.4)$$

where, a = pre-exponential factor, cc/hr. gm. of catalyst

E = activation energy, cals/gm.mole ^oK,

R_g = universal gas constant, cals/gm. mole ^oK, and

T = absolute temperature, ^oK

The value of activation energy, E, to be used in this equation is reported from 13,000 to 32,000 cal/gm mole [12, 15, 21,30] but mostly it lies in the range 21.4 to 27.3 Kcal/gm mole [35]. For the present catalyst (of P and D, FCI) the value of E is calculated as follows:

A pilot plant study using pellets of this catalyst and feed gas containing high CO content (40.6 per cent, dry basis) is reported in literature [13]. In this, the calculated value of energy of activation for the catalyst without taking into account any mass or heat transfer resistance between the

bulk gas and catalyst pores i.e. the apparent energy of activation for the catalyst pellets, is

$$E' = 13.88 \text{ Kcal/gm mole} \qquad (3.5)$$

For commercial shift reactor operating conditions, heat transfer and the external mass transfer resistances may be considered insignificant but the intra-pellet mass transfer resistance is very high [28]. In such a case, the true energy of activation, E, can be taken as twice the apparent energy of activation, E' [36]. Therefore,

$$E = 2E' = 27.76 \text{ Kcal/gm mole} \qquad (3.6)$$

In the above evaluation any temperature difference between the catalyst pellets and the bulk gas or between different points in a catalyst pellet has been taken to be insignificant. The close agreement in value of E thus obtained and those reported by different workers [14,21,35] who used small [$<$ 1 mm size] catalyst particles, lower pressures and lower CO concentrations in their studies, suggests that it is so. However, if some temperature difference exists, its effect is absorbed in the rate equation and hence need not be considered separately.

The pre-exponential factor, a, is not a constant. It depends on temperature because the specific surface area varies with temperature [18]. In this work, a has been

evaluated at a temperature of 350°C by equating experimentally determined intrinsic rate constant [33] to that given by equations (3.4) and (3.6). This value of

$$a = 2.865 \times 10^{13} \text{ cc/hr gm. of catalyst} \quad (3.7)$$

has been used throughout this work.

Error incurred in the calculation of a catalyst pellet activity due to taking a constant value of a is corrected for temperature as discussed in the section dealing with catalyst age. From equations (3.3), (3.4), (3.6) and (3.7) the intrinsic rate of reaction for the catalyst is given by,

$$r = 2.865 \times 10^{13} \exp\left(\frac{-27760.0}{R_g T}\right) \times (x_{CO} - x^*_{CO}) \quad (3.8)$$

Rate of reaction for the pellet is obtained by incorporating the effects of diffusional resistances, age of the catalyst, pressure and H_2S concentration in the reacting gases. These factors have been discussed in the above order in the following paragraphs.

(a) Diffusional Resistances:

As mentioned earlier only intra-pellet diffusional resistance is to be considered. This can be done by using a suitable effectiveness factor. For calculating effectiveness factor, catalyst pellets have been considered to be isothermal[10 and Wheeler's method [42] has been used. This gives

Effectiveness factor,

$$Eff = \frac{\tanh h}{h} \tag{3.9}$$

where,

$$h = L\sqrt{\frac{2k}{r_o D_e}}, \tag{3.10}$$

$$L = \sqrt{2}\,\frac{V_P}{S_x}, \tag{3.11}$$

$$D_e = \frac{1}{1/D_k + 1/D_B} \tag{3.12}$$

V_P = volume of the catalyst/pellet,

S_x = external surface area/pellet,

r_o = pore radius,

D_e = effective diffusivity,

D_B = bulk diffusivity and

D_k = Knudsen diffusivity

It has been shown [28,33] that for the shift catalysts at low pressure, Knudsen diffusion is the controlling mode of diffusion. So a method based on pore size distribution has been used. This method as well as the pore size distribution for the catalyst is reported elsewhere [33]. In this method effectiveness factor, $Eff(r_o)$ corresponding to different pore sizes (r_o) is calculated. This is multiplied with the total surface for the pore size, A_p. This gives the effective surface area

$$A_e = Eff\ (r_o) \times A_p$$

corresponding to pore size, r_o. A_e is calculated for values of r_o in the range of 90 to 250°A, which accounts for ninety per cent of the total surface area. Now effectiveness factor is calculated at one atmosphere from the following relation

$$\text{Eff} = \frac{\text{Total effective surface area}}{\text{Total pore area}}$$

$$= \frac{\sum_{r_o=90}^{250^\circ A} A_e}{\sum_{r_o=90}^{250^\circ A} A_p} \qquad (3.13)$$

(b) Age of the Catalyst:

A catalyst on-stream continuously loses its activity with time at a rate which depends on the operating conditions to which it is subjected. Above 500°C this loss in activity in the case of a shift catalyst corresponds to the loss in specific surface area, A. A is expressed in terms of the operating temperature, T, and the age of the catalyst, τ, as [18]

$$\frac{1}{A^n} - \frac{1}{A_o^n} = K_S \tau \, e^{-E_S/R_g T} \qquad (3.14)$$

where, A_o = specific surface area of a fresh catalyst,

K_S = a constant and

E_S = activation energy of sintering.

For large values of τ, this is reduced to a simpler form:

$$A = K_S^{-1/n} \times \tau^{-1/n} \times \exp(E_S/R_g T) \qquad (3.15)$$

The above equations show that the surface area for a given process time, τ, decreases with increase in temperature and for large process time (τ) (i.e. when eqn.3.15 holds) the variation in area is small for large variations in τ since n lies between 6.2 to 7.3. But the shift-converters are operated below 500°C where the correspondence of A to catalyst activity does not hold. The actual loss in catalyst activity is much more than the loss of surface area [13,28]. This has also been pointed out in the original work [18] on reduction in surface area due to sintering. Therefore, an empirical correlation has been obtained, which is based on a study of the quantitative variation in the activity of pellets of this catalyst with temperature and time [13]. A typical curve of catalyst activity vs time, from this study, at any particular temperature shows (Figure 3.1) that the activity falls very sharply in the initial stages. Then almost abruptly, the rate of fall in activity is reduced to a very low value. The activity of the catalyst at the turning point M has been compared with those calculated from intrinsic rate constant[33] for the catalyst reduced at the temperature for which the curve PML containing M has been obtained. Both these values turn out to be equal within the range of experimental accuracy. This implies that point M's on activity curves for different

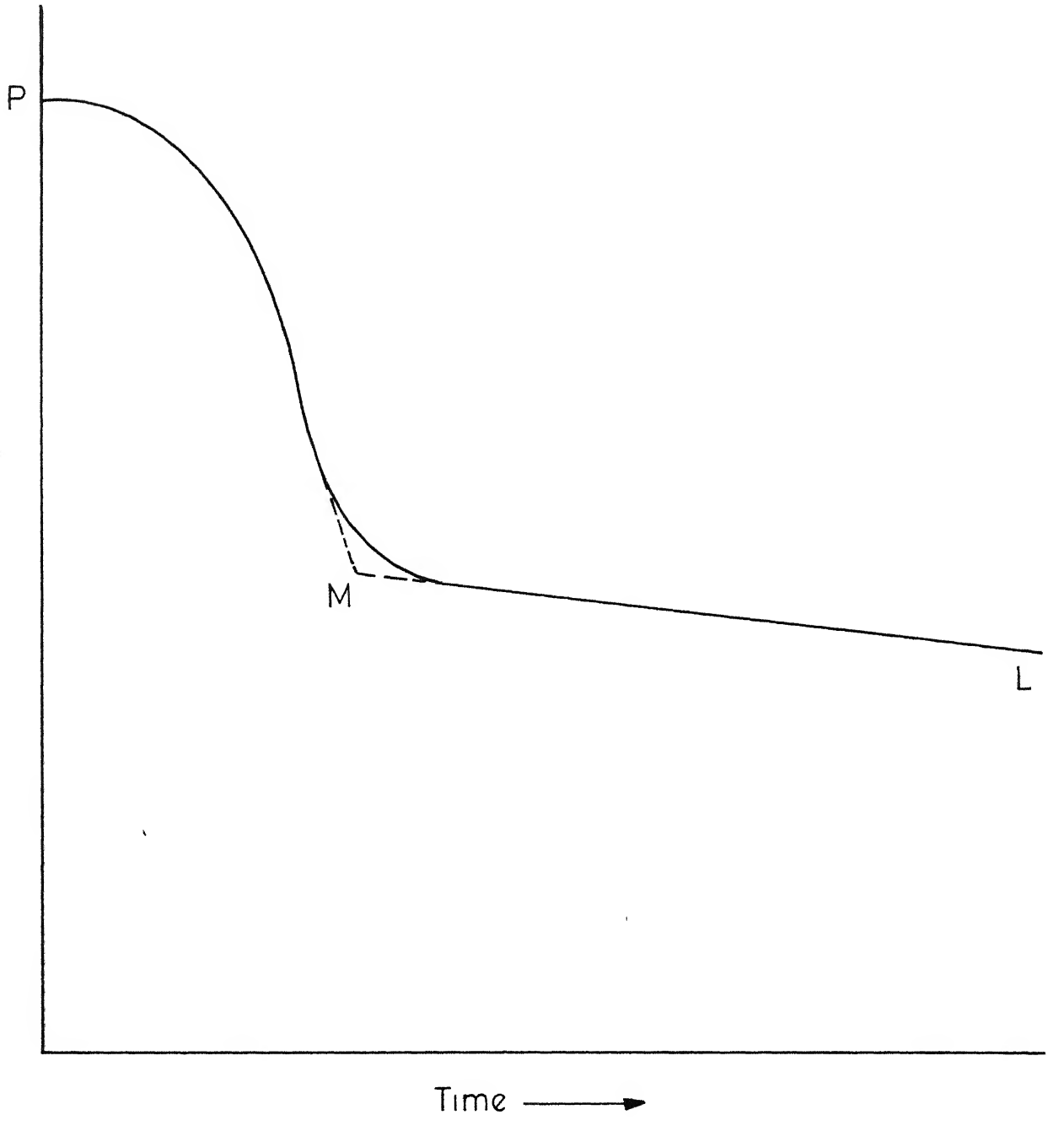

Fig 3 1 - A typical curve of variation in catalyst activity with time at constant temperature

temperatures represent the activities of the catalyst completely reduced at respective temperatures. Here, catalyst activity is considered only after it has completely been reduced i.e. the sharp fall period is not considered. There is not much loss of generality due to this since the catalyst at best takes a few days to steady its rate (i.e. to reach M) whereas the total estimated life of the catalyst is three years.

As the activity of a reduced catalyst is a function of the reduction temperature, a correlation of the relative activities of the catalyst pellets reduced at different temperatures is required. Relative activity ($R_a(T)$) has been defined as

$$R_a(T) = \frac{\text{Activity of a catalyst pellet reduced and working at } T^\circ K}{\text{Activity of the same catalyst reduced at a standard temperature } T_s \text{ and working at } T^\circ K} \qquad (3.16)$$

Taking standard temperature $T_s = 623.2^\circ K$ ($350^\circ C$),

$$R_a(T) = \frac{\text{Activity represented by M for } T^\circ K}{\text{Eff} \times 2.865 \times 10^{13} \times \exp\left(\frac{-27760}{R_G\, T}\right)} \qquad (3.17)$$

This relation gives $R_a(T)$ for different values of T. To correlate $R_a(T)$ with T, an exponential decrease in catalyst activity with increase in reduction temperature (as in Eqn.3.15) has been assumed as a first approximation i.e.

$$R_a(T) = \frac{\exp\ (C/T)}{\exp\ (C/T_S)} = \exp\ [C(1/T-1/T_S)] \qquad (3.18)$$

A plot of $-\ln R_a$ vs T gives a straight line. This validates the assumption and gives

$$R_a(T) = \exp\ (-10.831 + 6750/T) \qquad (3.19)$$

It is to be noted that one needs to consider the activities of only those catalyst pellets which are reduced at operating temperature, since one cannot do otherwise but to assume that in a converter the catalyst pellets are reduced at the operating temperatures only. In the present work the possibility of it being subjected to a higher temperature, for a period long enough to reduce it (even partially) at that temperature is not considered.

Now one can find out the activity of a reduced catalyst pellet at atmospheric pressure and any temperature (i.e. M) from Equations (3.8), (3.13) and (3.19). Any further fall in catalyst activity (i.e. along ML) with respect to T and τ can be expressed in terms of another factor (aging factor) which has been correlated as

$$\log_{10} A_{gf} = (14.66 \times 10^{-4} - 2 \times 10^{-6} \times T) \times \tau \qquad (3.20)$$

from data obtained from the same study [13] referred above.

(c) Pressure:

All investigators [3,8,12,29] but one [38] have reported that the rate of reaction increases with increase in pressure. In an investigation over the catalyst [12] the ratio by which the rate increases has been related to pressure as

$$\text{Pressure factor, } P_f = P^{(0.5 - P/250)} \qquad (3.21)$$

This is in very close agreement with results of others [3,29].

(d) H_2S Concentration:

The activity of an iron-oxide catalyst (HT . shift catalyst) is reduced by the presence of H_2S in the reacting gases due to reversible poisoning of the catalyst. The extent of the reduction in catalyst activity depends on the concentration of H_2S in the reacting gases. Many workers [7,8,28,38] have studied this effect quantitatively. The one reported for this catalyst [7] has been used to correlate the reduction in activity with H_2S concentration (in ppm) as

$$f_S = -0.276 \log_{10}([H_2S] + 2.78) + 1.127 \qquad (3.22)$$

where f_S stands for the factor by which the rate is reduced and $[H_2S]$ represents concentration of $[H_2S]$ in ppm.

Now the final rate equation can be written as,

$$r = Eff \times 2.865 \times 10^{13} \times \exp\left(\frac{-27760}{R_g T}\right) \times R_a \times A_{gf} \times P_f \times f_S \times (x_{CO} - x^*_{CO}) \qquad (3.23)$$

which gives the rate of reaction over the pellets of the catalyst, whose specifications are given below, under all operating conditions which may exist in any commercial HT shift converter.

Catalyst specification	Fresh	Reduced at 350°C
Chemical composition		
Fe_2O_3	72 per cent	
Cr_2O_3	8 per cent	
Real density, gm/cc		4.561
Density of the pellet, gm/cc		2.225
Specific surface area, m^2/gm	47.4	31.2
Porosity:		
$<$ 200 °A		0.2436 cm^3/gm
200 °A-75,000°A		0.0818 cm^3/gm
$>$ 7500 °A		0.0019 cm^3/gm
Total porosity	0.2901 cm^3/gm	0.3273cm^3/gm

3.1.2 DESCRIPTION OF THE MATHEMATICAL MODEL

The following mathematical model has been developed for a high-temperature shift reactor which may have single or

multiple adiabatic beds of catalyst with interstage cooling. One such reactor having three adiabatic beds with interstage cooling is shown in Figure 3.2.

Uniform distributionof temperature and composition throughout a general cross-section of the catalyst bed has been assumed and axial diffusion of mass and heat has been neglected. With these assumptions the material and energy balance equations which describe the composition and temperature of the reaction system along an adiabatic catalytic layer can be written as

$$\frac{d\xi}{dv} = \frac{r'}{G} \tag{3.24}$$

$$\frac{dT}{dv} = \frac{-\Delta H}{\bar{C}_p} \times \frac{r'}{G} \tag{3.25}$$

$$\xi = \frac{x_1 - x_1^o}{\alpha_j} \quad \text{for } j=1,\ldots 4 \tag{3.26}$$

where v = volume of catalyst

G = volume flow rate

r' = reaction rate,

ΔH = heat of reaction,

$\bar{C}_p$ = average specific heat of reacting system

x_j, x_j^o = mole fraction of component j at any point and the entrance respectively, and

α_j = stoichiometric coefficient of j, with a negative sign when it is a reactant.

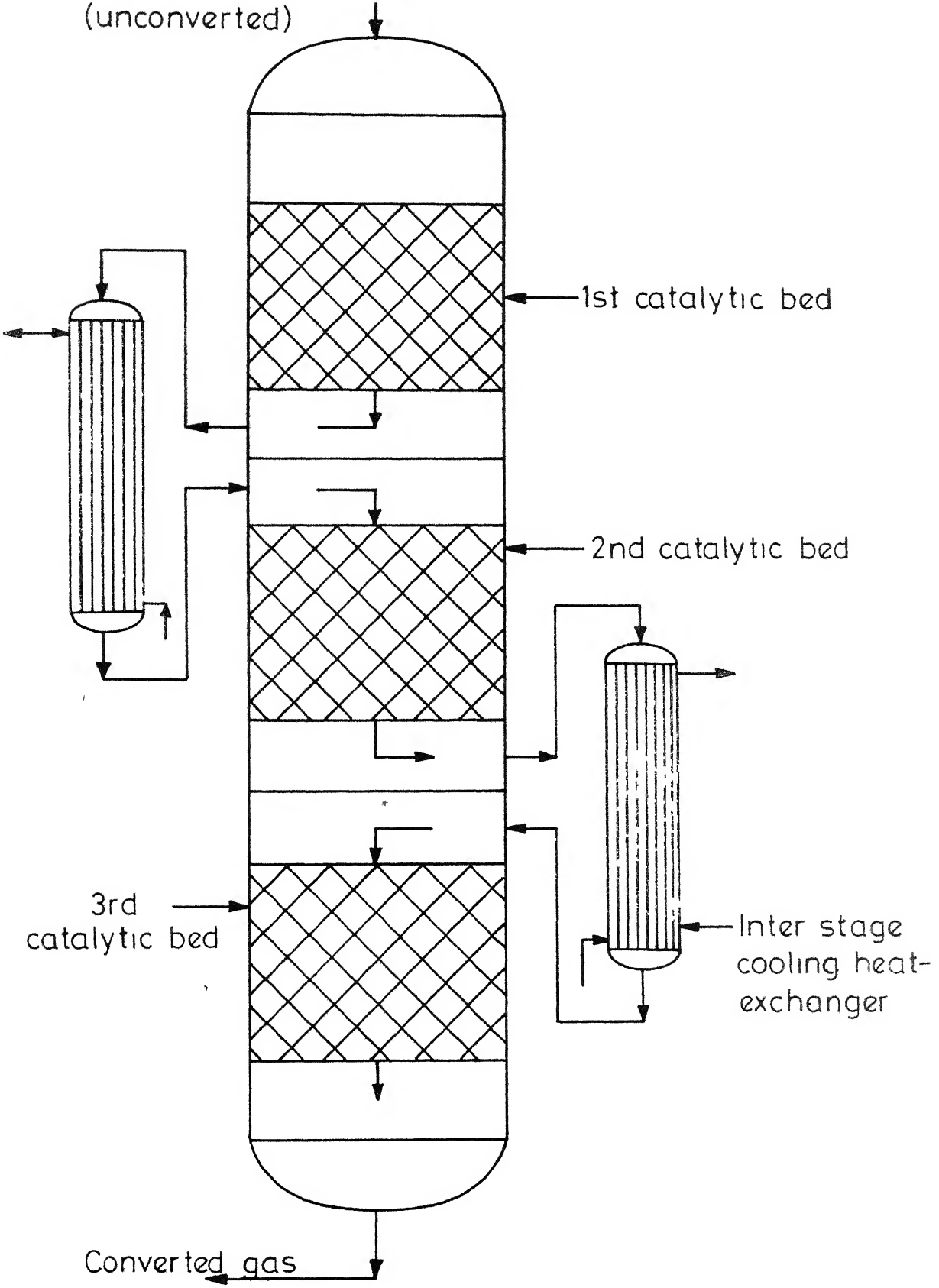

Fig 3 2 - Triple adiabatic bed reactor with interstage cooling

Since the reaction takes place at a moderately high pressure, reacting gaseous system can not be considered ideal. So the pressure dependence term has been included in the expression for specific heat [19] of each component using data [17] on different pressures (1-40 atms). The standard heat of reaction at 25°C and 1 atm pressure has been calculated from the heat of formation data [19] which has then been generalized for calculations at higher temperatures and pressures [17].

The composition and temperature of the reacting system at the inlet of any layer being known, the material balance equation (3.24) is solved to obtain the extent of reaction which in turn gives the mole fraction of individual components (eqn. 3.26). Solution of the energy balance equation (3.25) gives the outlet temperature. Runge Kutta method of fourth order [11] has been used for the simultaneous solution of mass and energy balance equations. The size of the integration step has been varied according to the volume of the catalyst used.

Calculation Program:

On the basis of the mathematical model described in the previous paragraph, a calculation program in Fortran IV has been prepared for IBM 7044 computer. The calculation time for checking the performance of a triple-bed reactor with

interstage cooling is 53 seconds when the step size for each bed is 1/100th of the bed volume. This program has been used only for checking the performance of shift reactors but it can conveniently be used for design purposes as well.

3.1.3 RESULTS AND DISCUSSION

The calculation results for five different units having single or multiple beds and working under different conditions of temperature (603 to 744°K), pressure (16.4 to 30 Kg/cm^2), composition of the reacting system (CO - 9.0 to 40.6 per cent), catalyst life (60 to 560 days), H_2S concentration (less than 0.5 to 60 ppm) and steam to CO ratio (5 to 21.7) are presented along with the plant data in Tables 3.1 to 3.4 and Figures 3.3 to 3.5.

For the purpose of discussion the reactors are considered separately (based on number of catalyst beds).

Triple Bed Reactor: The maximum difference in concentration of CO calculated from that measured exists at the outlet from 1st bed (Table 3.1, Fig. 3.4). Based on the model, the volume of catalyst in 1st bed required for the measured conversion (14.2 per cent of CO, dry basis) is 7 per cent less than the actual volume. Generally the experimental error upto ± 5 per cent is allowed. The result is slightly beyond that limit. But this would be of much less significance if the error in double bed reactor, to be discussed next, is considered.

TABLE 3.1

EXPERIMENTAL AND CALCULATED DATA FOR A TRIPLE BED HT REACTOR

Inlet dry gas flow rate, Nm^3/hr	17830.0
Inlet steam to gas ratio, S/G	1.07
Pressure, Kg/cm^2	29
Age of catalyst, days	270
H_2S, ppm	60

Bed	I			II			III		
Volume of catalyst, m^3	4.36			8.52			8.52		
Composition of gas, percent (dry basis)	Inlet	Outlet Cal.	Outlet Exptl.	Inlet	Outlet Cal.	Outlet Exptl.	Inlet	Outlet Cal.	Outlet Exptl.
CO	40.6	13.21	14.2	13.21	4.99	4.8	4.99	3.6	3.6
CO_2	3.2	22.06	23.0	22.06	27.75	29.4	27.75	28.69	30.0
H_2	53.2	62.32	59.6	62.32	65.03	63.1	65.03	65.50	64.6
CH_4	0.4	0.32	3.2	0.32	0.30	2.7	0.30	0.30	1.8
N_2+Ar	2.6	2.09		2.09	1.93		1.93	1.91	
Temperature, °C	351.0	471.1	460.0	400.00	447.3	459.0	406.0	415.3	414.0

TABLE 5.2

EXPERIMENTAL DATA AND CALCULATED RESULTS FOR A DOUBLE BED HT REACTOR

Inlet dry gas flow rate, Nm^3/hr	13085
Inlet steam to gas ratio, S/G	0.924
Pressure, Kg/cm^2	16.4
Age of catalyst, days	268
H_2S, ppm	<0.5

Bed	I			II		
Volume of catalyst, m^3	5.6			18.4		
Composition of gas, per cent (dry basis)	Inlet	Outlet Cal.	Outlet Exptl.	Inlet	Outlet Cal.	Outlet Exptl.
CO	9.0	1.96	1.9	1.96	0.67	0.6
CO_2	11.4	17.08	17.8	17.28	18.13	18.1
H_2	57.7	60.51	60.5	60.51	61.00	61.1
CH_4	0.4	0.42	0.4	0.42	0.41	0.4
N_2+Ar	21.5	20.03	19.4	20.03	19.79	19.8
Temperature, ^oC	399.0	441.3	442.5	330.0	338.3	340.0

TABLE 3.3

EXPERIMENTAL DATA WITH CALCULATED VALUES FOR SINGLE BED HT REACTORS

Reactor	I			II			III		
Inlet dry gas flow rate, Nm^3/hr	85570			84493			71649		
Inlet steam to gas ratio, S/G	0.693			0.711			0.697		
Pressure, Kg/cm^2	22.5			30.0			20.5		
Age of the catalyst, days	115			60			560		
Volume of catalyst, m^3	57.6			44.23			58.2		
Dry gas inlet composition, mole per cent	Inlet	Outlet Cal.	Outlet Exptl.	Inlet	Outlet Cal.	Outlet Exptl.	Inlet	Outlet Cal.	Outlet Exptl.
CO	15.10	2.79	3.20	11.96	1.83	2.16	13.36	3.11	3.10
CO_2	11.41	20.80	20.50	9.44	17.62	17.62	12.46	20.36	21.20
H_2	51.83	56.73	56.60	55.73	59.83	59.40	52.26	56.58	55.60
CH_4	0.34	0.31	0.35	0.34	0.31	0.23	0.29	0.25	0.10
N_2	20.04	19.12	19.10	22.26	20.37	20.12	21.42	19.47	19.30
Ar	0.28	0.25	0.25	0.27	0.24	0.23	0.25	0.23	0.20
Temperature, °C	360.0	434.8	432.0	366.6	423.4	424.0	364.0	430.5	436.0

TABLE 3.4

TEMPERATURE AT DIFFERENT VOLUME FRACTIONS OF SINGLE BED REACTORS

Reactor	I		II		III	
Reactor bed, Vol. fraction	Temperature, °C					
	Cal.	Exptl.	Cal.	Exptl.	Cal.	Exptl.
0.00	360.0	360.0	366.6	366.6	364.2	364.2
0.25	407.0	409.2	401.4	402.3	405.8	410.0
0.50	426.8	428.0	417.3	416.9	423.3	426.3
0.75	433.0	431.7	422.1	423.0	428.9	426.8
1.00	434.8	432.0	423.4	424.0	430.5	436.0

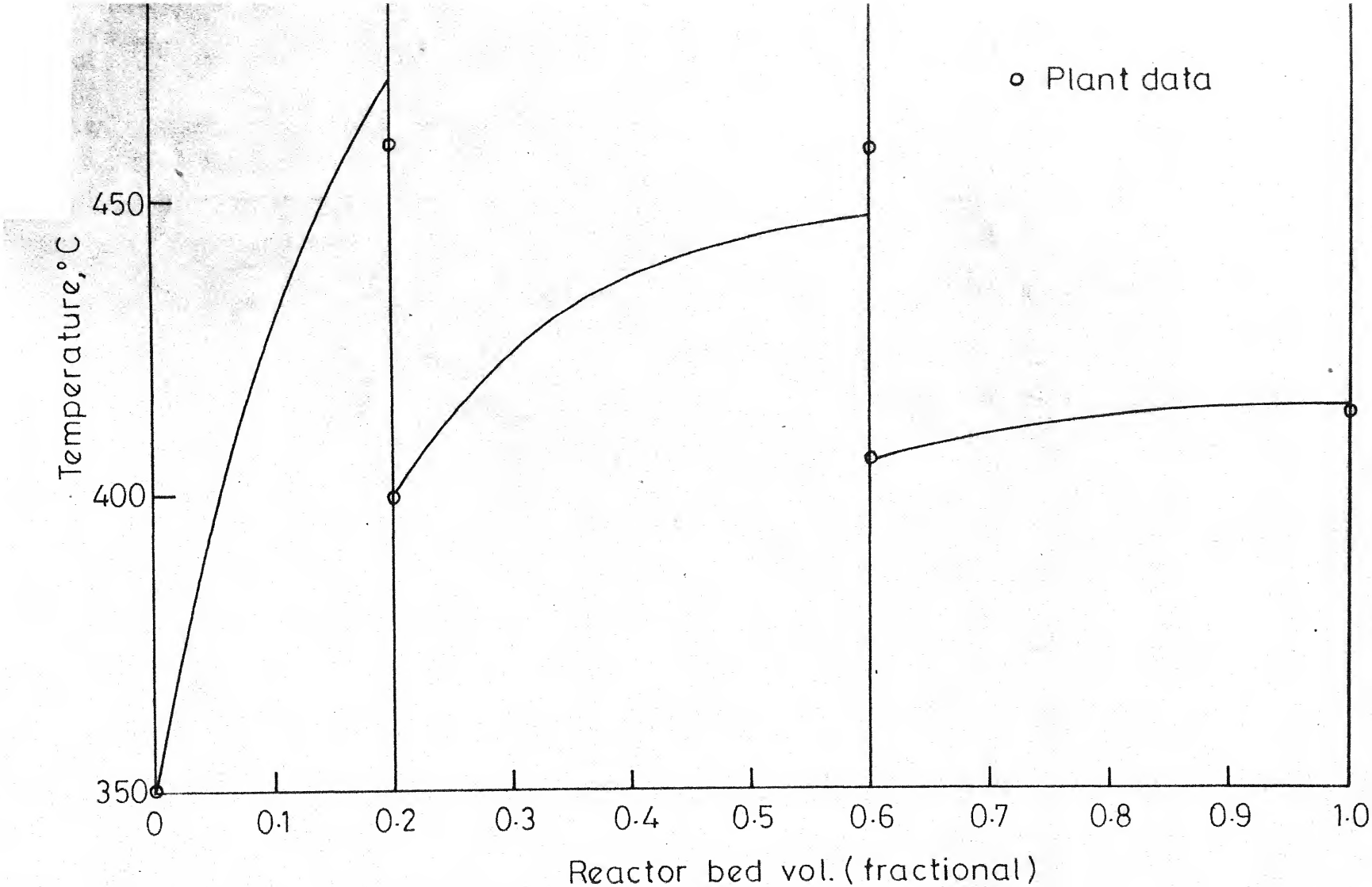

Fig. 3·3 - Temperature variation in a triple bed H.T. reactor.

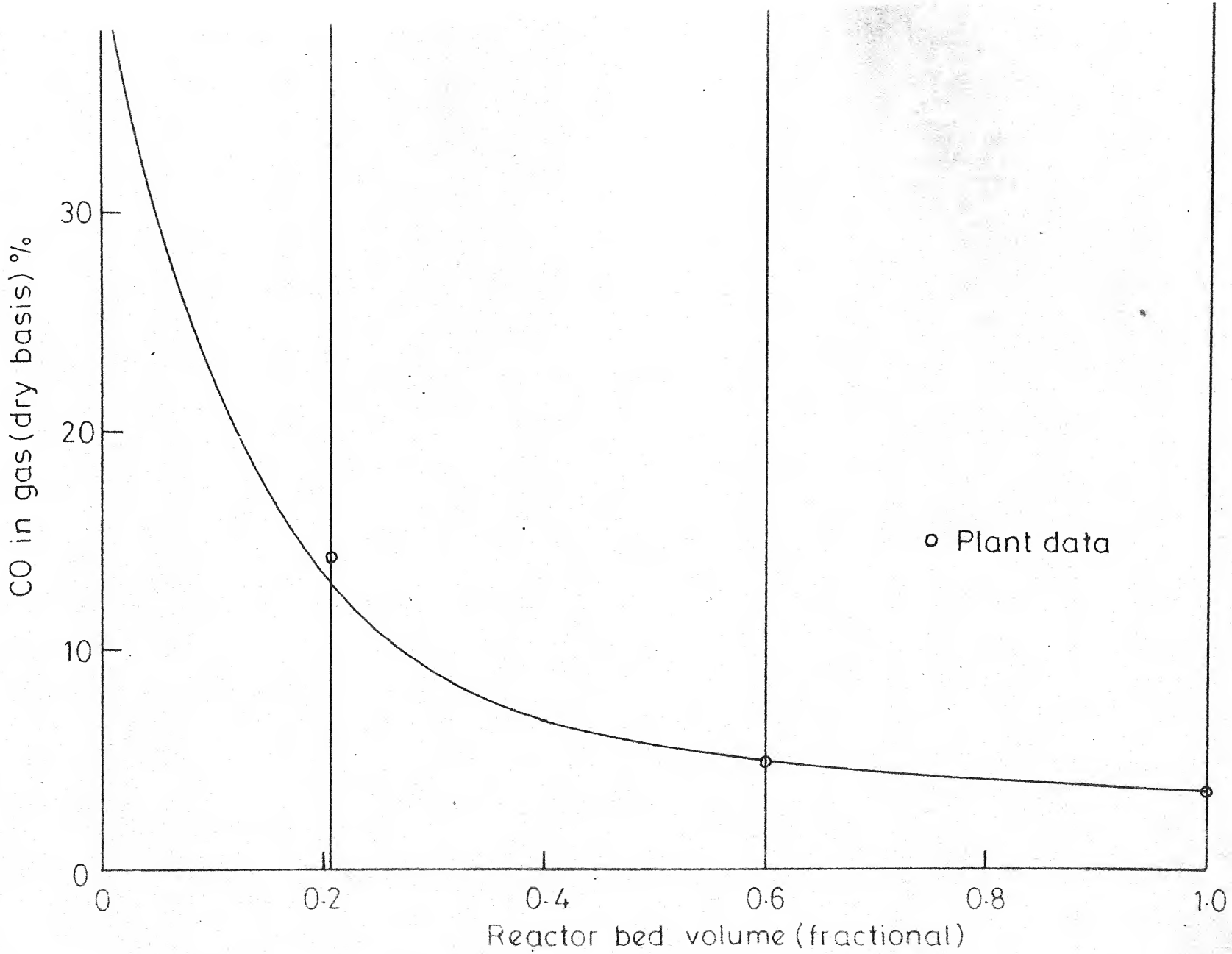

Fig. 3·4 – Carbon monoxide concentration in a triple bed H.T reactor

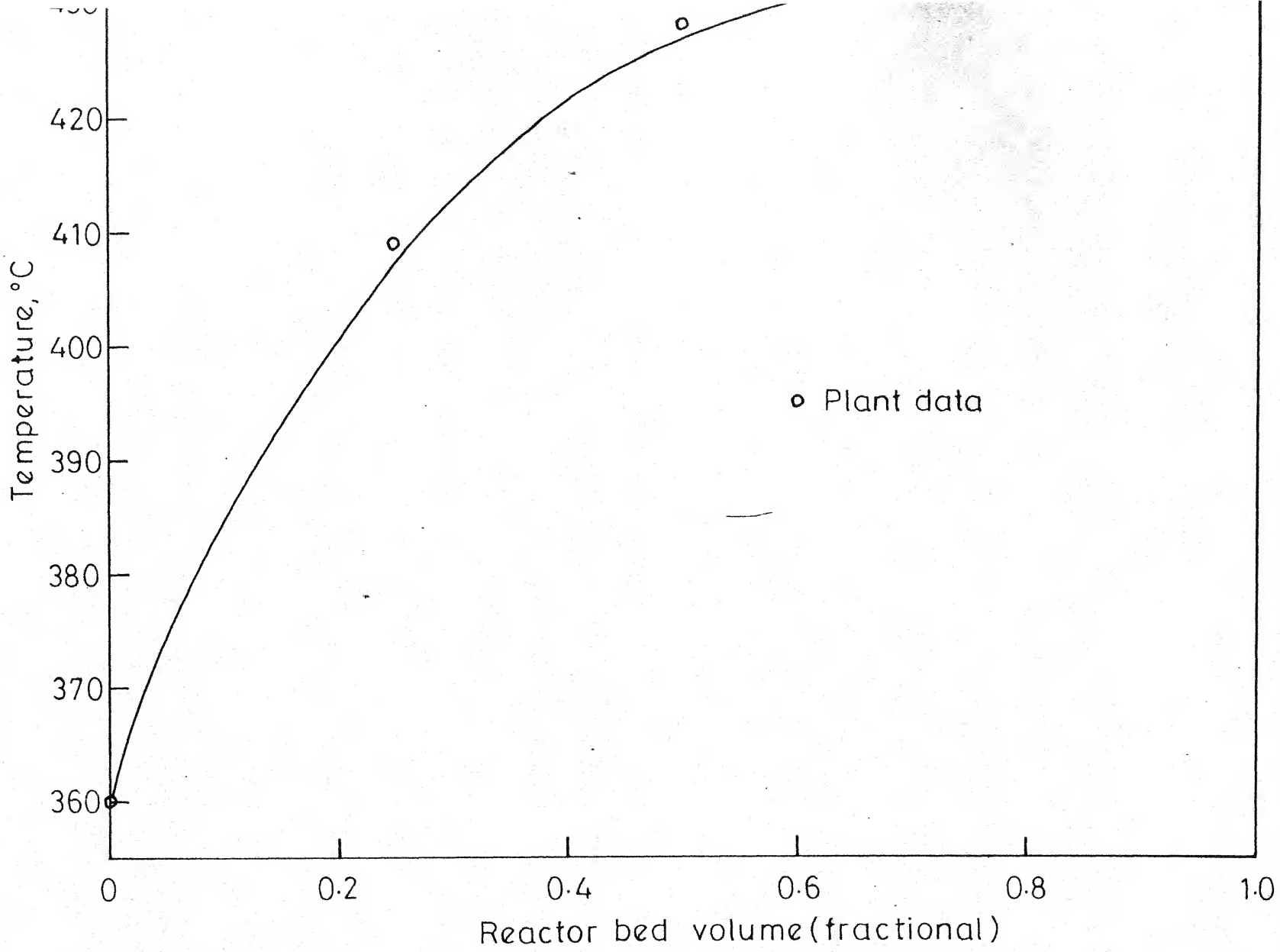

Fig. 3·5 -Temperature variation in, a H.T. reactor.

The maximum difference in temperature is 11.1°C (Table 3.1, Fig.3.3) which is only 2.4per cent.

Double Bed Reactor: Calculated volume of catalyst in the first bed required to obtain the desired conversion is 4 per cent more than the actual volume. This error compared to that in the Triple bed reactor makes it clear that the error is rather random. Temperature calculated and measured differ only by 1.7°C (Table 3.2) which is well within the experimental error.

Single Bed Reactors: Although the difference in calculated and measured composition and temperature at the exit is not high (Table 3.3), this alone is not sufficient, particularly when the equilibrium is closely approached at the exit. However, it can easily be shown, from thermodynamic considerations, that if the temperature at any section of the reactor is known, it can be used to predict the composition of the reacting gases. Hence, following the temperature profile is equivalent to knowing the conversion profile. This is particularly important in the absence of any method of knowing the concentration profile. In Table 3.4 the calculated and measured values of temperatures at different sections of the single bed reactors are presented. Figure 3.5 shows the temperature profile of Reactor I (in Table 3.3). The curve shows that the measured and calculated values are in very good agreement, within 2 per cent, and randomly distributed.

The results very clearly show that in general, the calculated values are in very good agreement with the plant data. This confirms that the developed rate equation as well as the assumptions made are valid under all plant conditions and effect of diffusion of reactants and products inside the catalyst pores has been correctly accounted for.

3.2 LOW TEMPERATURE WATER-GAS SHIFT REACTOR

The studies pertaining to the preparative and kinetic aspects of low temperature shift-catalyst (essentially a copper-zinc oxide system with various promoting components) operating in the range 180-250°C are relatively recent [14,16, 21, 39,40,41] and not as exhaustive as on HT catalyst. The kinetics of the reaction is reported to be same as that over a HT catalyst [14]. Kinetic studies leading to rate equations different from that for HT catalyst are also reported [39,41]. However, in general, a rate equation similar to that for reaction over high temperature catalyst is assumed to evaluate the constants and to compare activities of the two catalysts [1,14,21]. These are used in all calculations for LT reactors [27].

Equation (3.3) used to describe the rate of reaction at atmospheric pressure over a HT catalyst is used in this case also. To calculate the effective rate over catalyst pellets, the effects of intra particle diffusional resistance, age of catalyst and pressure are separately accounted for as in the case of HT catalyst.

Thus, the intrinsic rate at atmospheric pressure for the low temperature catalyst is expressed as

$$r = k(x_{CO} - x^*_{CO}) \qquad (3.3)$$

where

$$k = a\, e^{-E/R_g T} \qquad (3.4)$$

The value of activation energy, E, is reported between 20,600 to 26,800 k.cal/kg.mole [1,14,21] for the catalyst over which the model has been tested, the reported [1] values are

$$E = 20,960 \text{ K.cal/kg.mole}$$

and $a = 2.955 \times 10^{13}$ cc of CO/hr.gm of catalyst at atmospheric pressure.

With these values, the intrinsic rate at atmospheric pressure for the catalyst can be represented as

$$r = 2.955 \times 10^{13} \, e^{-\frac{20,960}{R_g T}} \, (x_{CO} - x^*_{CO}) \qquad (3.27)$$

The specifications of the catalyst over which the rate is described by equation (3.27) are as follows:

Catalyst Specifications:

Chemical composition	
CuO	- 33 per cent
ZnO	- 66 per cent
Real density, gm/cc	5.09
Density of the pellet, gm/cc	2.575
Specific surface area, m^2/gm	27.6
Porosity	
<200	0.208 cm^3/gm
Total porosity	0.243 cm^3/gm

(a) Diffusional Resistance:

Knudsen diffusion is the controlling mode of intra-particle diffusion. Therefore the effectiveness factor is calculated by the method described earlier using equations (3.9) through (3.13).

(b) Age of the Catalyst:

Since the reaction over this catalyst takes place at a low temperature, there is no loss due to sintering as in the case of HT catalyst. The loss in activity due to age is accounted for by the aging factor

$$A_{gf} = 10^{(4.66\times10^{-4}-1.6\times10^{-6}T)\times\tau} \qquad (3.28)$$

(c) Pressure:

Effect of pressure on the rate of reaction has been studied by some workers [1,39]. The one based on the catalyst under study is however inconclusive andhence on the basis of similarity the pressure effect is accounted for by the factor obtained for high temperature catalyst i.e.

$$P_f = P^{(0.5 - P/250)} \qquad (3.21)$$

The agreement of plant data and calculated results justifies its use.

Now the final rate equation can be expressed as

$$r = Eff \times 2.955 \times 10^{13} \, e^{\frac{-20960}{R_g T}} \times A_{gf} \times P_f \times (x_{CO} - x^*_{CO}) \qquad (3.29)$$

Description of Mathematical Model:

Assumptions made in the case of HT reactor are valid in this case also and the same set of equations (3.24 - 3.26) are used to describe the reaction system along an adiabatic catalytic layer. Heat of reaction is calculated from the same correlation and integration is also performed according to the same scheme.

RESULTS AND DISCUSSION

The calculation results for three different reactors using catalysts of different age (60 to 560 days) and working under different conditions of pressure (16.0 to 29.3 atms) and temperature (183 to 220°C), are presented along with the plant data in Tables 3.5 and 3.6. Figure 3.6 shows that the calculated temperature profile in Reactor II (Tables 3.5 and 3.6) along with the plant data.

The results show a very good agreement between the plant data and calculated values, the maximum difference being less than 2 per cent. However, the composition and temperature changes involved in these reactors are so small that the correctness of the model is not realized very easily as in the case of HT reactor.

TABLE 2.2

EXPERIMENTAL DATA AND CALCULATED RESULTS FOR LT REACTORS

Reactor	I			II			III		
Inlet dry gas flow rate, Nm^3/hr	13980			78813			92873		
Inlet steam to gas ratio, S/G	0.812			0.546			0.653		
Pressure, Kg/cm^2	16.0			20.7			29.3		
Volume of catalyst, m^3	18.4			56.0			50.2		
Age of catalyst, days	138			560			60		
Composition of the gas, per cent (dry basis)	Inlet	Outlet Cal.	Outlet Exptl.	Inlet	Outlet Cal.	Outlet Exptl.	Inlet	Outlet Cal.	Outlet Exptl
CO	1.9	0.15	0.2	3.11	0.32	0.30	1.83	0.16	0.18
CO_2	17.1	18.58	18.6	20.36	22.51	22.84	17.52	18.87	18.93
H_2	60.6	61.13	61.0	56.58	57.75	57.30	59.83	60.48	60.29
CH_4	0.2	0.19	0.2	0.25	0.24	0.28	0.31	0.31	0.34
N_2	19.9	19.57	19.6	19.47	18.95	19.03	20.37	20.03	20.01
Ar	0.3	0.28	0.3	0.23	0.23	0.25	0.24	0.23	0.25
Temperature, °C	183	193.1	193	200	218.7	220	200	208.4	213

TABLE 3.6

TEMPERATURES AT DIFFERENT VOLUME FRACTIONS OF LT REACTORS

Reactor	I		II		III	
Reactor bed volume	Temperature, ^{o}C					
	Cal.	Exptl.	Cal.	Exptl.	Cal.	Exptl.
0.00	183.0	183.0	200.0	200.0	200.0	200.0
0.25	188.9	189.1	210.0	211.0	205.1	206.0
0.50	191.6	190.8	216.1	215.0	207.3	207.0
0.75	192.3	191.9	217.9	218.0	208.0	209.0
1.00	193.1	193.0	218.7	220.0	208.7	213.0

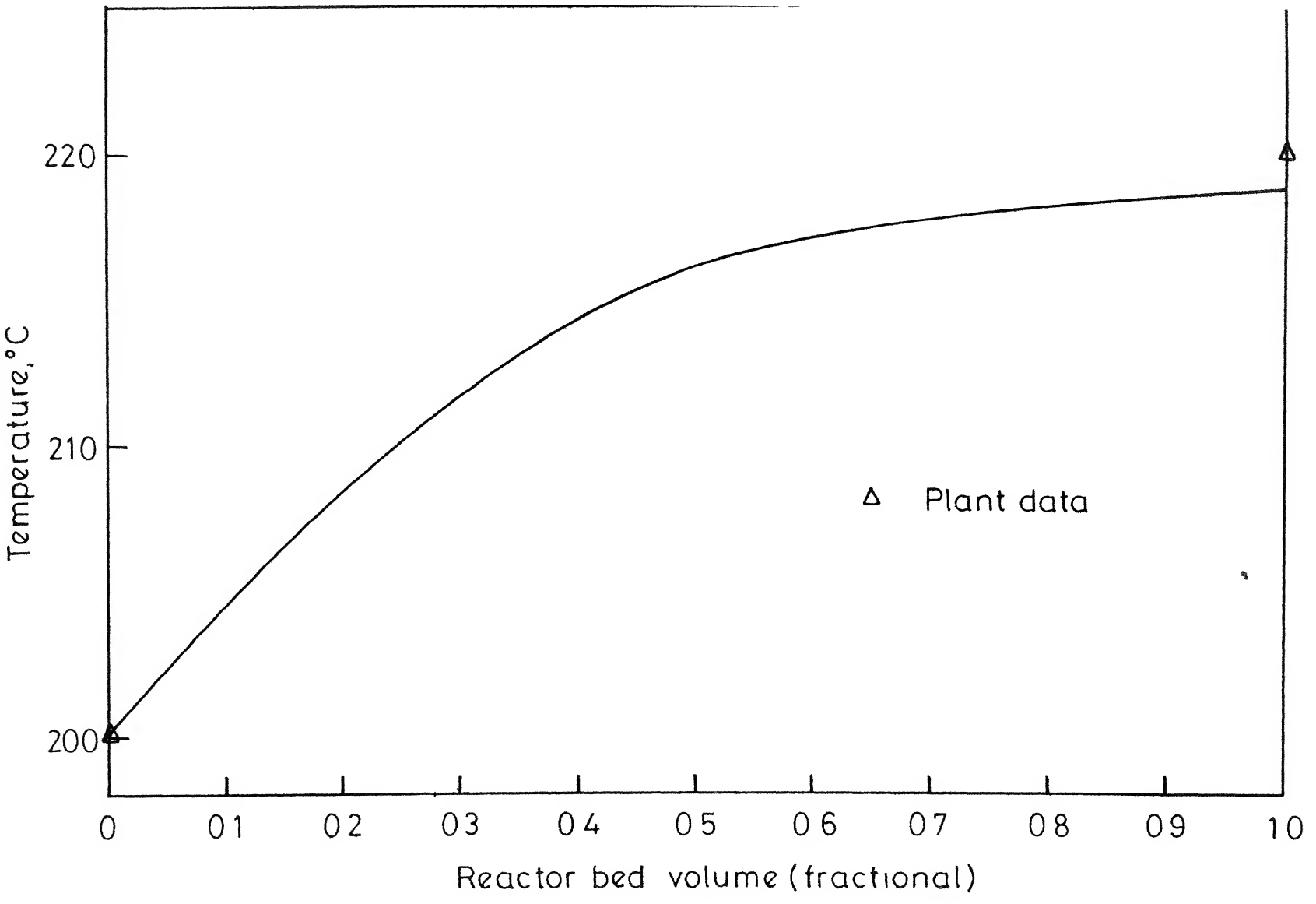

Fig 3 6 - Temperature profile in LT reactor

NOMENCLATURE

A	Specific surface of catalyst, m^2/gm
A_o	Specific surface of fresh catalyst, m^2/gm
a	Frequency factor, cc/hr. gm. of catalyst
$\bar{C}_p$	Specific heat capacity of reacting gaseous mixture, Cals/gm mole ^oK.
D_e	Effective diffusivity, cm^2/sec
D_B	Bulk diffusivity, cm^2/sec
D_k	Knudsen diffusivity, cm^2/sec
E	Intrinsic energy of activation, cals/gm mole ^oK
E'	Apparent intrinsic energy of activation, cals/gm mole ^oK
E_S	Energy of activation for sintering, cals/gm of catalyst, ^oK
G	Volume flow rate, Nm^3/hr
ΔH	Heat of reaction, cals/gm mole of CO reacted
j	Number used to represent different components
k	Rate constant, cc/hr. gm. of catalyst
k'	Rate constant cc/hr. gm of catalyst, atms
P	Total pressure, atms
p	Partial pressure, atms
R_g	Gas constant, cal/gm mole ^oK
r	Rate of reaction, cc/hr gm of catalyst
r'	Rate of reaction, cc/hr cc of catalyst
r_o	Pore radius, cms
T	Temperature, ^oK

V Volume of catalyst, cc

x Mole fraction

C, K_s, n Constants

α Stoichiometric coefficient (-ve value is used for reactants and +ve for products of the reaction)

τ Age of the catalyst, days

Subscripts

j Component j

CO Component carbon monoxide

Superscript

0 Inlet conditions

* Equilibrium conditions

REFERENCES

1 Ahmed, S., Sengupta, A., Bhattacharya, N.B. and Sen, S.P., Technology (India) 8, 218 (1971).

2 Ahmed, S., Sengupta, A., Sen,B. and Bhattacharya, N.B., Technology (India) 9, 301 (1972).

3 Atwood, K., Arnold, M.R. and Appel, E.G., I and EC 42, 1600 (1950).

4 Atroshchenko, V.I. and Bibr, B., 'Zhur. Priklad. Khim. 32, 997 (1959).

5 Atroshchenko, V.I., Zhidkev, B.A. and Zasorin, A.P., Kinet. Catal. 3, 529 (1962).

6 Barkley, L.W., Corrigan, T.E., Wainwright, H.W. and Sands, A.E., I and EC 44, 1066 (1952).

7 Bannerjee, B., Chandra, M. and Ghoshal, S.R., Technology (India) 19, 368 (1972).

8 Bohlbro, H., J.Catalysis, 3,207 (1964).

9 Bortolini, P., Chem.Eng. Sci. 9, 135 (1958).

10 Carberry, J.J., AIChE. J., 7, 350 (1961).

11 Carnahan, B., Luther, H.A. and Wilkes, J.O., 'Applied Numerical Methods', John Wiley and Sons Inc. 1969.

12 Chandra, M., Singh, S.S., Banerjee, B., Sinha, A.K. and Sinha, N.K., Technology (India) 9, 358 (1972).

13 Chandra, M., Singh, S.S., Sinha, A.K., Sinha, N.K. Banerjee, B. and Ghoshal, S.R., Technology (India), 10, 208 (1973).

27 Mahapatra, H., et al. Technology (India) 8, 211(1971).

28 Mars, P., Chem. Eng.Sci. 14, 375 (1961).

29 Moe, J.M., Chem. Eng. Prog. 58(3), 33 (1962).

30 Nakanishi, K. and Tamaru, K., Trans. Faraday Soc. 59, 1470 (1963).

31 Padovani, C. and Lotteri, A., J.Soc. Chem. Ind. 56, 391T (1937).

32 Popov, B.I., Zhur. Fiz. Khim. 31, 1033 (1957).

33 Puri, V.K., Mahapatra, H., Kursetji, R.M., Ganguly, N.C. and Sen, S.P., Technology (India), 10, 224 (1973).

34 Ruthven,D.M., Chem.Eng.Sci. 23, 759 (1968).

35 Ruthven, D.M., Canadian J.Chem.Eng. 47, 327 (1969).

36 Smith, J.M., 'Chemical Engineering Kinetics' IInd Ed., McGraw Hill Book Company 1970.

37 Stilling, O. and Krusunstierna, O.U., Acta. Chem.Scand. 12, 1095 (1958).

38 Ting, A.P. and Wan, S.W., Chem.Eng. May 19, 185 (1969).

39 Tsuchimoto, K., Oda, Y. and Morita, Y., Kogyo Kagaku Zasshi 73, 137 (1970).

40 Yureva, T.M., Boreskov, G.K. and Gruver, V.Sh., Kinet. Katal. 10, 294 (1969).

41 Yureva, T.M., Boreskov, G.K. and Gruver, Y.Sh. Kinet. Katal. 10, 862 (1969).

42 Wheeler, A. in 'Catalysis', Vol. II, P.H.Emmett, Ed., Reinhold, New York, 1955.

CHAPTER 4

SIMULATION OF AMMONIA SYNTHESIS REACTORS

The exit gas from methanator contains nitrogen and hydrogen in appropriate proportion for the ammonia synthesis reaction. This gas also contains some methane and argon as inert components. The gas mixture is compressed to 200-350 atmospheres and fed to ammonia reactor along with the recycle gas. The reaction between nitrogen and hydrogen is one of the simplest kinetic reactions. The synthesis is straight forward, there is no side reaction and the product is stable. The physical and thermodynamic properties of the reactants and products are well known [15]. However, the mechanism of this reaction over the synthesis catalyst [Iron Catalyst] is not well understood. This has led to numerous rate equations, all of which are of complex order. Because of complexity of these rate equations it is difficult to account for the diffusional resistances to the transport of reactants and product in catalyst pores. This, in addition to limited reliability of rate equation, makes it difficult to have a mathematical description of the processes taking place inside an ammonia synthesis reactor.

Major changes have taken place in the design of ammonia synthesis reactors since the first commercial production

started in 1925 [19]. Most of these changes have been based on historical plant data rather than an insight into the physical and chemical processes taking place in the reactors. However, the use of computers in design, optimization and control made it necessary to have a mathematical description of the process. Simulation models for ammonia synthesis converters of different types have been developed for design, optimization [26, 35] and control [31,32] purposes.

To describe the reactor operating conditions as accurately as possible, the simulation model should take into consideration all the physical and chemical processes taking place in the reactor. In order to avoid the complexity resulting from such a consideration, earlier workers have attempted only approximate simulations.

The mathematical model described here considers all physical and chemical processes in the reactor. Method to solve transport equations to evaluate effectiveness factor, upto desired accuracy is developed and used in the model calculations.

4.1 RATE EXPRESSIONS

The literature contains innumerable rate expressions. Those reported till early thirties have been summarized by Frankenburg [14] and Emmett [11, 12]. In 1940 Temkin and Pyzhev [37] developed a rate equation which offered a satisfactory

kinetic approach to the synthesis and decomposition of ammonia over doubly promoted iron catalysts. Since then this rate equation as such or in modified forms has been most extensively used, although some doubts about the generality of the equation have been raised [1, 13,17]. The modified form of the Temkin equation [10], used in this work, is as follows:

$$r_{NH_3} = K_2[k_a^2 \times f_{N_2} \times \left(\frac{f_{H_2}^3}{f_{NH_3}^2}\right)^a - \left(\frac{f_{NH_3}^2}{f_{H_2}^3}\right)^{1-a}] \qquad (4.1)$$

where r_{NH_3} = reaction rate, kg. mole. $NH_3/hr/m^3$ of catalyst, K_2=velocity constant of the reverse reaction, kg. mole/hr/m^3, f_{N_2}, f_{H_2}, f_{NH_3} = fugacities of nitrogen, hydrogen and ammonia respectively, k_a = equilibrium constant of the reaction: 1.5 H_2 + 0.5 $N_2 \rightleftharpoons NH_3$ and a=constant. According to some workers a=0.5 for all iron catalysts [25,36,37] whereas others obtained values ranging from 0.4 to 0.8 [2-7,10, 13, 16, 18, 22, 23, 24, 28, 29, 33, 34].

Having found different values of a, many authors suggest that it depends upon catalyst characteristics. It appears reasonable, considering that catalysts of different make differ in their promoter contents and physical characteristics. However, difference of the same order in the value of a has been reported for the same catalyst operating under two different conditions (before and after thermoresistancy test). Even for

two arbitrary sets of runs over the same catalyst, values of a show similar differences [16].

Generally to evaluate a, K_2 is expressed as a function of temperature in Arrhenius equation form i.e.

$$K_2 = K_{20}\, e^{-E_2/R_g T} \qquad (4.2)$$

where K_{20} is a constant, E_2 is the energy of activation, R_g is gas constant and T is the absolute temperature. The experimental results are then fitted with K_{20}, E_2 and a as parameters. Such a method of evaluation could lead to variations in values of a with a corresponding change in values of E_2 and K_{20}. It has been suggested that there is a linear relationship between the value of log K_2 and a. This shows that to differentiate the effect of catalyst characteristics or promoter content from those associated with measurement errors or method of calculation is difficult. Based on this it has been suggested that a constant value of a, independent of catalyst make, could be used [16]. However, for a fixed value of a, other parameters K_{20} and E_2 are not available for the two catalysts over which the present model has been tested. The values used for Montecatini Edison catalyst are a = 0.647, E_2 = 38690 Kcal/Kg mole, log K_{20}=14.206 and the corresponding rate equation is

$$r_{NH_3} = \text{Exp}\ (2.303 \times 14.206 - \frac{38690}{R_g T}) \times$$

$$[k_a^2 \times f_{N_2} \times (\frac{f_H^3}{f_{NH_3}^2})^{0.647} - (\frac{f_{NH_3}^2}{f_{H_2}^3})^{0.353} \qquad (4.3)$$

For Halder Topsoe catalyst, a = 0.692, E_2 = 42893 and log K_{20} = 15.2059 and the rate equation is

$$r_{NH_3} = \text{Exp}\ (2.303 \times 15.2059 - \frac{42893}{R_g T}) \times$$

$$[k_a^2 \times f_{N_2} \times (\frac{f_{H_2}^3}{f_{NH_3}^2})^{0.692} - (\frac{f_{NH_3}^2}{f_{H_2}^3})^{0.308}] \qquad (4.4)$$

All the above values of a, E_2 and log K_{20} have been obtained from the published work of Guacci et al. [16].

4.2 EFFECTIVENESS FACTOR

The above expressions represent the intrinsic rate of reaction i.e., the rate of reaction for small particles in which there is no resistance to transfer of mass or heat to the active surface. The large size industrial catalyst particles (6-12 mm for axial flow converters) are, however, subject to diffusion restriction in their pore structure.

This effect can be taken care of by effectiveness factor, η, which is defined as the rate at which the reaction occurs in a pellet divided by the rate at which the reaction would occur if the concentration and temperature throughout the pellet were same as those at the outer surface i.e.

$$\eta = \frac{\text{[Molar flux of component i across surface]}}{\text{[Volume of pellet]}} \times \frac{\text{[Surface area of pellet]}}{\text{[Rate of formation of component i at surface comp., T,P]}} \qquad (4.5)$$

Several authors [4,10,20,21,28] have calculated this factor for ammonia synthesis reaction. In all these calculations but those due to Dyson and Simon [10] either pseudo first order kinetics was used or the bulk flow terms in the equations for transport within the catalyst pellet were omitted. Dyson and Simon [10] have formulated the problem by considering all the aspects. But unable to solve within practicable computation time limits, they also suggest the use of an empirical correlation to obtain effectiveness factor. The development of transport equations, to follow, are similar to those done by Dyson and Simon [10].

Catalyst particles are assumed to be spherical [28] and isothermal [30]. Knudsen diffusion is neglected [4] and diffusion coefficients of each component are assumed to be independent of position within a particle.

The reaction considered for the development of diffusion equation is

$$\frac{1}{2} N_2 + \frac{3}{2} H_2 \rightleftharpoons NH_3 \qquad (4.6)$$

A mole balance for component i gives

$$\frac{1}{r^2}\frac{d}{dr}(r^2 N_i) = \alpha_i \frac{r_{NH_3}}{1-\varepsilon} \qquad (4.7)$$

where r is the radial coordinate of spherical particle, N_i is the molar flux of the ith component in the r-direction, r_{NH_3} is the rate of formation of ammonia given by equation (4.1), ε is the void fraction of the packed bed and α_i represents the stoichiometric coefficient of the ith component in the reaction scheme given by equation (4.6). Following the ordinary convention, α_i, is taken to be positive if the component is a product, negative if the component is a reactant, and zero if the component is an inert substance. Nitrogen, hydrogen, ammonia, methane and argon have been designated as components 1,2,3,4 and 5 respectively.

Boundary conditions for equation (4.7) are

$$N_i = 0 \quad \text{at } r=0 \text{ or, } \frac{dx_i}{dr} = 0 \text{ at } r=0 \text{ and}$$
$$x_i = x_{ig} \text{ at } r=R' \qquad (4.8)$$

where R' is radius of spherical particle, x_i is the mole fraction of component i at any point of the catalyst particle and x_{ig} is that at the surface. It is taken to be same as that in gas.

The molar fluxes of any two components i and j at steady state are related as follows:

$$\alpha_i N_j = \alpha_j N_i \qquad (4.9)$$

This implies that molar flux of any inert component is equal to zero. The molar flux, N_i of any active component i can be expressed in terms of its concentration gradient and the molar fluxes of other active components as

$$N_i = -C\, D_{ie} \frac{dx_i}{dr} + x_i \sum_{j=1}^{3} N_j \qquad (4.10)$$

where C is the total concentration of reacting gas mixture Kgmole/m^3 and D_{ie} is the effective diffusion coefficient of component i. Substitution of equation (4.9) into equation (4.10) and utilization of the relationship

$$\sum_{i=1}^{3} \alpha_i = -1 \qquad (4.11)$$

gives

$$N_i = \frac{-C\, D_{ie} \dfrac{dx_i}{dr}}{1 + \dfrac{x_i}{\alpha_i}} \qquad (4.12)$$

Substituting for N_i and N_j from equation (4.12) in equation (4.9) yields

$$\alpha_i \left[\frac{-CD_{je} \dfrac{dx_j}{dr}}{1 + \dfrac{x_i}{\alpha_j}}\right] = \alpha_j \left[\frac{-C\, D_{ie} \dfrac{dx_i}{dr}}{1 + \dfrac{x_i}{\alpha_i}}\right] \qquad (4.13)$$

Integrating this equation subject to boundary conditions (4.8), the following equation is obtained

$$x_j = -\alpha_j + (\alpha_j + x_{jg})\left(\frac{\alpha_i + x_1}{\alpha_i + x_{1g}}\right)^{D_{ie}/D_{je}} \qquad (4.14)$$

As a consequence of this relationship, the solution of only one mole balance (equation 4.7) need be considered.

Substituting for N_i from equation (4.12) into equation (4.7) yields

$$\frac{d^2x_i}{dr^2} - \frac{1}{(\alpha_i+x_1)}\left(\frac{dx_1}{dr}\right)^2 + \frac{2}{r}\frac{dx_i}{dr} = -\left(\frac{\alpha_i+x_i}{CD_{1e}}\right)\frac{r_{NH_3}}{1-\varepsilon} \qquad (4.15)$$

Normalising equation (4.15) by defining $Z = \frac{r}{R'}$, gives

$$\frac{d^2x_i}{dZ^2} - \frac{1}{(\alpha_1+x_1)}\left(\frac{dx_1}{dZ}\right)^2 + \frac{2}{Z}\frac{dx_1}{dZ} = -\left[\frac{R'^2}{CD_{ie}}\right](\alpha_1+x_1)\frac{r_{NH_3}}{1-\varepsilon} \qquad (4.16)$$

and the boundary conditions in terms of Z are

$$\frac{dx_i}{dz} = 0 \text{ at } Z=0; \quad x_i = x_{ig} \text{ at } z=1 \qquad (4.17)$$

This is a two point boundary value problem and may be solved by either choosing the unknown condition at the centre (i.e. x_i at Z=0) and integrating equation (4.16) towards the surface (Z=1) for choosing the unknown condition at the surface ($\frac{dx_i}{dZ}$ at Z=1) and integrating inward. To solve the

problem, in both cases, the value of the chosen quantity is varied and integration repeated until the boundary condition at the other point is satisfied. It is convenient to write equation (4.16) for the product component (NH_3), thereby ensuring that the denominator in the second term of equation (4.16) cannot go to zero. If the integration is carried out from centre towards the surface, it is necessary to rewrite equation (4.16) because of the third term. This type of problem has been treated by Weisz and Hicks [38]. Here the inward integration procedure is used. It is reported [10] that to satisfy the boundary conditions at the centre with tolerable accuracy it is necessary to determine the flux at the surface (i.e. dx_3/dZ) to within 1 part in 10^5. However, it may not be necessary to satisfy the boundary condition at the centre, if it is recognized that the direction of rapid deviation of the calculated value of $\frac{dx_3}{dZ}$ from the true one i.e. direction of shooting of $\frac{dx_3}{dZ}$ value as integration proceeds, depends on whether the assumed value of $\frac{dx_3}{dZ}$ (at Z=1) is smaller or greater than the true value. As shown in Figure 4.1, if the assumed value of $\frac{dx_3}{dZ}$ is smaller (A) integration would lead to shooting of its value in one direction as the centre is approached whereas it would have the opposite direction if the assumed value (B) is greater than the true one. Therefore, by observing the direction of shooting, it is possible to obtain a range (AB) within which the true value lies. This range could be reduced

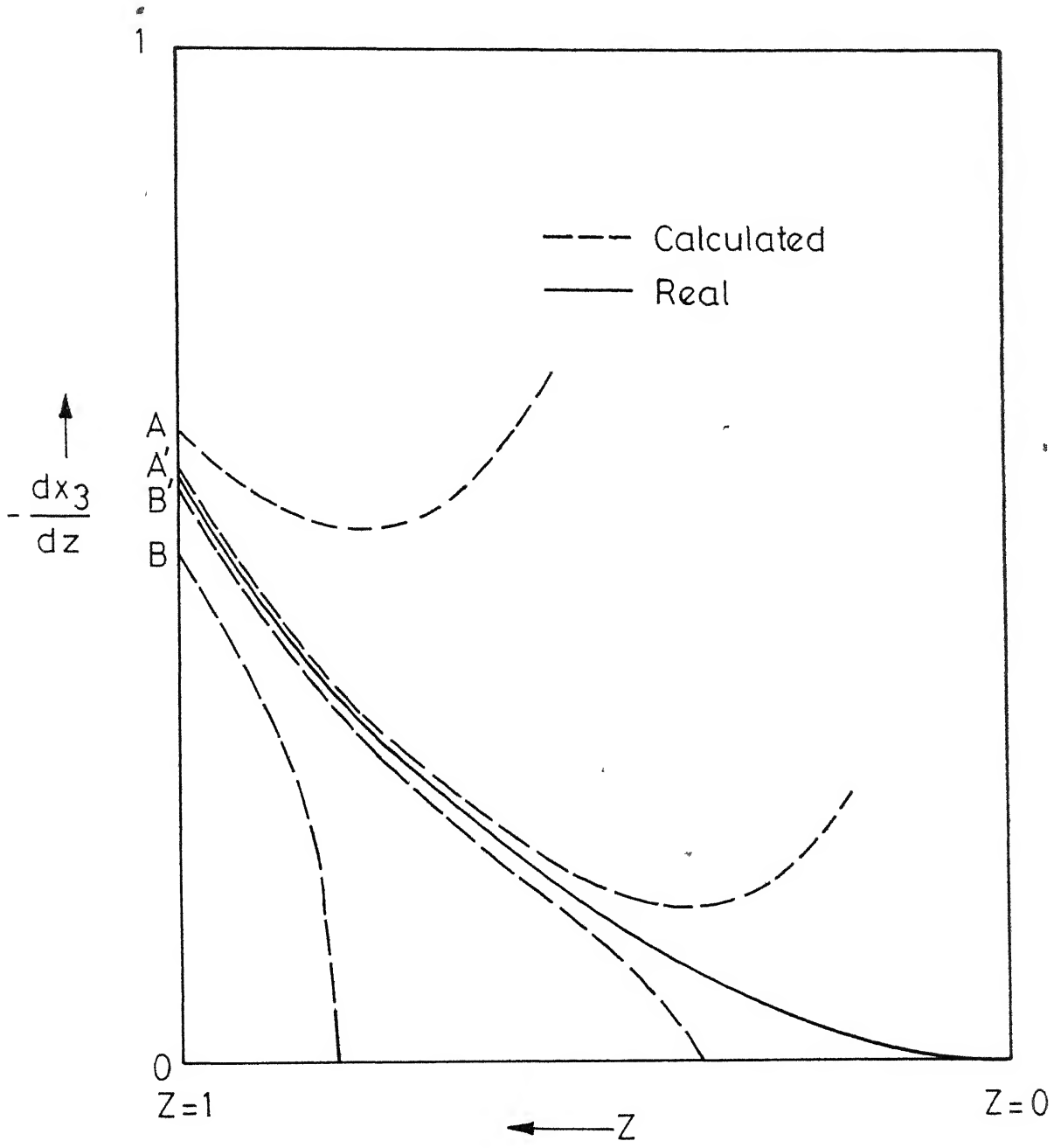

Fig 4 1 - Calculated integration path of concentration gradient of ammonia in the catalyst pellet

to desired accuracy (A'B') by repeated integration. After achieving the desired accuracy (range of $\frac{dx_3}{dZ}$ value reduced to A'B') no further integration is called for although the boundary condition at the centre has not been satisfied. In this work range A'B' representing less than0.5 per cent of the true value of $\frac{dx_3}{dZ}$ has been used. Mean of the two extreme values (A' and B') is taken to represent the true values of $\frac{dx_3}{dZ}$.

The surface flux may now be substituted along with other terms in equation (4.5) to get the effectiveness factor,

$$\eta = \frac{3\left(-\frac{dx_3}{dZ}\right)}{\left(\frac{R'^2}{CD_{3e}}\right) r_{NH_3}(x_{ig}, T, P)(1+x_{3g})\left(\frac{1}{1-\varepsilon}\right)} \qquad (4.18)$$

The total concentration c is obtained from

$$C = \frac{\sum_{i=1}^{n} f_i}{RT} \qquad (4.19)$$

where f_i is the fugacity of component i. The radius, R', for spheres equivalent to industrial size particles may be calculated from

$$R' = \frac{\Lambda}{2\psi} \qquad (4.20)$$

where Λ and ψ are equivalent diameter and shape factor respectively. Effective diffusion coefficient is calculated

from the relation given by Wheeler [39].

$$D_{ie} = \frac{1}{2} \theta D_1 \tag{4.21}$$

where θ is the intra-particle porosity and D_1 is the bulk diffusion coefficient of component i. This coefficient at $0^{o}C$ and 1 atmosphere is calculated from the following relation

$$D_i^o = \frac{1-x_i}{\sum_{J=1}^{n} \frac{x_i}{D_{j1}}} \tag{4.22}$$

where D_{j1} is the diffusion coefficient of component j in component i. The diffusion coefficients calculated from equation (4.22) are then corrected for the temperature and pressure at the surface of the catalyst pellet by

$$D_i = D_1^o \left(\frac{T}{273}\right)^{1.5} x \frac{1}{P} \tag{4.23}$$

where P is in atmospheres.

4,3 DESCRIPTION OF THE MATHEMATICAL MODEL

Since the reaction is exothermic all reactor designs have arrangements for removing the heat generated in the catalyst bed by the progress of the reaction. The reactor also serves as its own heat exchanger to heat the incoming synthesis gas. Apart from flow pattern (axial or radial) the designs differ on heat removal strategy. In autothermic designs, heat is removed throughout the bed volume whereas

other designs have adiabatic beds with cooling in between them either by external exchangers or by quench gas mixing. Figure 4.2 shows schematic diagrams of a reactor having three adiabatic beds with external cooling of the reaction mixture and an autothermal reactor. Both adiabatic as well as non-adiabatic beds, in an axial flow reactor, have been considered in the present study.

Adiabatic Catalyst Bed:

The temperature and composition throughout a general cross-section of the bed is assumed uniform. Axial diffusion of mass and heat is neglected. Pressure drop is very small compared to the total pressure therefore an uniform pressure equal to the average pressure in the reactor has been assumed. On the basis of these assumptions the material and heat balance equations which describe the evolution of the composition and temperature of the system along an adiabatic catalytic layer can be written as

$$\frac{d\xi''}{dV} = \frac{\eta\, r_{NH_3}(\xi'', P, T)}{G} \qquad (4.24)$$

$$\frac{dT}{dV} = \frac{\Delta H}{C_P} \frac{\eta\, r_{NH_3}(\xi'', P, T)}{G} \qquad (4.25)$$

where G = mass flow rate,

ΔH = heat of reaction, K.cal/Kg.mole

V = catalyst volume, m^3 and ξ'' is the extent of

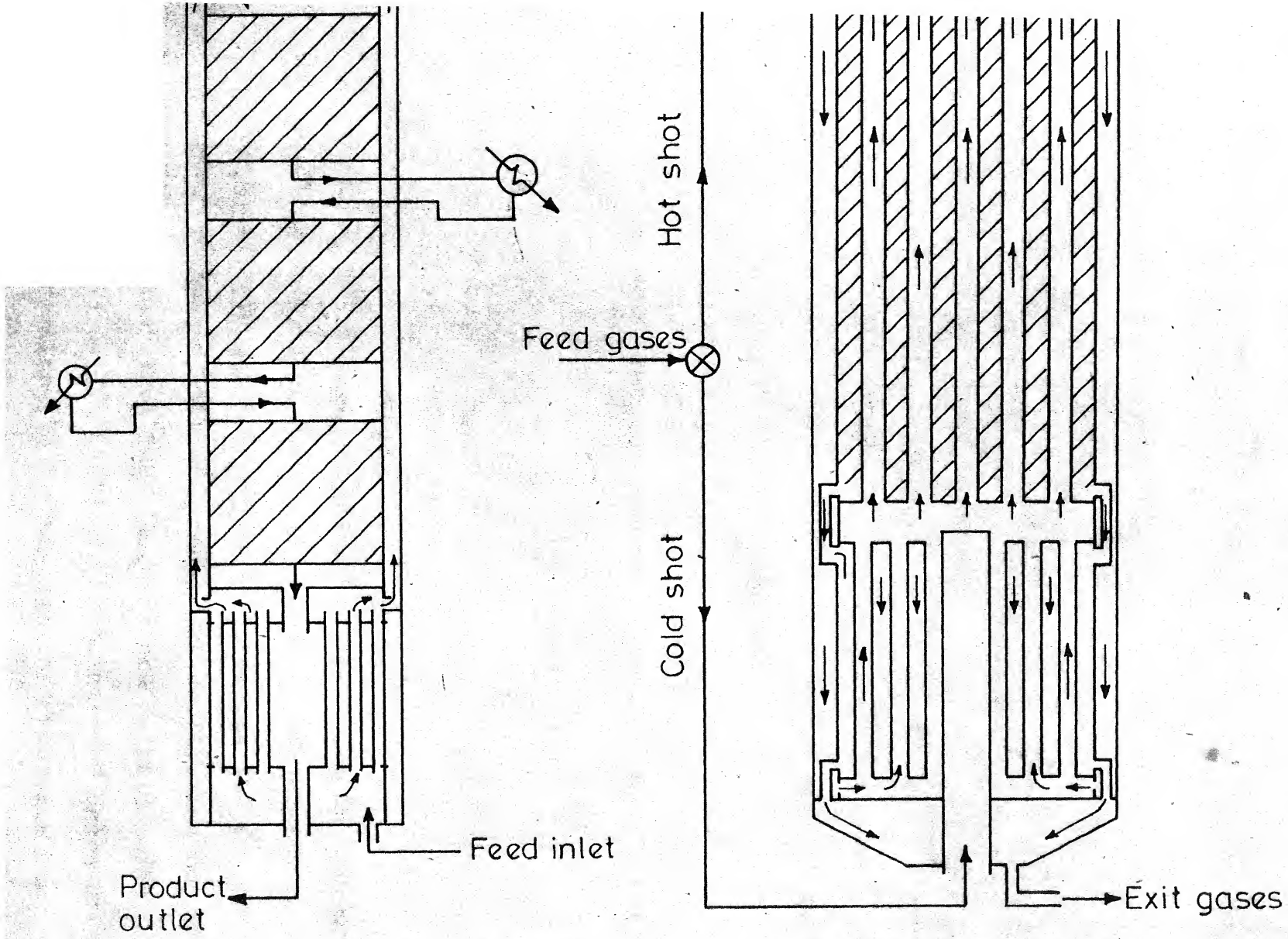

Reactor with three adiabatic beds.

Autothermal reactor.

Fig. 4·2 - Schematic diagrams of ammonia synthesis reactors.

reaction defined by

$$g_J = g_{Jo} + \alpha_J \, m_J \, \xi'' \tag{4.26}$$

where g_J, g_{Jo} = mass fraction of component J at any point and at the inlet, m_J = molecular weight of component J.

Non-Adiabatic Catalyst Bed:

Assumptions same as those in case of adiabatic bed are made. Mass balance equation (4.24) holds for this case also. The heat balance is described by the following equations:

$$\frac{dT_g}{dV} = \frac{U.A.(T-T_g)}{G\ \bar{C}_{Pg}} \tag{4.27}$$

$$\frac{dT}{dV} = \frac{-\Delta H}{\bar{C}_P} \frac{\eta\ r_{NH_3}}{G} - \frac{U.A.(T-T_g)}{G.\ \bar{C}_P}$$

$$= \frac{-\Delta H}{\bar{C}_P} \frac{\eta\ r_{NH_3}}{G} - \frac{dT_g}{dV} \frac{\bar{C}_{Pg}}{\bar{C}_P} \tag{4.28}$$

where T_g is the temperature of the feed gas in imbedded cooling tube, U is the heat transfer coefficient, A is the exchange area per unit volume of catalyst and $\bar{C}_{Pg}$ is the specific heat of the feed gas. The equilibrium constant K_a is obtained from the Gillispie and Beattie equation [15]. The fugacity coefficients are calculated by means of the Cooper expression [9] for nitrogen and hydrogen and by the Newton expression [27] for ammonia.

The composition and temperature of the reacting system at the inlet of any layer being known, the material balance equation (4.24) is solved to obtain the extent of reaction which in turn gives the mole fraction of individual components (equation 4.26). For adiabatic bed the solution of energy balance equation (4.25) gives the outlet temperature whereas for non-adiabatic bed (cooling tubes imbedded in catalyst bed) equations (4.27) and (4.28) are to be solved simultaneously for the same purpose. Runge Kutta method of fourth order [8] has been used for the simultaneous solution of mass and energy balance equations. The size of the integration step has been varied according to the volume of catalyst used.

Calculation Program:

On the basis of the mathematical model described above, a calculation program in Fortran IV has been prepared for IBM 7044 computer. The calculation time for checking the performance of a triple-bed reactor with interstage cooling is 3 minutes and 3 seconds, when the step size for each bed is 1/100th of the bed volume.

4.4 RESULTS AND DISCUSSION

The calculation results for six different cases having adiabatic as well as non-adiabatic beds (autothermal reactors), working under different conditions of pressure and composition of the reacting system are presented along with the plant data

in Tables 4.1 to 4.4 and Figures 4.3 to 4.5.

For the purpose of discussion the reactors having adiabatic beds and those with non-adiabatic beds would be considered separately. The adiabatic reactors have Montecatini Catalyst whereas in autothermal reactors (non-adiabatic beds) Haldor Topsoe catalyst is in use.

Reactors with Adiabatic Catalyst Beds: Each reactor under consideration has three adiabatic catalyst beds. The results for these are presented in Tables 4.1 to 4.3. Figures 4.3 and 4.4 show the temperature and ammonia per cent profile for Case I (Table 4.1). The maximum difference in measured and calculated ammonia concentration exists for case I at the outlet from first catalyst bed (Table 4.1). The measured value is 4 per cent less than the calculated one. This difference is well within the experimental error limits. Maximum difference in temperature is recorded in Case III for exit from bed III (Table 4.3). The difference, being only 1.5 per cent, could be considered insignificant.

Autothermal Reactors: Results for these reactors are tabulated in Table 4.4. The maximum difference in measured and calculated composition exists at the outlet of Case IV (Table 4.4). This difference of 3.2 per cent is well within the allowable error limits. Moreover, the measured and calculated temperature profiles for this case (Fig. 4.5) almost overlap, showing

TABLE 4.1

EXPERIMENTAL DATA AND CALCULATED RESULTS FOR TRIPLE BED REACTOR [CASE I]

Total feed flow, Nm^3/hr 242160

Pressure, Kg/cm^2 232

Bed	I			II			III		
Volume of Catalyst, m^3	5.05			7.19			8.02		
Composition of gas, per cent	Inlet	Outlet		Inlet	Outlet		Inlet	Outlet	
		Cal.	Exptl.		Cal.	Exptl.		Cal.	Exptl.
N_2	22.19	20.00	20.1	20.00	18.59	18.2	18.59	17.64	17.8
H_2	67.03	60.42	61.0	60.42	56.31	57.1	56.31	53.46	53.9
NH_3	2.76	10.93	10.5	10.93	16.03	15.9	16.03	19.55	19.2
CH_4	5.46	5.89	5.7	5.89	6.17	6.1	6.17	6.36	6.3
Ar	2.56	2.76	2.7	2.76	2.90	2.7	2.90	2.99	2.9
Temperature, ^oC	385	507	507	433	501	502	415	469	455

TABLE 4.2

EXPERIMENTAL DATA AND CALCULATED RESULTS FOR TRIPLE BED REACTOR [CASE II]

Total feed flow, Nm^3/hr 180000

Pressure, Kg/cm^2 182

Bed	I			II			III		
Volume of Catalyst, m^3	5.05			7.12			8.10		
Composition of gas, per cent	Inlet	Outlet Cal.	Outlet Exptl.	Inlet	Outlet Cal.	Outlet Exptl.	Inlet	Outlet Cal.	Outlet Exptl.
N_2	19.6	17.71	17.2	17.71	16.63	15.7	16.63	15.70	15.5
H_2	65.1	59.83	60.3	59.83	56.79	57.2	56.79	54.20	54.5
NH_3	3.2	9.60	9.7	9.60	13.30	13.8	13.30	16.45	16.4
CH_4	7.4	7.86	7.8	7.86	8.12	8.2	8.12	8.35	8.3
Ar	4.7	5.00	5.0	5.00	5.16	5.1	5.16	5.30	5.3
Temperature, ^oC	395	490	496	442	492	502	404	445	440

TABLE 4.3

EXPERIMENTAL DATA AND CALCULATED RESULTS FOR TRIPLE BED REACTOR [CASE III]

Total feed flow, NM^3/hr 19500

Pressure, Kg/cm^2 212

Bed	I			II			III		
Volume of Catalyst, m^3	5.25			7.35			8.30		
Composition of gas, per cent	Inlet	Outlet Cal.	Outlet Exptl.	Inlet	Outlet Cal.	Outlet Exptl.	Inlet	Outlet Cal.	Outlet Exptl.
N_2	20.6	18.23	18.4	18.23	17.00	16.1	17.00	16.12	16.1
H_2	65.1	59.13	59.0	59.13	55.62	57.4	55.62	52.70	53.0
NH_3	3.2	10.60	10.7	10.60	14.90	14.2	14.90	18.28	18.3
CH_4	7.3	7.92	7.8	7.92	8.08	7.9	8.48	8.48	8.1
Ar	3.8	4.12	4.1	4.12	4.40	4.4	4.40	4.42	4.5
Temperature, ^oC	390	504	512	443	500	502	400	446	439

TABLE 4.4

EXPERIMENTAL DATA AND CALCULATED VALUES FOR AUTOTHERMAL REACTORS

Case	4			5			6		
Total feed flow, Nm^3/hr	47200			51700			24259		
Pressure, Kg/cm^2	285			275			365		
Volume of catalyst, m^3	4.07			2.3			2.3		
Total heat transfer surface, m^2	50.0			31.2			25.2		
Heat transfer coefficient, K.cal/(m^2 °C)	400			500			400		
Composition of gas, per cent	Inlet	Outlet		Inlet	Outlet		Inlet	Outlet	
		Cal.	Exptl.		Cal.	Exptl.		Cal.	Exptl.
N_2	21.9	17.65	17.7	21.2	17.60	17.21	18.82	13.74	14.2
H_2	65.0	52.11	52.8	65.8	55.26	55.41	59.45	44.75	45.1
NH_3	5.2	21.16	20.5	3.0	15.89	16.10	3.00	20.55	20.0
CH_4	4.3	4.93	4.9	6.7	7.54	7.53	13.21	15.62	15.9
Ar	3.6	4.15	4.1	3.3	3.71	3.75	4.52	5.34	5.3
Temperature, °C	421	438	438	437	501	505	417	447	443

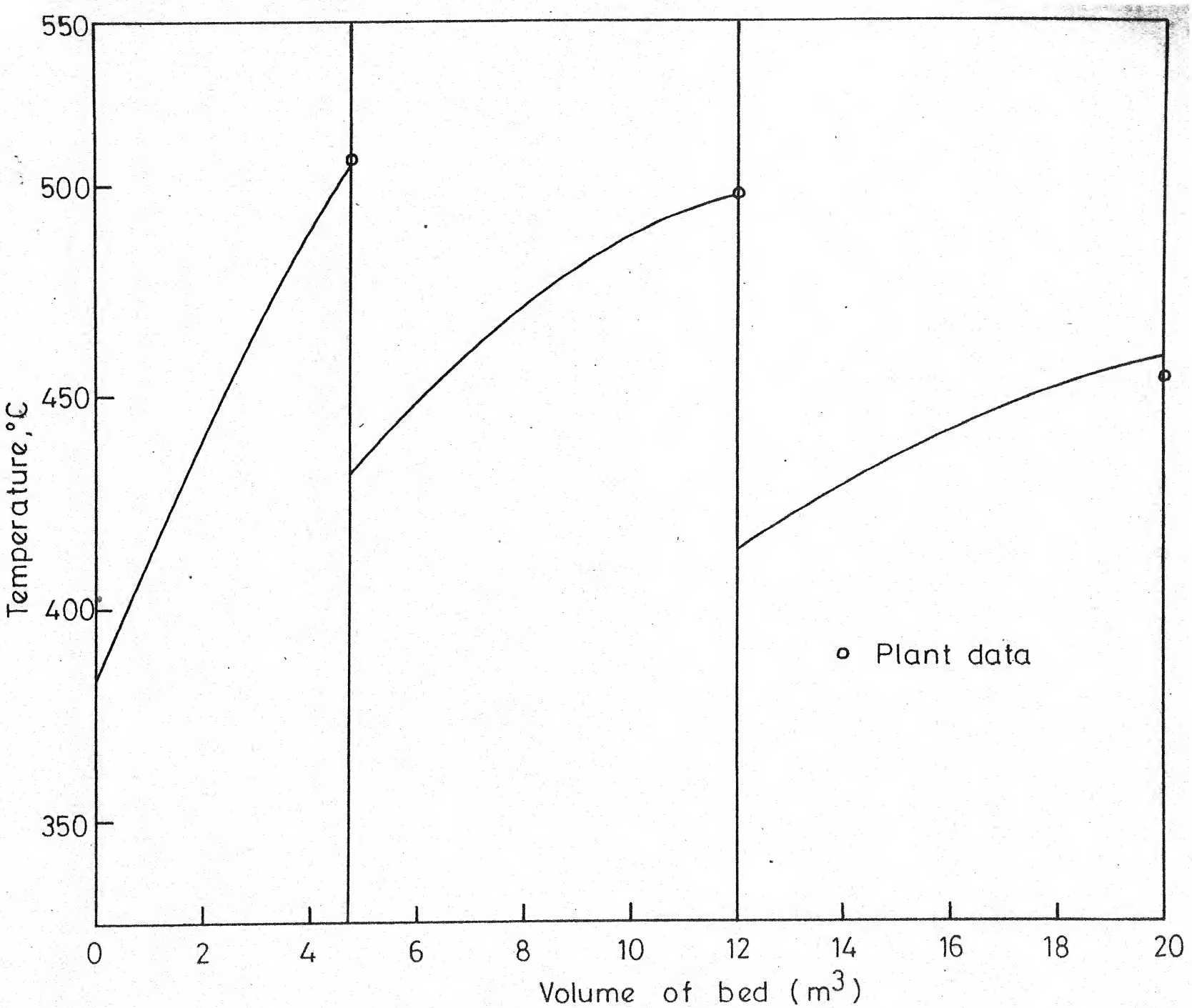

Fig. 4.3 - Temperature change in a triple adiabatic bed synthesis reactor.

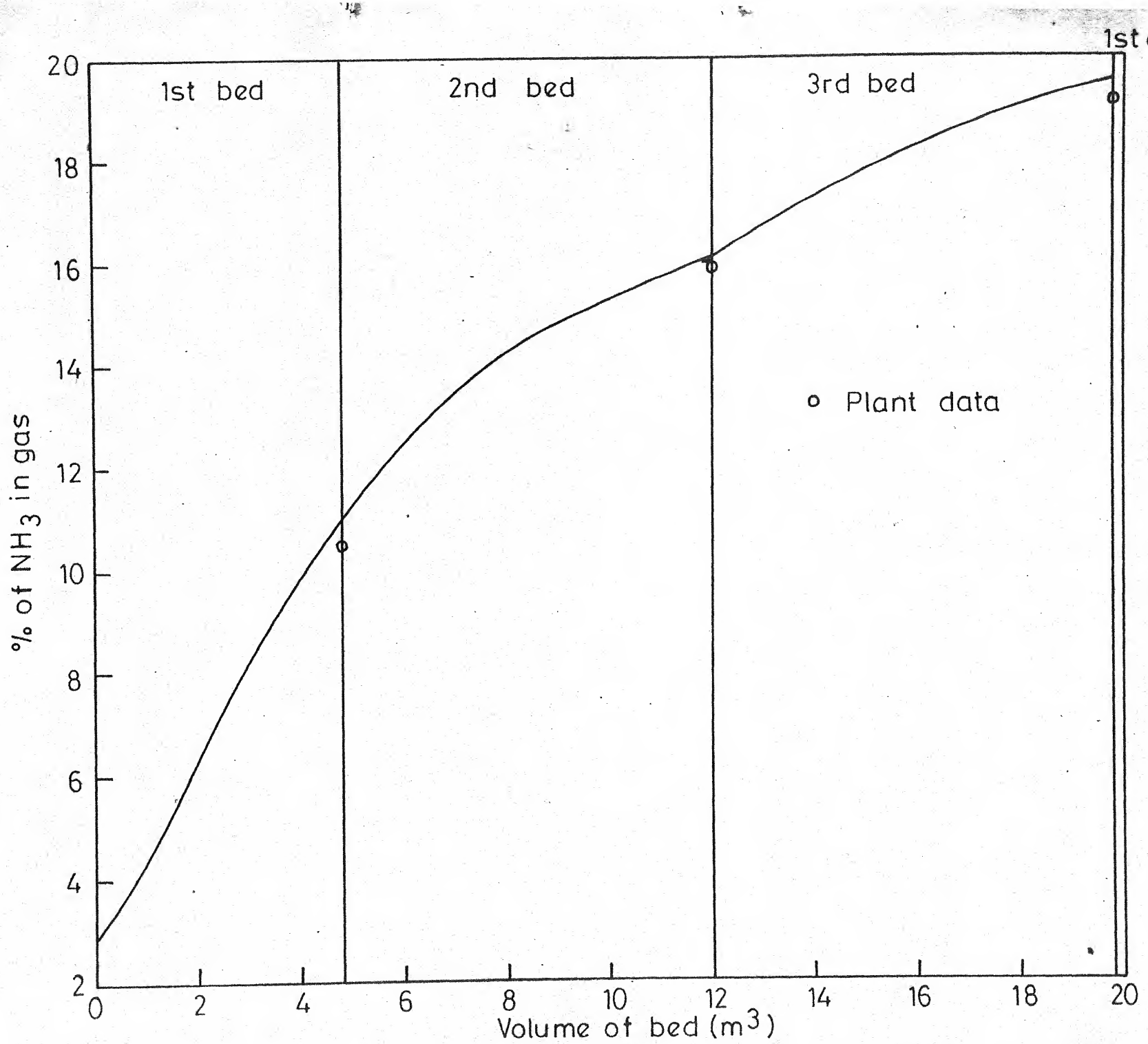

Fig. 4.4 -Ammonia concentration in a triple adiabatic bed synthesis reator.

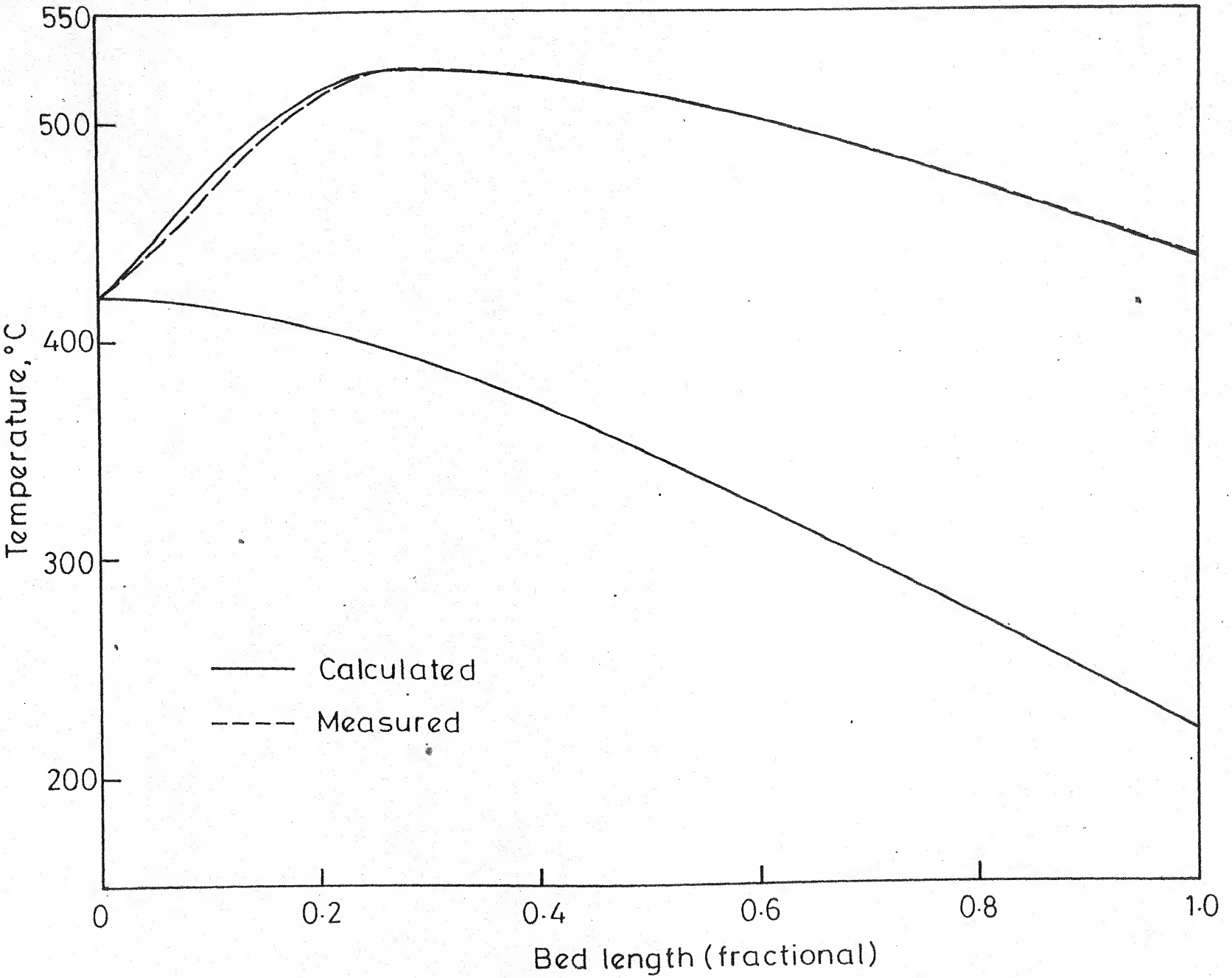

Fig. 4·5 - Temperature of synthesis gas in cooling tubes and catalyst bed of an autothermal reactor.

complete agreement between the model values and the actual ones. A complete match of temperature profiles would mean, from thermodynamic considerations, a match in composition also, indicating thereby that the difference observed in composition may be because of measurement errors. Also shown in Figure 4.5 is the calculated temperature profile of the feed gas in the tubes embedded in the catalyst bed. Maximum temperature difference of 4 per cent is observed for Case V. For this case the measured and calculated temperature profiles show a difference of 2 to 3 per cent over most part of the reactor. In view of very good agreement for other cases this small difference could be considered insignificant. Moreover, since the comparison is made over the entire profile and not at selected points, the reliability is high inspite of small deviations.

The results very clearly show that in general, the calculated values are in very good agreement with the plant data. It is to be noted that the deviations, in addition to being small, are randomly distributed with respect to actual plant observations both for temperature and composition. This confirms the reliability of the rate equations used as well as the validity of assumptions made under all plant conditions. This also shows that the effect of diffusion of reactants and products inside the catalyst pores has been correctly accounted for.

NOMENCLATURE

a	Constant
A	Heat exchange area, m^2
c	Total concentration of reacting gas mixture, kg.mole/m^3
C_P	Specific heat of reacting gas mixture, Kcal/kg.^oK.
C_{Pg}	Specific heat of feed gas, Kcal/kg ^oK
D_i^o	Diffusion coefficient of component i at 0^oC and 1 atm.
D_{ie}	Effective diffusion coefficient of component i
E_2	Activation energy for ammonia decomposition, Kcal/kg.mole
f_i	Fugacity of component i
$f_{N_2}, f_{H_2}, f_{NH_3}$	Fugacity of nitrogen, hydrogen and ammonia respectively
g_j	Mass fraction of component j
g_{jo}	Mass fraction of component j at inlet
G	Mass flow rate, Kg/hr
ΔH	Heat of reaction, Kcal/kg.mole
K_{20}	Frequency factor in Arrhenius equation for K_2
K_2	Velocity constant of reverse reaction
K_a	Equilibrium constant of the reaction: $0.5\ N_2 + 1.5\ H_2 \rightleftarrows NH_3$
m_j	Molecular weight of component j
N_i	Molar flux of component i
P	Pressure, atm.
r	Radial coordinate of spherical catalyst particle
D_i	Diffusion coefficient of component i

r_{NH_3}	Rate of ammonia formation, Kg.mole·NH_3/hr/m^3 of catalyst
R_g	Universal gas constant
R'	Radius of spherical particle
T	Temperature, ^oK
T_g	Temperature of gas in cooling tubes, ^oK
U	Heat transfer coefficient, Kcal/hr/m^2
V	Catalyst volume, m^3
x_i	Mole fraction of component i
x_{ig}	Mole fraction of component i in gas (bulk phase)

Greek Symbols:

α_i	Stoichiometric coefficient of component i
η	Effectiveness factor
ξ''	Extent of reaction
ε	Void fraction of packed bed
Λ	Equivalent diameter
ψ	Shape factor
θ	Intraparticle porosity

REFERENCES

1 Adams, R.M. and Commings, E.W., Chem.Eng. Progr. 49(7) 359 (1953).

2 Anderson, R.B., I and EC., 52, 89 (1960).

3 Bokhoven, C., VanHeerden, C., Westrik, R., Zwietering, P., 'Catalysis' Vol. III, Reinhold, New York, 1955.

4 Bokhoven, C., van Raayen, W., J. Phys. Chem. 58, 471 (1954).

5 Brill, R., J.Chem. Phys., 19, 1047 (1951).

6 Buzzi Ferraris, G., Donati, G., Ing.Chim. Ital. 6, 1(1970).

7 Cappelli, A., Collina, A., I. Chem.E. Symp. Ser. No. 35,5; 10(1972).

8 Carnahan, B., Luther, H.A. and Wilkes, J.O., 'Applied Numerical Methods', John Wiley and Sons, Inc., 1969.

9 Cooper, H.W., Hydro. Proc. Pet. Ref., 46(2), 159 (1967).

10 Dyson, D.C., Simon, J.M., I and EC Fund., 7, 605 (1968).

11 Emmett, P.H., in curtis 'Fixed Nitrogen' Chap. VIII, New York, Chemical Catalogue Co., 1932.

12 Emmett, P.H., 12th Report of Committee on Catalysis, National Research Council, Chap XIII, New York, John Wiley and Sons, 1940.

13 Emmett, P.H., Kummer, J.T., I and EC, 35, 677 (1943).

14 Frankenburg, W., Z. Electrochem. 39, 45-50, 97-103, 269-81, 818-20 (1933).

15 Gillespie, L.J., Beattie, J.A., Phys. Rev., 36, 734 (1930).

16 Guacci, U., Traina, F., BuzziFerraris, G. and Barisone, R., I and EC., Proc. Des. Dev., 16, 166 (1977).

17 Hays, G.E., Poska, F.L. and Stafford, J.D., Chem.Eng. Progr. 60, 61 (1964).

18 Huber, A., Chem. Ing. Techn., 3, 147 (1962).

19 Johansen, K., Chem.Eng. World 5(6), 107 (1970).

20 Kubota, H. and Shindo, M., Chem.Eng. (Japan), 20,11(1956).

21 Kubota, H., et al., Chem.Eng. (Japan), 23, 284 (1959).

22 Livshits, V.D., Sidorov, I.P.,Zh. Fiz. Khim. 26, 538(1952).

23 Lov, K.S., Emmett, P.H., J.Am.Chem.Soc., 63, 3297(1941).

24 Mills, A.K., Bennett, C.O., AIChE. J., 5, 539 (1959).

25 Morozov, N.M., Luk'yanova, L.I., Temkin, M.I., Kinet. Katal., 6, 82(1965).

26 Murase, A., Roberts, H.L. and Converse, A.O., I and EC. Proc. Des. Dev., 9, 503 (1970).

27 Newton, R.H., I and EC., 27, 302 (1935).

28 Nielsen, A., 'An Investigation on Promoted Iron Catalysts for the Synthesis of Ammonia' 3rd Ed. Jul Gjellerups Forlang Copenhagen, 1968.

29 Ozaki, A., Taylor,H.S., Boudart, M., Proc. Roy. Soc. London,Ser. A. 258, 47 (1960).

30 Prater, C.D., Chem.Eng. Sci. 8, 284 (1958).

31 Shah, M.J., I and E.C. 59, 72 (1967).

32 Shah, M.J., Weisenfelder, A.J., Automatica 5, 319 (1969).

33 Sholten, J.J.F., Thesis, Delft, the Netherlands, 1959.

34 Sidorov, I.P., Livshifts, V.D., Zh.Fiz. Khim. 21, 1177 (1947).

35 Singh, V.B., M.Tech. Thesis, I.I.T. Kanpur, India 1975.

36 Temkin, M.I., Morozov, N.M. Shapatina, E.N., Kinet. Katal. 4, 260, 565 (1963).

37 Temkin, M.I. and Pyzhev, V., Acta. Physicochem. 12, 327 (1940).

38 Weisz, P.B., Hicks, J.S., Chem.Eng.Sci., 17, 265 (1962).

39 Wheeler, A., 'Catalysis', P.H.Emmett, Ed., Chap. 2, Reinhold, New York, 1955.

CHAPTER 5

PROCESS SIMULATION OF AMMONIA PLANT

There is no recycle of process gas between the point of inlet to the PR and the exit from methanator. The outlet from one reactor makes the feed to subsequent one. Air and steam added at SR and HT inlets respectively are accounted for by mass balance. Temperature change associated with heat removal in between any two reactors is not considered, instead the measured value of temperature after cooling is used in simulation calculations. The ammonia synthesis reactor involves recycle of a major part of the product gas, to feed, after separation of ammonia from it. This recycle gas mixed with make up synthesis gas i.e. methanator exit, is the synthesis reactor feed. The process simulation includes a scheme for calculating flow and composition of feed to ammonia synthesis reactor. The model for this reactor calculates the rate of ammonia production.

In the PR model, dimensions of tube, burner and furnace, the number of tubes and burners in use and the amount, shape and size of catalyst are required to specify the primary reformer. The data on H_2/C ratio in hydrocarbon, steam, process and fuel hydrocarbon flow rates, inlet pressure, inlet temperature, calorific value of fuel, excess

air used by burners and the flue gas temperature are required by the PR model to calculate the flow, composition, temperature and pressure throughout the reformer tube length and at the exit. In addition, the total heat absorbed in the furnace, the inside and outside tube wall temperatures along the entire length are also calculated.

The outlet from PR is mixed with appropriate amount of air at SR inlet, to provide required nitrogen for ammonia synthesis and heat for steam reformation of remaining methane. The SR simulation model calculates the amount of air required, the composition and temperature after its mixing with PR exit and the subsequent changes in composition, temperature and pressure along the entire length of SR catalyst bed. Only data required by the model are dimensions of catalyst filled space and amount and specific surface of catalyst pellets.

The SR exit stream is cooled and in some cases small amount of steam is also added before it is fed to the H.T. The inlet temperature needs to be specified whereas composition of the process gas after mixing with known amount of steam is calculated. Volume and bulk density of the catalyst being known the HT model calculates composition and temperature throughout the catalyst volume.

The HT outlet is the feed to the LT with removal of heat in between. The flow and composition remains unaffected

but the feed temperature needs to be specified in addition to the volume and bulk density of catalyst. The LT model calculates composition and temperature throughout the catalyst bed.

The process simulation assumes complete removal of steam from LT exit and complete absorption of CO_2 in the CO_2 absorber. It further assumes complete conversion of CO in the process gas to CH_4 in the methanator. The exit from the methanator i.e. the make up synthesis gas therefore contains only N_2, H_2, CH_4 and Ar.

The recycle scheme of ammonia synthesis reactor is shown in Figure 5.1. CH_4 and Ar which do not take part in the reaction are continuously added to the ammonia synthesis loop [ABCD] by the make up gas. For continuous operation of the process it is, therefore, necessary that the amount of inerts being added to the synthesis loop is continuously taken out of it. Operating at higher concentration of inerts means lower production and higher circulation of synthesis gas through the reactor whereas low concentration of inerts in recycle gas would require high purge loss. An optimum concentration of inerts is therefore maintained. The flow and composition of purge, recycle and feed is obtained from the following component mass balance equations.

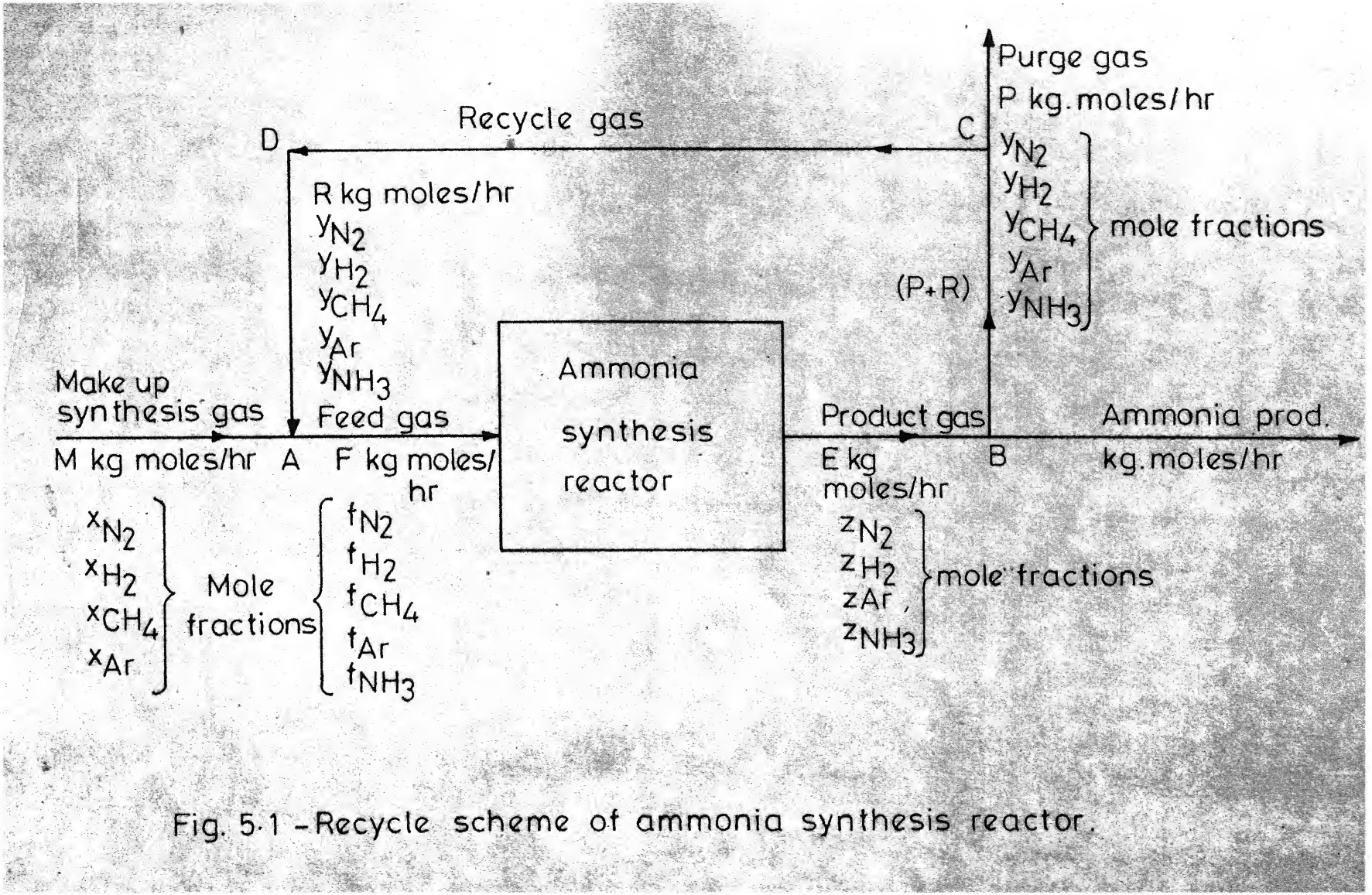

Fig. 5.1 - Recycle scheme of ammonia synthesis reactor.

Mass Balance Around Synthesis Loop (Figure 5.1):

$$M \cdot x_{N_2} = P\left(y_{N_2} + \frac{y_{NH_3}}{2}\right) + \frac{Prod}{2} \qquad (5.1)$$

$$M \cdot x_{H_2} = P \cdot (y_{H_2} + 1.5\ y_{NH_3}) + 1.5\ Prod \qquad (5.2)$$

$$M \cdot x_{CH_4} = P \cdot y_{CH_4} \qquad (5.3)$$

$$M \cdot x_{Ar} = P \cdot y_{Ar} \qquad (5.4)$$

Mass Balance Around Point A (Figure 5.1):

$$M + R = F \qquad (5.5)$$

$$M \cdot x_{N_2} + R \cdot y_{N_2} = F \cdot f_{N_2} \qquad (5.6)$$

$$M \cdot x_{H_2} + R \cdot y_{H_2} = F \cdot f_{H_2} \qquad (5.7)$$

$$M \cdot x_{CH_4} + R \cdot y_{CH_4} = F \cdot f_{CH_4} \qquad (5.8)$$

$$M \cdot x_{Ar} + R \cdot y_{Ar} = F \cdot f_{Ar} \qquad (5.9)$$

$$R \cdot y_{NH_3} = F \cdot f_{NH_3} \qquad (5.10)$$

Mass Balance Around Point B. (Figure 5.1):

$$E = P + R + Prod \qquad (5.11)$$

$$E \cdot Z_{N_2} = (P+R) \cdot y_{N_2} \qquad (5.12)$$

$$E \cdot Z_{H_2} = (P+R) \cdot y_{H_2} \qquad (5.13)$$

$$E \cdot Z_{CH_4} = (P+R) \cdot y_{CH_4} \qquad (5.14)$$

$$E \cdot Z_{Ar} = (P+R) \cdot y_{Ar} \qquad (5.15)$$

$$E \cdot Z_{NH_3} = (P+R) \cdot y_{NH_3} + Prod \qquad (5.16)$$

obtained from equations (5.11) and (5.16),

$$R = \frac{\text{Prod } (1-Z_{NH_3})}{Z_{NH_3} - y_{NH_3}} - P \quad . \qquad (5.20)$$

if Z_{NH_3} i.e. mole fraction of ammonia at the synthesis reactor exit is known. Once flow and composition of purge and recycle are known, equations (5.5) through (5.10) can be solved to obtain the feed flow and composition. However, Z_{NH_3} is the product composition and hence objective of synthesis reactor calculation and cannot be known apriori. Therefore, Z_{NH_3} value is assumed and equations (5.20), (5.5) through (5.10) are solved to obtain feed flow and composition. The synthesis reactor model calculates the exit concentration, Z_{NH_3}, which is compared with its assumed value. In case of significant difference a new value for Z_{NH_3}, based on calculated value, is chosen and equations (5.20), (5.5) through (5.10) solved again to obtain feed conditions. The process is repeated till the assumed value agrees with the calculated one within desired limit of accuracy.

The rate equations used by the synthesis reactor model in the present simulation are those for Montedison catalyst. In case of a different catalyst it would need to be suitably changed. Pressure, volume of catalyst in different beds and the inlet temperature for each of them being specified,

the synthesis reactor model calculates flow, temperature and composition of the process gas at each point in the reactor and at the exit. The agreement between assumed and calculated ammonia concentration in the product gas yields the rate of ammonia production. From the ammonia concentration in the synthesis reacted product gas the rate of ammonia production is obtained. The calculation scheme for the process simulation is described in detail in Appendix which also includes listing of the program.

Results and Discussion:

The calculation results alongwith the measured values for two plants at two different levels of operations are presented in Tables 5.1 and 5.2. The agreement between the measured and calculated values of flow, composition, temperature and pressure at various point throughout the plant, in all the four cases reported, is generally very good. It is to be noted that information on process variables required by the plant simulation, in addition to process unit specifications and inlet conditions, include inlet temperatures to HT and LT reactors and to the different beds in ammonia synthesis reactor, pressure and the allowable level of inerts in ammonia synthesis loop and the per cent of ammonia remaining in the gas after separation of the product. The information called for by the process simulation is rather very limited whereas

TABLE 5.1

MEASURED AND CALCULATED DATA FOR NAPHTHA BASED AMMONIA PLANT

Number of PR tubes	160
Dia of PR tubes	115.3 mm I.D./147.7 mm O.D.
Heated length of PR tubes	11.36 meters
SR catalyst	25 tons/19.4 m^3
HT Catalyst	75 tons/58.2 m^3
LT catalyst	73 tons/56 m^3
Synthesis catalyst	57.2 tons/20.9 m^3

Process Inlet PR	Case I	Case II
Process naphtha flow, kg/hr	14100	11900
Steam flow, kg/hr	67200	56000
Pressure, Kg/cm^2	24.8	24.3
Temperature, ^oC	443	440
SR inlet air temperature, ^oC	231	231
HT inlet temperature, ^oC	377	364
LT inlet temperature, ^oC	202	200
Synthesis reactor inlet temperature, ^oC		
1st bed	395	389
2nd bed	412	428
3rd bed	406	404
Pressure at synthesis reactor inlet, kg/cm^2	228	214

Table 5.1 (contd) Case I

ANALYSIS OF PROCESS GAS AT DIFFERENT POINTS IN AMMONIA PLANT

Location		CO	CO_2	H_2	CH_4	N_2	Ar	NH_3	Pressure, kg/cm^2	Temp., ^oC	S/G ratio	Flow, Nm^3/hr
Exit PR	Exptl.	9.93	17.43	64.16	8.13				21.90	761	0.927	118100
	Cal.	11.21	16.97	64.44	7.38				21.75	770	0.864	118839
Exit SR	Exptl.	13.36	13.06	52.26	0.36	20.73	0.23		21.10	905	0.703	143100
	Cal.	13.18	12.74	52.14	0.34	21.34	0.26		21.10	902	0.693	145980
Exit HT	Exptl.	3.21	21.42	55.86	0.32	18.95	0.24		20.50	445	0.530	143100
	Cal.	3.08	20.61	56.38	0.31	19.38	0.24			443	0.527	145980
Exit LT	Exptl.	0.31	23.29	57.03	0.32	18.81	0.24		20.00	220	0.480	143100
	Cal.	0.33	22.71	57.60	0.30	18.83	0.23			221	0.487	145980
Make up Syn.gas	Exptl.			74.59	0.80	24.32	0.29					72900
	Cal.			74.19	0.83	24.68	0.30					74898
Inlet NH_3 Reactor	Exptl.			65.90	6.54	22.03	2.51	3.02		228		248000
	Cal.			66.56	6.52	21.74	2.34	2.84				259116
Exit NH_3 Reactor	Exptl.			53.46	7.32	18.12	3.10	18.00		222		216000
	Cal.			53.45	7.50	17.52	2.72	18.43				225126
Recycle gas	Cal.			63.40	8.82	20.60	3.18	4.00				184218
Purge gas	Cal.			63.40	8.82	20.60	3.18	4.00				7062

Total amount of ammonia produced, tons/day Plant 619 Calculated 616

Table 5.1 (contd) Case II

ANALYSIS OF PROCESS GAS AT DIFFERENT POINTS IN AMMONIA PLANT

Location		CO	CO_2	H_2	CH_4	N_2	Ar	NH_3	Pressure, kg/cm^2	Temp., ^oC	S/G ratio	Flow NM^3/hr
Exit PR	Exptl.	12.60	17.20	63.30	6.90				21.60	775	0.821	98800
	Cal.	11.32	17.01	64.38	7.29				21.65	772	0.892	98700
Exit SR	Exptl.	14.10	12.80	50.78	0.10	21.90	0.20		21.00	925	0.674	123900
	Cal.	13.36	12.42	52.26	0.29	21.42	0.25		20.92	905	0.694	122037
Exit HT	Exptl.	3.10	21.20	55.60	0.10	19.30	0.20		19.90	436	0.550	123900
	Cal.	3.11	20.36	56.58	0.25	19.47	0.23			431	0.546	122037
Exit LT	Exptl.	0.30	22.84	57.30	0.28	19.03	0.25		19.30	220	0.510	123900
	Cal.	0.32	22.51	57.75	0.24	18.95	0.23			219	0.508	122037
Make up Syn.gas	Exptl.			74.99	0.67	25.01	0.33					65700
	Cal.			74.22	0.73	24.75	0.30					62836
Inlet NH_3 Reactor	Exptl.			65.14	6.35	22.32	2.65	3.54	214			22600
	Cal.			65.20	6.88	21.79	2.84	3.29				23421
Exit NH_3 Reactor	Exptl.			53.62	6.97	18.33	2.76	18.32	207			19700
	Cal.			52.97	7.91	17.77	3.25	18.10				20549
Recycle gas	Cal.			61.78	9.21	20.72	3.79					17137
Purge gas	Cal.			61.78	9.21	20.72	3.79					497

Total amount of ammonia produced, tons/day — Plant 543, Calculated 533

TABLE 5.2

MEASURED AND CALCULATED DATA FOR NATURAL GAS BASED AMMONIA PLANT

Number of PR tubes	200	
Dia of PR tubes	96 mm I.D./133.8 mm O.D.	
Heated length of PR tubes	12.2 meters	
SR catalyst	14.83 tons/12.4 m^3	
HT catalyst	53.5 tons/44.23 m^3	
LT catalyst	70.3 tons/50.2 m^3	
Synthesis catalyst	52.8 tons/20.26 m^3	
Process inlet PR	Case I	Case II
Process natural gas inlet, Nm^3/hr	13920	12014
Steam flow, kg/hr	61000	55000
Pressure, kg/cm^2	35.0	32.3
Temperature, ^oC	456.4	447.4
Air temperature at SR inlet, ^oC	460.0	460.0
Steam added at HT inlet, kg/hr	7200	6000
HT inlet temperature, ^oC	367	357
LT inlet temperature, ^oC	198	200
Synthesis reactor inlet temperature, ^oC		
1st bed	385	406
2nd bed	433	430
3rd bed	415	407
Pressure at synthesis reactor inlet, kg/cm^2	235	210

Table 5.2 (contd) Case I

ANALYSIS OF PROCESS GAS AT DIFFERENT POINTS IN AMMONIA PLANT

Location		CO	CO_2	H_2	CH_4	N_2	Ar	NH_3	Pressure, Kg/cm^2	Temp., °C	S/G ratio	F. Nr
Exit PR	Exptl.	10.17	12.27	67.22	9.83				31.30	773	0.878	11
	Cal.	9.56	12.56	69.61	8.27				31.56	796	0.898	116
Exit SR	Exptl.	12.20	9.40	55.58	0.32	22.11	0.38		30.20	962	0.694	14
	Cal.	11.96	9.44	55.73	0.34	22.26	0.27		30.40	957	0.711	144
Exit HT	Exptl.	2.16	17.62	59.40	0.23	20.12	0.23		29.50	425	0.649	151
	Cal.	1.83	17.52	59.83	0.31	20.37	0.24			424	0.653	153
Exit LT	Exptl.	0.18	18.93	60.29	0.34	20.01	0.25		28.70	213	0.630	151
	Cal.	0.16	18.87	60.48	0.31	20.03	0.23			208	0.626	153
Make up Synthesis gas	Exptl.			74.55	0.75	24.37	0.32					78
	Cal.			74.39	0.57	24.74	0.30					76
Inlet Ammonia Reactor	Exptl.			67.03	5.46	22.19	2.56	2.76	235			242
	Cal.			67.25	5.65	21.80	2.95	2.35				247
Exit Ammonia Reactor	Exptl.			53.90	6.30	17.80	2.90	19.10	228			216
	Cal.			53.38	6.59	17.08	3.44	19.51				212
Recycle gas	Cal.			64.31	7.90	20.44	4.10	3.25				171
Purge gas	Cal.			64.31	7.90	20.44	4.10	3.25				55

Total amount of ammonia produced, tons/day Plant - 618
Cal. - 641

Table 5.2 (contd) Case II

ANALYSIS OF PROCESS GAS AT DIFFERENT POINTS IN AMMONIA PLANT

Location		CO	CO_2	H_2	CH_4	N_2	Ar	NH_3	Pressure kg/cm^2	Temp., ^oC	S/G ratio	Flow, Nm^3/hr
Exit PR	Exptl.	9.86	11.79	69.03	9.32				28.80	793	0.910	103500
	Cal.	9.90	12.01	69.59	8.90				29.12	784	0.931	101098
Exit SR	Exptl.	12.40	9.60	55.37	0.33	22.10	0.40		28.00	932	0.735	125800
	Cal.	12.52	9.26	55.43	0.33	22.25	0.36		28.30	927	0.748	127553
Exit HT	Exptl.	1.18	18.05	60.02	0.30	20.09	0.36		27.50	415	0.670	134000
	Cal.	1.23	18.13	59.80	0.30	20.22	0.32		27.70	414	0.667	135019
Exit LT	Exptl.	0.13	18.00	61.60	0.25	19.63	0.39		27.00	209	0.650	134000
	Cal.	0.13	19.02	60.24	0.29	19.99	0.31		27.00	207	0.649	135019
Make up Syngas	Exptl.			74.37	0.49	24.72	0.42					
	Cal.			74.32	0.52	24.78	0.38					65383
Inlet NH_3 Reactor	Exptl.			64.85	5.48	21.54	5.16	2.97	216			228300
	Cal.			65.57	5.55	21.94	4.06	2.88				234106
Exit NH_3 Reactor	Exptl.			52.61	6.23	18.21	4.63	18.32	210			20400
	Cal.			53.00	6.40	17.76	4.68	18.16				203176
Recycle gas	Cal.			62.18	7.51	20.82	5.49	4.0				168723
Purge gas	Cal.			62.18	7.51	20.82	5.49	4.0				4497

Total amount of ammonia produced, tons/day Plant 548
Calculated 546

the measured and calculated values, for different plants, compare very well at any point along the flow of process gas. The close agreement in all cases studied shows the versatility of the process simulation presented here.

NOMENCLATURE

E	Flow of synthesis reactor exit, kg.mole/hr
F	Flow of feed to synthesis reactor, kg.mole/hr
f_i	Mole fraction of component i in feed
P	Flow of purge gas, kg.mole/hr
Prod	Rate of ammonia production, kg.mole/hr
R	Flow of recycle, kg.mole/hr
x_i	Mole fraction of component i in make up synthesis gas
y_i	Mole fraction of component i in purge and recycle gas
Z_i	Mole fraction of component i in synthesis reactor exit

Chemical formula is used as subscript to represent the respective component molecules.

CHAPTER 6

CONCLUSIONS AND RECOMMENDATIONS

Mathematical models for simulation of all the important process units of ammonia plant, namely, primary and secondary reformers, high temperature and low temperature shift reactors and ammonia synthesis reactor, have been developed. These have been subsequently used for process simulation of an ammonia synthesis plant.

In primary reformer model, rate equations for steam methane reactions and heat transfer equations have been successfully developed and used. Transfer of heat from flames which accounts for 25-35 per cent of the total heat transfer has separately been considered.

Secondary reformer model calculates the amount of air to be mixed, with PR exit, at the inlet to SR, the resulting temperature of process gas and the subsequent change in composition and temperature over the catalyst bed. Rate of reformation reaction in the SR is obtained by considering the reaction to be limited by the rate of diffusion of reactants from bulk to the catalyst pellet surface.

A rate equation for water-gas shift reaction over chromia promoted iron-oxide (HT catalyst) has been successfully developed and used in simulation of several industrial

reactors. Rate of shift reaction over LT catalyst (CuO-ZnO) has also been developed and used.

A suitable homogeneous rate expression for ammonia synthesis reaction has been selected. A method of calculating effectiveness factor for industrial catalysts, by partially solving the transport equations has been developed. Subsequently, these have been used in a mathematical model developed for design and simulation calculations of axial flow ammonia synthesis reactors. Reactors having adiabatic as well as those with non-adiabatic beds have been considered.

The process simulation of ammonia plant has been obtained using these models and considering other process units to be ideal. Recycle of gas at the synthesis reactor is also considered. The calculation results and the measured values of process variables at different locations in a plant are in close agreement.

The models developed in this work have been used only to check the performance of various units but it can be claimed that their use for design work would yield very good results.

Recommendations:

Efforts are required to develope methods to calculate transfer of heat to PR tubes where the flue gas temperature is not uniform.

Rate equations developed here for water gas shift reaction over HT and LT catalysts and ammonia synthesis reaction over iron catalyst are valid for the catalysts being used. More extensive work is required to develop truely general rate equations which will be valid for any catalyst.

Attempts should be made to develop such a simulation of ammonia plant which would account for the performance of all the units and also consider the recovery of heat from SR exit, PR exit, flue and synthesis gas and power generated for compression of synthesis gas.

APPENDIX

PROCESS SIMULATION PROGRAM FOR AMMONIA PLANT

The process simulation program consists of a main program and fifteen subprograms, namely FIREBX, EQMC, WALL, COMP, SRINTC, SHIFT AMMONIA, HTCF, REACR, REANH, EFF, EFFNH, HTRXN, CP and RUNCE.

Main Program:

All relevant data about the plant is obtained by this program through READ statements. These data are printed in the same format to enable a check on the possible errors. The required data are transferred to the subprograms whenever, they are called in by the main program, through the arguments and COMMON statements and in turn these are transferred as required to the subprograms that these subprograms call and so on.

After reading and printing data the main program calls FIREBX to calculate emissivities of flue gas and flames and the total amount of heat absorbed in reforming furnace. These values along with the flow and composition of flue gas are printed by the subprogram. Composition of PR inlet stream is calculated in main program by assuming conversion of feed to methane and carbon dioxide only. Subsequently EQMC is called to calculate the real composition of feed containing CH_4, CO, CO_2 and H_2. Flow, composition, temperature and

pressure along the flow over the catalyst in the PR tube are calculated by the integration subprogram RUNGE which calls in WALL to calculate inside and outside tube wall temperatures, REACR to calculate rates of steam-methane and water-gas shift reactions, HTRXN to calculate heat of the two reactions, CP to calculate specific heat of reaction mixture, COMP to calculate the composition of the process gas and HTCF to calculate inside tube heat transfer coefficient. Temperature, component flow rates and pressure of the process gas, outside and inside tube wall temperatures and amount of heat transferred to a differential section of the reformer tube length are calculated and printed at each integration step.

SRINTC is called by the main program to calculate the amount of air required and the temperature and composition of the mixed feed. RUNGE is again called to integrate the changes in flow, composition, temperature and pressure over the SR catalyst bed. Rate of steam-methane reaction is calculated from diffusivity considerations which involves equilibrium calculations to be done by EQMC. REACR is called to calculate rate of shift reaction. Heat of reactions, specific heat of process gas and composition of the reaction product at any point along the path of integration are evaluated by HTRXN, CP and COMP respectively. Volume of the catalyst and correspondin

temperature, pressure and flow rates of each component of process gas are printed for the entire volume of the catalyst.

Any steam added to the process gas at the inlet is accounted for to obtain the inlet process gas composition and this information along with inlet temperatures, pressures and catalyst volumes for HT and LT reactors are transferred to SHIFT which is called in to calculate the performance of HT and LT reactors. SHIFT calls in RUNGE to perform integration of mass and heat balance equations whereas REACR, HTRXN and CP are called to calculate reaction rate, heat of reaction and specific heat respectively. Volume of the catalyst alongwith the calculated temperature and composition of the gas throughout the entire volume of HT and LT reactors are printed.

The CO_2 and H_2O content are taken as zero. The composition change associated with the removal of CO_2 and H_2O and complete conversion of CO to CH_4 is calculated. This gives the make up synthesis gas composition. Flow and composition of recycle gas is calculated by assuming the ammonia concentration in synthesis reactor outlet gas. The composition of feed gas i.e. the mixture of make up and recycle synthesis gas is calculated and this along with the volume of the catalyst in each bed and the corresponding inlet temperature

is transferred to AMONIA. This subprogram calls EFFNH to calculate the effectiveness factor of the synthesis catalyst at each step of integration which is done by RUNGE. EFFNH cannot be called by RUNGE since this itself calls RUNGE. Therefore for the four substeps taken by RUNGE to complete one integration step, the effectiveness factor is taken constant. RUNGE calls REANH, HTRXN and CP to calculate the rate of ammonia synthesis reaction, heat of reaction and specific heat of synthesis gas respectively. Effectiveness factor, volume of the catalyst, temperature and composition of gas are printed at each integration step. If the calculated ammonia concentration of the product gas does not agree with the assumed value, calculation is repeated with a new value of ammonia concentration in product gas. In case of agreement between the assumed and calculated value of ammonia concentration at the synthesis reactor outlet, the rate of ammonia production is evaluated and printed.

Subprogram:

FIREBX: Data required by this subprogram are - Hydrocarbon fuel used, H_2/C ratio, flow rate and calorific value of the fuel, beam lengths of flames and flue gas, ambient temperature, excess air used in burning the fuel and temperature of flue gas. It calculates the adiabatic flame temperature by equating sum of the calorific heat in fuel and the sensible heats in flue and flames to the sensible heat in flames.

Amount of heat absorbed in reformer is the difference between sensible heat in flames and that in flue gas leaving the reformer. Adiabatic flame temperature, emissivities of flue and flames, and the total heat absorbed in primary reformer are printed.

EQMC: Data required are component molar flow rates, pressure and temperature. Equilibrium composition at the given pressure and temperature is calculated by repeatedly evaluating mole fractions of H_2 and CO from equilibrium of steam-methane and water-gas shift reactions respectively. Calculated equilibrium composition is transferred to the point which called the subprogram and no values are printed.

WALL: In addition to the reformer specifications, data required are the temperatures and emissivities of flue gas and flames, mass flow rate, pressure, temperature and composition of process gas and specific heat of reaction mixture. Inside and outside wall temperatures, heat transferred from flue gas and flames to the differential section under consideration are obtained by equating the amount of heat transferred from flames and flue gas to that from inner wall of the tube to the process gas. No values are printed.

COMP: Stoichiometric coefficients, molecular weights and mass fractions of all component molecules, total mass flow rate and extents of reactions are the data required. Composition

of the process gas for given extent of reactions is calculated by the subprogram.

SRINTC: Molecular weight, temperature and molar flow rates of different components in PR exit and temperature of air is to be provided for this subprogram to calculate amount of air required to be mixed to process gas and resulting temperature, composition and flow.

SHIFT: Stoichiometric coefficients for shift reaction and molar flow rates of different components at the inlet to HT, pressure, volume of catalysts in HT and LT and the inlet temperatures for the two reactors are the information called for. Mass and energy balance equations over a differential section of reactor are integrated over the entire volume, from inlet to exit, with RUNGL. The reaction rates over the HT and the LT catalysts are calculated by REACR. Effectiveness factor is obtained from EFF, heat of reaction from HTRXN and specific heat from CP. At each integration step, volume of catalyst, temperature and composition of the process gas are printed.

AMONIA: Data required include stoichiometric coefficients for synthesis reaction, molecular weights, molar flow rates of all components and volume of catalyst and inlet temperatures for all the catalyst beds. EFFNH is called to calculate effectiveness factor for the catalyst and subsequently RUNGE

is called to integrate the mass and heat balance equations over a differential section which needs REANH, HTRXN and CP to calculate rate of synthesis reaction, heat of reaction and specific heat of the process gas respectively. Volume of the catalyst, temperature and composition of process gas and effectiveness factor are printed at each integration step.

HTCF: Diameter of the catalyst pellet, specific heat, temperature and process gas mass flow rate per unit area are supplied to this subprogram for calculating reformer tube internal heat transfer coefficient.

REACR: Composition, temperature and pressure of the process gas along with the catalyst under consideration being specified this subprogram calculates the rate of methane-steam reaction over reformation catalyst and that of shift reaction over reformation, HT and LT catalysts.

CP: This subprogram calculates the specific heat of process gas throughout the ammonia plant which has components from among the eight considered by this subprogram. Composition, temperature and pressure being specified, this subprogram calculates the average molar specific heat of process gas.

REANH: This subprogram calculates rate of ammonia synthesis reaction from component gas fugacities and temperature of process gas.

EFF: Effectiveness factors for HT and LT catalysts are obtained from this subprogram given the forward rate constant, temperature of reaction and the reactor under consideration.

EFFNH: Fugacity coefficients, bulk diffusivities and mole fractions of component molecules, stoichiometric coefficients for synthesis reaction, temperature and pressure of the gas are the data required. The subprogram calculates effectiveness factor for the ammonia synthesis catalyst particles.

HTRXN: Pressure and temperature of process gas and the reaction under consideration being specified, this subprogram calculates the heat of the specified reaction. Heat of reformation, shift and synthesis reactions, one at a time, can be obtained from this subprogram.

RUNGE: All integrations involved in the program are performed by this subprogram. This employs the fourth order Runge-Kutta method with Kutta's coefficients to integrate a system of N simultaneous first order ordinary differential equations

$$F(J) = DY(J)/DX, \quad (J=1,2,\ldots,N)$$

accross one step of length H in the independent variable X, subject to initial conditions Y(J), (J = 1,2,...,N). N, H, F and initial values of X and Y(J), (J=1,2,...,N) are required to perform the integration.

LISTING OF COMPUTER PROGRAM

Available with Professor D.N. Saraf,
Department of Chemical Engineering,
Indian Institute of Technology, Kanpur,
India